Improving Agreement Between Static Method and Dynamic Formula for Driven Cast-In-Place Piles in Wisconsin

James H. Long, PhD, P.E.

University of Illinois at Urbana/Champaign
Department of Civil Engineering

WisDOT ID no. 0092-10-09
June 2013

Research & Library Unit

Wisconsin Highway Research Program

WISCONSIN DOT
PUTTING RESEARCH TO WORK

Wisconsin Highway Research Program #0092-10-09

Improving Agreement Between Static Method and Dynamic Formula for Driven Cast-In-Place Piles in Wisconsin

FINAL REPORT

James H. Long

University of Illinois at Urbana/Champaign
Department of Civil Engineering
College of Engineering

Submitted to Wisconsin Department of Transportation

June 2013

DISCLAIMER

This research was funded by the Wisconsin Department of Transportation and the Federal Highway Administration under Project 0092-10-09. The contents of this report reflect the views of the authors who are responsible for the facts and accuracy of the data presented herein. The contents do not necessarily reflect the official views of the Wisconsin Department of Transportation or the Federal Highway Administration at the time of publication.

This document is disseminated under the sponsorship of the Department of Transportation in the interest of information exchange. The United States Government assumes no liability for its contents or use thereof. This report does not constitute a standard, specification or regulation.

The United States Government does not endorse products or manufacturers. Trade and manufacturers' names appear in this report only because they are considered essential to the object of the document.

TECHNICAL REPORT DOCUMENTATION PAGE

1. Report No. 0092-10-09	2. Government Accession No	3. Recipient's Catalog No
4. Title and Subtitle Improving Agreement Between Static Method and Dynamic Formula for Driven Cast-In-Place Piles in Wisconsin		5. Report Date June, 2013 6. Performing Organization Code Wisconsin Highway Research Program
7. Authors James H. Long		8. Performing Organization Report No.
9. Performing Organization Name and Address University of Illinois at Urbana/Champaign Department of Civil Engineering 205 North Mathews / Urbana, IL 61801		10. Work Unit No. (TRAIS) 11. Contract or Grant No. WisDOT SPR# 0092-10-09
12. Sponsoring Agency Name and Address Wisconsin Department of Transportation Division of Business Services, Research Coordination Section 4802 Sheboygon Avf. Rm 104 Madison, WI 53707		13. Type of Report and Period Covered Final Report 2009-2013 14. Sponsoring Agency Code

15. Supplementary Notes
Research was funded by the Wisconsin Department of Transportation through the Wisconsin Highway Research Program. Wisconsin Department of Transportation Contact: Jeffrey Horsfall (608) 243-5993

16. Abstract
This study focuses on comparing the capacities and lengths of piling necessary as determined with a static method and with a dynamic formula. Pile capacities and their required lengths are determined two ways: 1) using a design and computed method, such as the static method (Nordlund/Thurman/Tomlinson) identified in the Wisconsin Bridge Manual, and 2) using as-driven information, such as the Wisconsin-modified Engineering News Formula, the modified-Gates method.

A collection of 182 cases was used to compare predictions made with the static method with prediction made using the FHWA-modified Gates driving formula. The most effective factors influencing the agreement between predictions made by DRIVEN and FHWA-Gates were the effective stress at the tip of the pile, the friction angle for coarse-grained soils, and whether load was carried in side resistance or end bearing. Correction factors are developed to correct the static method for overburden stress at the tip of the pile. Furthermore, conditional limits are suggested for the friction angle for coarse-grained soils.

Improvements were attained in the agreement for pile length required for many of the cases, however, in about 10 percent of the cases, the prediction of length of piling was not as accurate and the overall coefficient of variation increased. However, predictions of capacity at the depth driven in the field was significantly improved. Coefficients of variation for the agreement between methods improved to 0.28 from the original 0.98.

17. Key Words	18. Distribution Statement
metal shell piles, CIP piles, pile formula, pile capacity.	No restriction. This document is available to the public through the National Technical Information Service 5285 Port Royal Road Springfield VA 22161

18. Security Classif.(of this report)	19. Security Classif. (of this page)	20. No. of Pages	21. Price
Unclassified	Unclassified	103	

Form DOT F 1700.7 (8-72) Reproduction of completed page authorized

ACKNOWLEDGEMENTS

The authors acknowledge the contributions from the technical oversight committee: Mr. Jeffrey Horsfall and Mr. Robert Andorfer of the Wisconsin Department of Transportation. These members provided helpful guidance to ensure the project addressed issues relevant to Wisconsin Department of Transportation.

EXECUTIVE SUMMARY

PROBLEM STATEMENT

Many transportation facility structures in Wisconsin are founded on driven piling. Round, closed-end, steel, pipe piles are commonly used as friction piles in many structures including bridges and retaining walls. These cast-in-place (CIP) piles have shell thicknesses typically ranging from 0.219 - 0.375 inches and diameters ranging from 10.75 – 16 inches. The piles are driven to capacity and then filled with concrete.

Wisconsin DOT's experience indicates that design pile length estimations have generally been fairly accurate when compared to driven pile lengths. Driven lengths have been determined based on penetration resistance measured in the field using the Wisconsin-modified Engineering News (EN) driving formula, as described in Section 508 of the Standard Specifications for Highway and Structure Construction.

However, the Wisconsin Department of Transportation (Wisconsin DOT) no longer uses the EN formula nor the LFD design methodologies and now designs structural transportation facilities using AASHTO Load and Resistance Factor Design (LRFD) methodologies and the FHWA-modified Gates formula.

This study focuses on comparing the capacities and lengths of piling necessary as determined with a static method and with a dynamic formula. Pile capacities and their required lengths are determined two ways: 1) using a design and compute method, such as the static method (Nordlund/Thurman/Tomlinson) identified in the Wisconsin Bridge Manual, and 2) using as-driven information, such as the Wisconsin-modified Engineering News Formula, the modified-Gates method, and WEAP.

PROCESS

One hundred and eighty two cases were collected, interpreted, and analyzed in which driven cast-in-place (CIP) piles were used foundation elements for bridge structures. For each case the soil boring logs and the geotechnical reports were reviewed to develop a soil profile. Construction records for pile driving were collected and recorded to determine the pile hammer characteristics and the driving behavior of the pile during installation.

Axial capacities for the piling were determined using static methods. Specifically, the static method estimates were made using the computer program DRIVEN with the options for selecting Tomlinson's recommendations for the relationship between unit side soil strength in fine-grained soil and Nordlund/Thurman's methods for unit side resistance and end bearing in coarse grained soil.

FINDINGS AND CONCLUSIONS

The collection of cases was used to compare predictions made with the static method with prediction made using the FHWA-modified Gates driving formula. Statistics for the 182 cases were determined for the ratio of capacity predicted with DRIVEN/capacity predicted with FHWA-modified Gates. The average was 1.35 with a coefficient of variation equal to 0.98 which corresponds to considerable scatter. Several investigations were conducted in an attempt to improve the predictions between the two methods. Modifications were focused on the static method used in DRIVEN. The most effective factors influencing the agreement between predictions made by DRIVEN and FHWA-Gates were the effective stress at the tip of the pile, the friction angle for coarse-grained soils, and whether the load was carried in side resistance or end bearing.

The following modifications to the static method are proposed:

1) conditionally limit the friction angle to a maximum of 36 degrees (if the Standard Penetration Test values exceed 80 bpf, then friction angles up to 40 degrees can be used),

2) apply a correction factor to the side capacity (Q_{side}) as follows:

$$Q_{side\ corr} = Q_{side}/CF_{side}$$

where, CFside is determined as

$$CF_{side} = 0.2 \leq -0.4615 + 1.4615 \cdot \sigma'_{v\ tip}/4750 \leq 1.2$$

where, $\sigma'_{v\ tip}$ is the vertical effective stress (psf) at the tip of the pile, and

3) apply a correction factor for end bearing (Q_{end}) as follows:

$$Q_{end\ corr} = Q_{end}/CF_{end}$$

where

$$CF_{end} = 0.2 \leq -0.185 + 1.185 \cdot \sigma'_{v\ tip}/4750 \leq 1.2$$

Comparing pile lengths necessary to develop pile capacity is one way to assess the agreement between methods. Pile lengths driven in the field were assigned a capacity as defined by FHWA-modified Gates based on the pile's driving behavior measured during pile installation. DRIVEN was used to estimate the pile lengths necessary to develop the capacity determined with FHWA-modified Gates. The effect of applying the correction factors was to improve the agreement between estimated lengths and lengths driven in the field for most of the piling; however, the agreement for about 10 percent of the piling was less accurate than with the original predictions.

However, the combination of correction factors and conditional limits for the friction angle were very successful in reducing the scatter between capacity estimates from DRIVEN and FHWA-modified Gates. The average of the ratio of capacity predicted with DRIVEN/capacity predicted with FHWA-modified Gates for the 182 cases was determined to have a mean of 1.06 and a coefficient of variation of 0.28. These correction factors were very successful in improving the agreement of capacity predicted.

TABLE OF CONTENTS

1.0 INTRODUCTION

Cast-In-Place pile foundations are driven in the field to a depth sufficient to develop enough axial capacity to support the bridge structure. The depth required to drive the pile is estimated from consideration of the load the pile must support, the level of safety required, and the soil conditions at the site and the dimensions of the pile. The capacity of the pile is determined using a design method that relates side resistance and end bearing to soil type, soil strength, vertical stress, and pile dimensions. Design methods that use laboratory and/or field measurements of soil strength to determine the static capacity of a pile are termed static methods. Wisconsin Department of Transportation uses a static method consistent with those in the computer program "DRIVEN."

However, piles are typically driven in the field using a predictive method different from the static method because soil conditions can vary with distance from the original soil boring. Accordingly, the pile may or may not develop sufficient capacity at the depth estimated using static methods. There are predictive methods based on pile-driving behavior in the field that predict capacity with greater precision than static methods. Therefore, there is a "disconnect" between the pile length estimated using static methods, and the pile length driven in the field based on the resistance of the pile during pile driving. These two different methods result in different estimated and driven lengths. In many cases, the estimated and driven lengths are similar; however, the two lengths can sometimes vary significantly.

One hundred and eighty two cases were reviewed where CIP piles were driven in soils for the support of bridge structures throughout the state of Wisconsin. Comparisons were made between estimated pile penetration and pile penetration observed in the field. This report adjusts the estimates of capacity using the static method to predict pile penetration requirements in better agreement with pile penetration observed in the field.

Chapter 2 reviews observations made in the literature documenting the agreement between estimates of pile capacity based on static methods and pile capacity, and the agreement between estimates of capacity based on dynamic methods and pile capacity. Descriptions for the static method used by the computer program "DRIVEN" and several dynamic methods are given in Chapter 3. Chapter 4 briefly identifies how soil properties were determined from soil exploration, laboratory, and field tests. The collection of cases is described in Chapter 5 to provide characteristics of the soil conditions, pile dimensions, pile capacities, and driven lengths. Chapter 6 compare the results of estimated and driven capacities (and lengths) while Chapter 7 adopts methods to improve the agreement between estimated and observed and quantifies the uncertainty with which capacity and length can be estimated. Chapter 8 summarizes the report and provides final conclusions. References are listed in Chapter 9.

2.0 BACKGROUND AND LITERATURE REVIEW – AXIAL PILE BEHAVIOR

2.1 INTRODUCTION

An understanding of the behavior of piles when subjected to axial load is important for selecting design methods for predicting axial capacity of driven piling. The results of selected studies on axial pile behavior are presented herein to provide a background for understanding the advantages and shortcomings of design methods for predicting axial capacity. This section focuses on describing observed behavior of piles, and then compares the behavior observed with common assumptions used in design methods (static methods) for predicting axial capacity of piles.

The behavior of piles driven into coarse-grained soil is discussed first. The development of end bearing and side resistance with depth is discussed and results of an extensive testing program are presented to provide a comparison of behavior observed versus what design methods use for modeling pile response. Similar discussion follows for piles driven into fine-grained soil.

2.2 DRIVEN PILES IN COARSE-GRAINED SOILS

Piles driven into sands and gravel are included in the category of coarse-grained soils. The soils exhibit high enough permeability to dissipate excess water pressures during the time it takes to conduct a static load test. Vesic (1967) conducted a series of large-scale model tests on piles to examine the behavior of piles in sand subjected to axial load. Vesic's test results form a basis for understanding pile behavior and are discussed below.

Vesic (1967) conducted pile load tests in a cylindrically-shaped test chamber that measured approximately 8 ft in diameter and 22 ft in depth. The test chamber was carefully filled with sand to control the in-place density. Sand was filled to a specific level, then the pile was placed on the sand surface, and then sand was again added to embed the pile to the ground surface. Load tests were conducted on the piles with instrumentation that allowed the determination of load carried in side resistance and load carried in end bearing. Vesic conducted several tests to vary the soil density, pile length, pile size and shape. Vesic also conducted some field tests, which were in agreement with the more extensive laboratory testing program. Results are discussed below for both side resistance and end bearing.

2.2.1 End Bearing Resistance (Vesic, 1967)

Results of model pile tests are shown in Fig. 2.1 to illustrate the effect of soil density and depth on the development of end bearing. Two important observations are as follows: 1) end bearing is affected by the density, or strength, of the soil, and 2) the end bearing capacity increases non-linearly with depth.

Shown in Fig. 2.1 are several curves of end bearing capacity versus depth. The end bearing pressure for loose sand is shown to increase linearly with depth to a depth of about 25 inches, and the curve becomes increasingly non-linear at depths greater than 25 inches. The end bearing resistance becomes constant, or nearly constant for depths greater than 45 inches. In summary, the end bearing resistance is shown to increase linearly with depth, but the rate of increase with depth does not stay constant. At some depth, the rate of increase in capacity with depth decreases with the end bearing capacity becoming almost constant with depth.

Piles in soil with greater density, and therefore greater strength, exhibit significantly greater end bearing resistance for any given depth (Fig. 2.1). At a depth of 10 ft, the end bearing pressure for medium dense sand is about 2.5 times greater than end bearing in loose sand, and the bearing pressure for a pile in dense sand is 12 times the end bearing pressure in loose sand. Accordingly, soil density greatly affects the bearing pressure developed at the tip of a pile. Furthermore, the shape of the curve that defines the increase in capacity with depth is affected by soil strength. The transition point where the increase in capacity with depth becomes non-linear gets deeper. Additionally, the depth which the end bearing capacity becomes nearly constant is deeper for stronger soils.

2.2.2 Side Resistance (Vesic, 1967)

The overall trend for side resistance is similar to that observed for end bearing resistance (Fig. 2.2). The two observations made for end bearing are also appropriate for side resistance, namely 1) side resistance is affected by the density, or strength, of the soil, and 2) side resistance increases non-linearly with depth.

Shown in Fig. 2.2 are several curves of side resistance versus depth. The side resistance for loose sand increases linearly with depth to a depth of about 25 inches, and then the curve becomes increasingly non-linear at greater depths. The side resistance becomes constant, or nearly constant for depths greater than 45 inches. Therefore, similar to trends observed for end bearing, the side resistance increases linearly with depth, but the rate of increase with depth is not constant. The rate of increase in side resistance with depth decreases and becomes constant, or nearly constant with depth (Fig. 2.2).

Piles embedded in soil with greater strength (density) exhibit greater unit side resistance at any given depth (Fig. 2.2). At a depth of 10 ft, the unit side resistance for medium dense sand is about 1.7 times greater than unit side resistance in loose sand, and the unit side resistance for a pile in dense sand is 4.8 times that observed in loose sand. Accordingly, soil density greatly affects the unit side resistance developed along the side of the pile. Furthermore, the shape of the curve that defines the increase in unit side resistance with depth is affected by soil strength. The transition point gets deeper where the increase in unit side resistance with depth becomes non-linear. It also appears that the depth which the unit side resistance becomes nearly constant is deeper for stronger soils.

2.2.3 Design Equations for Unit End Bearing and Unit Side Resistance

The classical design equation for piles embedded in sand computes the contribution of unit end bearing and unit side resistance, and then applies these unit values to the end bearing area or surface area of the pile. The design equation for unit end bearing is typically simplified to be proportional to the effective stress at the tip of the pile as follows:

$$q_{eb} = \sigma_v' N_q^* \tag{2.1}$$

where σ_v' is the vertical effective stress at the tip of the pile, N_q^* is a bearing capacity factor. Equation 2.1 identifies a unit end bearing that increases linearly with vertical effective stress. This equation would predict a linear increase in unit end bearing pressure with depth for a pile embedded in a uniform soil with constant unit weight. Obviously, the trend predicted by Eqn. 2.1 are not representative of the unit end bearing with depth observed by Vesic (1967) as discussed above. Vesic observed the unit end bearing to vary non-linearly with depth.

A popular modification to Eqn. 2.1 is to restrict the unit end bearing from getting too large. Accordingly, a limiting end bearing pressure is prescribed, and Eqn. 2.1 is re-written as:

$$q_{eb} = \sigma_v' N_q^* \leq q_{eb\ lim} \tag{2.2}$$

where, $q_{eb\ lim}$ is a limiting unit end bearing pressure. The limiting end bearing pressure depends on the strength of the soil and is greater for higher strength soils.

Equation 2.2 represents a common equation for determining unit end bearing in practice. For uniform soil conditions, this equation predicts a unit end bearing pressure that increases linearly with depth until it reaches a limit value, and then the unit end bearing remains constant for all greater depths. Therefore, this equation models the non-linear increase in unit end bearing with depth, as shown in Fig. 2.1, as a bilinear curve.

Likewise, common design equations for determining the unit side resistance for piles follow similar trends, such as

$$f_s = \sigma_v' K \tan\delta \leq f_{s\,lim} \tag{2.3}$$

where, f_s is the unit side resistance, σ_v' is the effective vertical stress, K is the coefficient of lateral earth pressure, and may be a function of the volume of soil displaced during insertion. δ is the interface friction angle between the pile and soil, and $f_{s\ lim}$ is the upper limit for unit side resistance for the soil/pile interface. The value of $f_{s\ lim}$ will vary with soil strength. Limiting unit side resistance values will be greater for values higher strength soils.

Equation 2.3 models the non-linearity of unit side resistance as shown in Fig. 2.2 as a bilinear relationship of unit side resistance versus depth.

2.2.4 Coyle and Castello (1981)

Coyle and Castello(1981) collected the results of over 24 load tests on piles in sand, separated the contributions by side resistance and end bearing, and determined the effect of soil strength and pile depth on pile capacity. They modeled unit end bearing as defined in Eqn. 2.1 and modeled unit side resistance as defined in equation 2.3, but without prescribing a limit value for unit side resistance.

Coyle and Castello back-calculated values for N_q^* for all the piles in their collection and showed the effect of depth and soil strength on N_q^* (Fig. 2.3). The values of N_q^* are seen to increase with depth to a maximum value and then decrease with depth. The initial increase in N_q^* with depth is due to increasing vertical stress and increasing effect of embedment. However, at a depth ratio (depth/pile diameter) of around 20, C is shown to decrease with depth. The effect of depth is significant. For example (Fig. 2.3), the value of N_q^* is about 100 for a soil with a friction angle equal to 40 degrees at a relative depth of 30 pile diameters. However, the value of N_q^* is only 60 at a depth of 60 diameters. Accordingly, the form of the equation for end bearing as given in Eqn. 2.2 may be too simple and therefore unrepresentative of the variation in unit end bearing with depth.

Coyle and Castello also investigated the effect of soil strength and pile depth on the development of unit side resistance (Fig. 2.4). Knowing the average unit side resistance from their collection of load test results, and the average effective vertical stress along the length of the pile, they determined unit side resistance and back calculated values of Ktanδ using the relationship given in Eqn. 2.3. The resulting values of Ktanδ are seen to decrease significantly with depth. For example (Fig. 2.4), a value of Ktanδ is shown to be 1.1 at a depth of 10 diameters for a soil with a friction angle of 36 degrees. However, a value of Ktanδ at an average depth of 30 diameters is only 0.48 for the same soil. This represents a significant decrease in Ktanδ with depth. Trends shown by Coyle and Castello demonstrate that Eqn. 2.3, with the simple application of a limiting side resistance does not model observations.

2.2.5 Dennis (1982)

Dennis interpreted the results of over 1000 load tests on driven piles and investigated the ability of several different methods for calculating pile capacity. One of the methods was the API method for cohesionless soil, which determines unit side resistance and unit end bearing according to Eqns. 2.2 and 2.3, respectively. Dennis found that the method tended to predict axial load capacity much less than measured pile capacity for short piles, whereas the method predicted capacity better for piles driven to depths greater than 100 ft. He quantified the depth effect by plotting the ratio of calculated/measured capacity versus depth (Fig. 2.5). Some of the piles embedded 20 ft exhibit a ration of calculated/measured capacity equal to 0.2, which means the measured capacity was 5 times greater than the predicted capacity. Accordingly, Dennis reports a significant depth effect for methods that calculate capacity based on Eqns. 2.2 and 2.3.

2.3 DRIVEN PILES IN FINE-GRAINED SOIL

Driving piles into fine grained soils results in displacing the soil around the pile during driving, remolding the soil adjacent to the pile and disturbing the soil to a distance of several pile diameters from the pile. After pile driving stops, excess water pressure generated during installation is allowed to dissipate. Modeling the installation process, the disturbance, the dissipation of pore pressures and the re-consolidation of the soil is complex, and generally not performed in typical highway design for pile foundations. Simple models for predicting unit side resistance and unit end bearing are more typically applied.

Tomlinson (1957) and Tomlinson (1971) developed relationships between unit side resistance and soil strength that are commonly used in pile design. Tomlinson (1957) collected a database of 56 driven piles and back-calculated the unit side resistance. These pile load tests were not instrumented, thus Tomlinson took the end bearing resistance as

$$Q_{eb} = 9 s_u A_P \tag{2.4}$$

where, Q_{eb} is the load in end bearing, s_u is the undrained shear strength for the soil at the tip of the pile, and A_p is the area of the pile at the tip. Tomlinson then subtracted the estimated end bearing capacity from the measured total pile load to back-calculate the load carried in side resistance. The load in side resistance was divided by the surface area of the pile embedded in soil to get an estimate of the unit side resistance. Tomlinson (1957) observed that the unit side resistance increased non-linearly with the average undrained shear strength along the side of the pile, and therefore developed a relationship as shown in Figure 2.6. Tomlinson used the ratio of unit side resistance / undrained soil strength and termed the ratio alpha. The relationship of alpha versus undrained strength is shown in Fig. 2.7. An alpha value of 1.0 corresponds to a unit side resistance equal to the soil strength. Tomlinson observed that alpha values of 1.0 occurred for piles driven into very soft soils. Accordingly, alpha values are seen to equal 1.0 for low strength soil, and alpha values decrease as the strength of the soil decrease. Tomlinson attributed the reduction in alpha to lateral pile displacements that occurred during driving. After driving, soft soils would reconsolidate and re-contact with the sides of the pile and therefore develop good side resistance. However, stiffer soil would be less inclined to re-establish good contact with the pile because the soil was stiff and resistance to movement. Tomlinson looked at effects of depth, but did not have enough information to draw any significant conclusions regarding effects of depth on capacity.

Tomlinson (1971) included more case histories than in his earlier study and investigated depth effects. Tomlinson concluded that for a pile driven into clay with uniform strength, the unit side resistance would be greater with greater with depth. Tomlinson quantified the effect of undrained soil strength and depth on unit side resistance (Fig. 2.8) and also suggested a variation for the alpha value as a function of both soil strength and pile depth (Fig. 2.9).

Some current methods Randolph (API, 1986) relate the alpha value to the ratio of undrained strength to vertical effective stress. It is expected that these proposed relationships are indirect methods to quantify and relate the over-consolidation ratio to the value of alpha. Piles driven into normally consolidated clays would be expected to develop unit side resistance close to the soil strength (alpha = 1.0), whereas stiff clays at shallow depths (overconsolidated clays) would be expected to develop alpha values lower than unity. Accordingly, depth effects are accounted for in Tomlinson (1971) and in methods that use the ratio of undrained strength to effective stress.

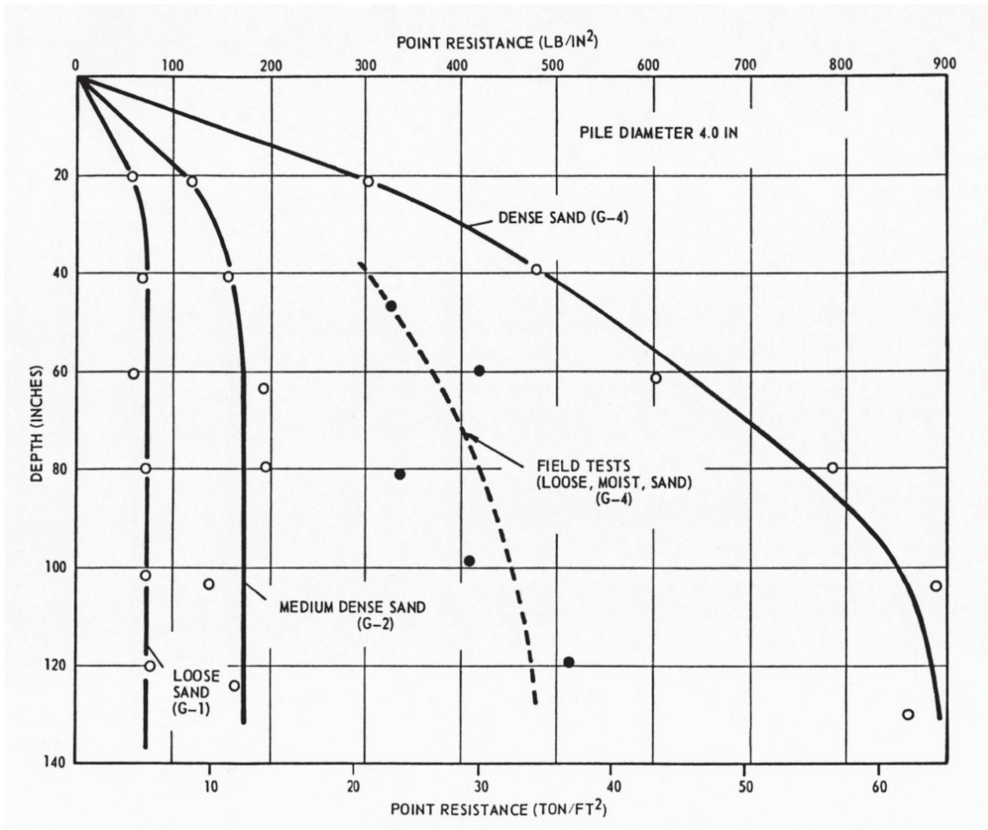

Figure 2.1 Effect of soil density and depth on end bearing resistance (Vesic, 1967)

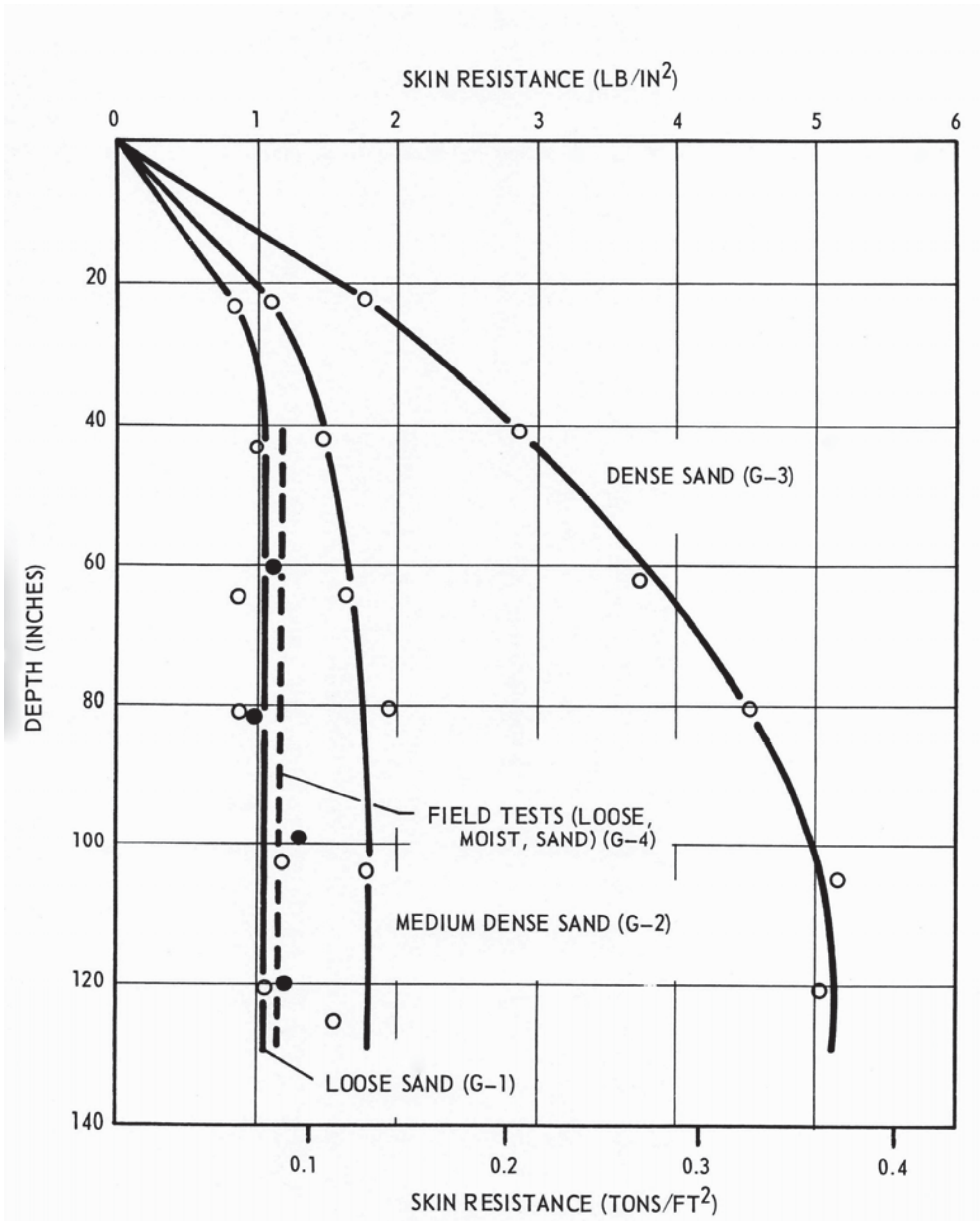

Figure 2.2 Effect of soil density and depth on unit side resistance (Vesic, 1967)

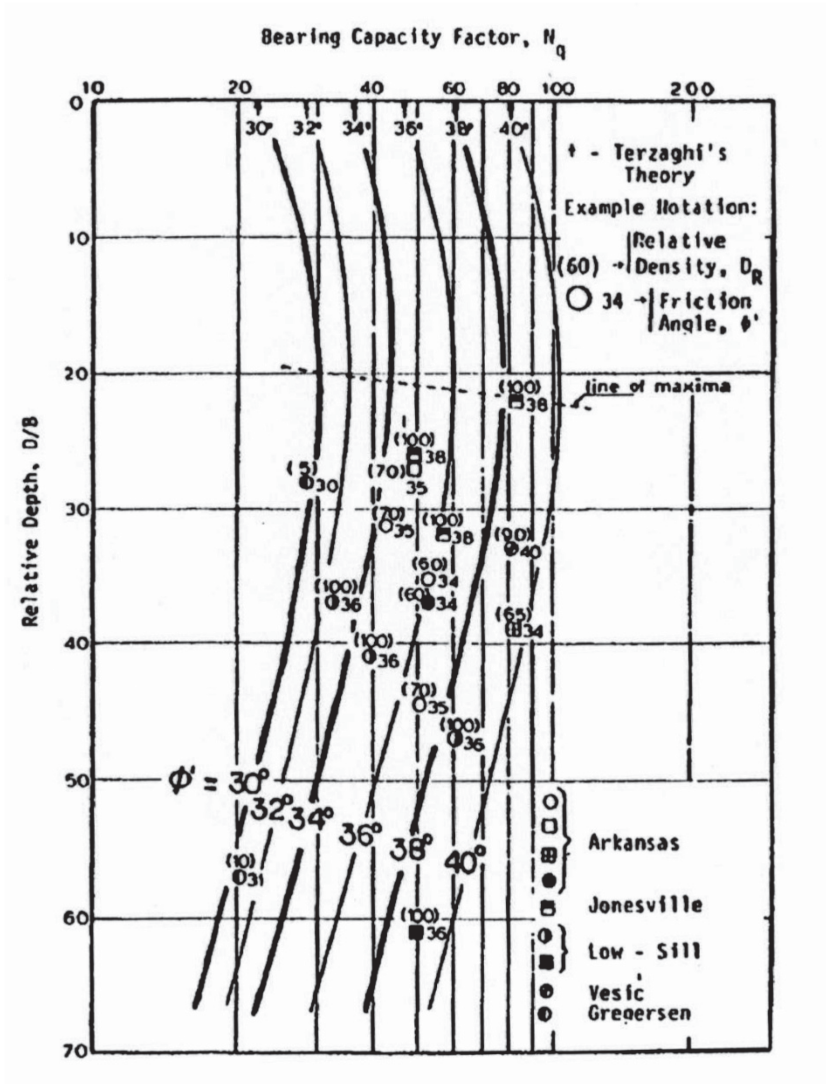

Figure 2.3 Effect of pile depth and soil strength on bearing capacity factor.

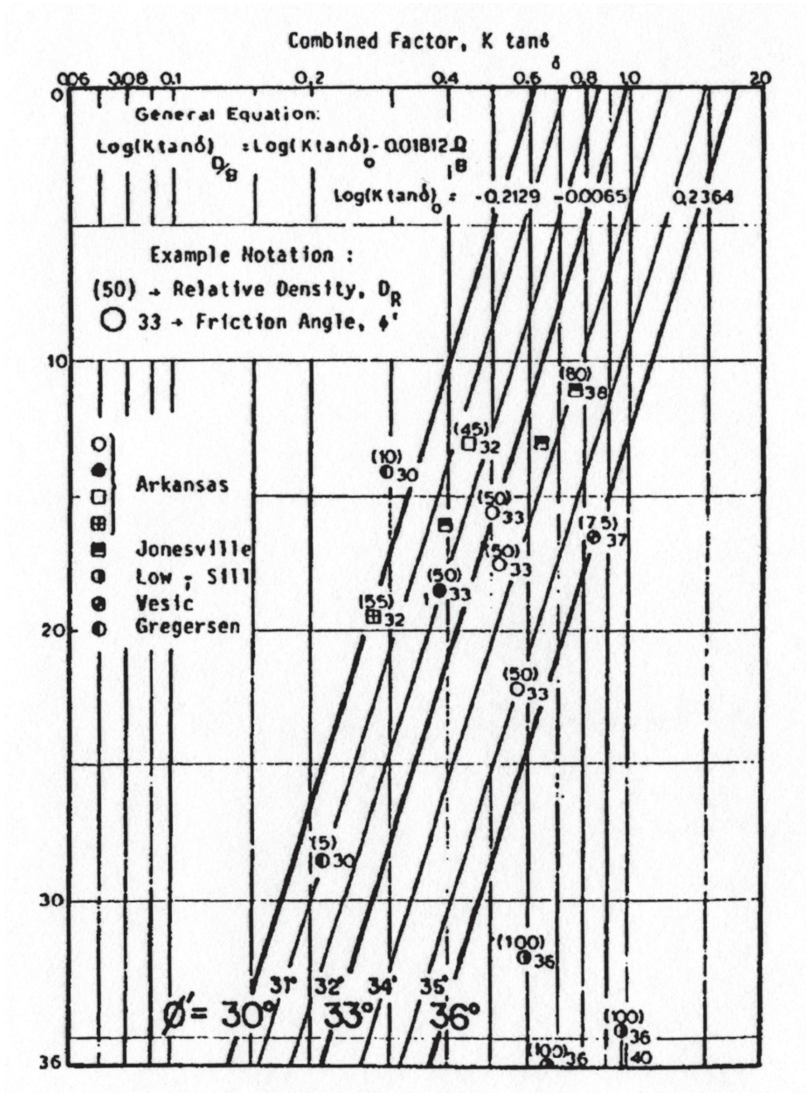

Figure 2.4 Effect of average pile depth and soil strength on Ktanδ.

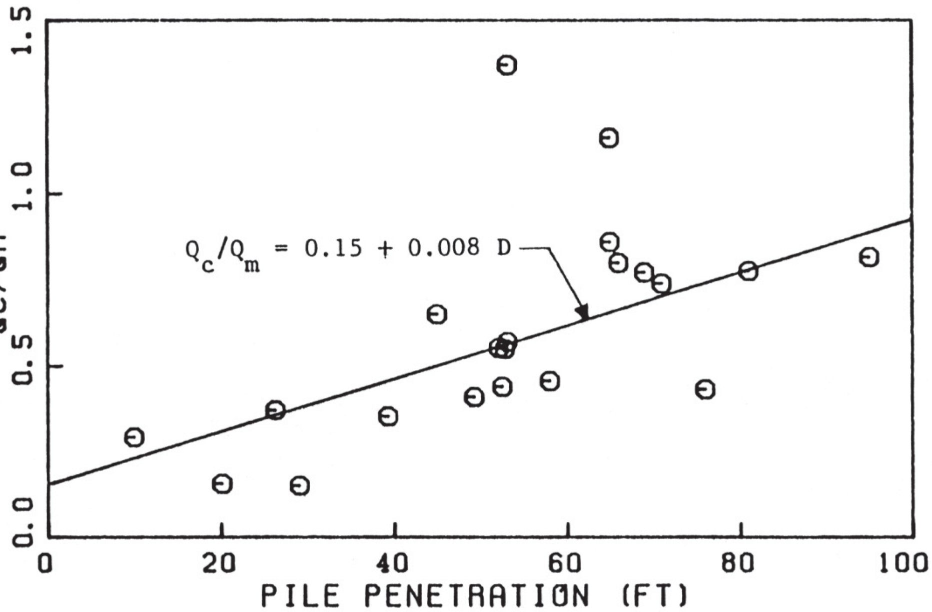

Figure 2.5 Ratio of calculated/measured capacity for piles driven into coarse-grained soils (Dennis, 1982)

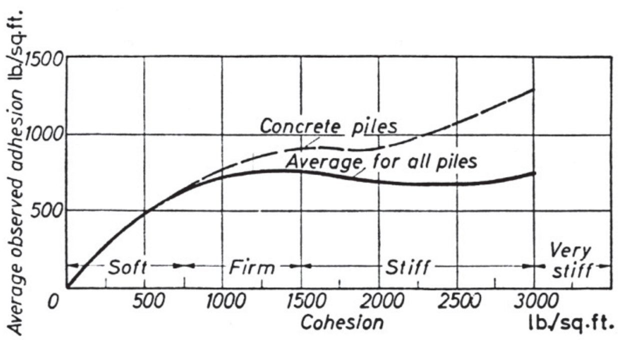

Figure 2.6 Effect of soil strength on unit side resistance (Tomlinson, 1957).

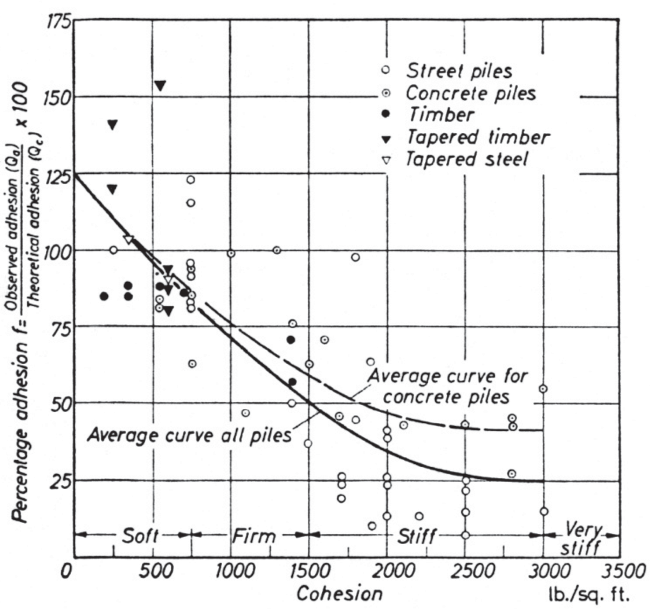

Figure 2.7 Effect of soil strength on alpha factor (Tomlinson, 1957).

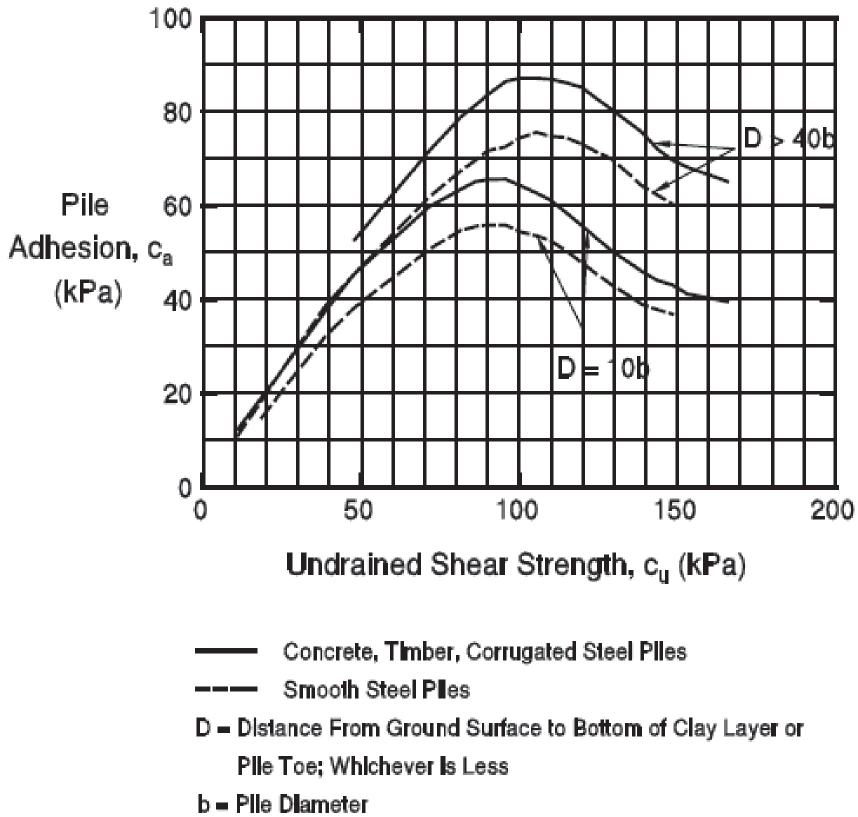

Figure 2.8 Effect of soil strength and depth on unit side resistance (Tomlinson, 1971).

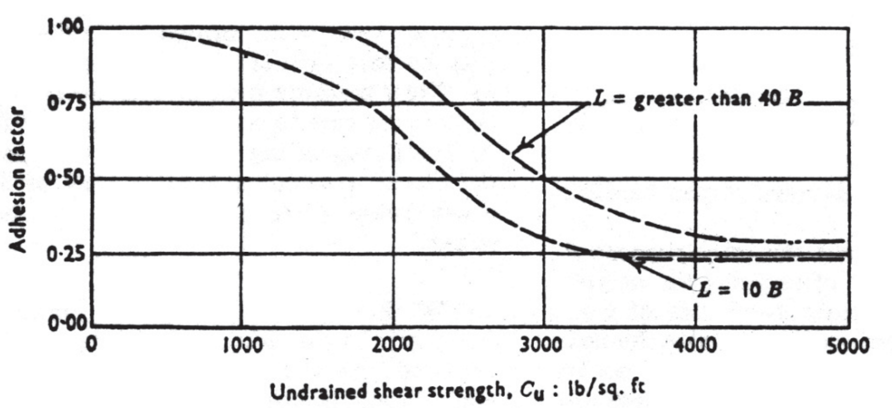

Figure 2.9 Effect of soil strength and depth on alpha factor (Tomlinson, 1971).

3.0 BACKGROUND AND LITERATURE REVIEW - STATISTICS

3.1 INTRODUCTION

The comparison of predicted pile capacity with measured pile capacity, or the comparison of two predicted pile capacities have been a subject of interest to foundation engineers for over a century. Reviewed herein are several studies that have compared capacity using various predictive methods with results from static load tests. Predictive methods include static methods, those that use soil properties and strengths to estimate pile capacity, and methods that estimate pile capacity based on the behavior during pile driving. Some studies have also compared predictions from one method with predictions from another to assess agreement between predictive methods, although these types of studies are less common. Comparative studies provide precedent and perspective for the agreement that should be expected by predictive methods.

Comparisons require the use of a metric capable of quantifying the overall agreement and scatter of the agreement. A metric commonly adopted for quantifying agreement between two methods is the ratio of the value for method 1 to the value of method 2 or mathematically, value 1/value 2. Simple statistical parameters such as mean are used to quantify the overall agreement, while the coefficient of variation is often used to quantify the scatter of the agreement.

3.2 STATIC METHODS

A static method is defined as a method that determines axial pile capacity based on the dimensions of the pile (diameter and length), and the strength of the soil profile in which the pile is embedded. The static methods reported herein have similarities to the methods used by the computer program DRIVEN, which used by Wisconsin DOT.

Briaud and Tucker (1988) compiled the results of 98 pile load tests provided by the Mississippi State Highway department. Each load test was reviewed to provide a soil profile, and pile driving record. Predictions for capacity were investigated using 13 different predictive methods. Two static methods based on the work of Coyle and Castello (1981) and API(1986) were reported and are given in Table 3.1. The mean (μ) for the ratio of predicted to measured capacity for the Coyle and Castello method was reported as 1.19 with a coefficient of variation (cov) equal to 0.66. The API method was reported to have a mean of 0.92 and a cov of 0.58.

Dennis(1982) conducted a study of driven piling to investigate the performance of several static methods. The study collected the results of over 8000 piles, however, only about 1004 were able to be analyzed. About one-third of those piles were steel pipe piles. Static methods that are of interest in this study are the methods developed for driven piles in clay by Tomlinson (1957) and Tomlinson (1970) because these employ alpha-methods similar to the computer program DRIVEN which is used by Wisconsin DOT. The Tomlinson (1957) method was determined to have a mean equal to 0.61 and a cov of 0.53, while the Tomlinson (1971) method exhibited a mean value of 0.97 and a cov of 0.45 as shown in Table 3.1. Static methods for piles driven in sand include the Coyle and Castello (1981) (μ=0.99 and cov = 0.55) method and the API(1986) method (μ=1.00 and cov=0.66). The API method models side resistance and end bearing pressures in a similar manner to methods used in the computer program DRIVEN.

The NCHRP–507 report by Paikowski, et al, (2004) reviewed pile load tests and compared static and dynamic predictions of capacity with static load test values. Of particular interest are the results for pile piles driven in clays, sands, and mixed soil profiles in which capacities were predicted using static methods by Tomlinson (1970) where μ was determined to be 1.95 with a cov of 0.50 for clays. Nordlund's (1963) methods results in μ equal to 0.86 with a cov equal to 0.52 in sand. Combining the analyses of Tomlinson and Nordlund in a manner consistent with DRIVEN resulted in a μ equal to 1.83 and a cov of 0.59 in mixed soils. These results are summarized in Table 3.1.

Coyle and Castello (1981) developed a static method for driven piles in sand. They collected over 24 load test results and developed a method for varying the development of unit side resistance and unit end bearing with depth. Upon completion of the correlation, the method was assessed with (primarily) the same data used to develop the correlations. Accordingly, very good agreement and low scatter was exhibited (μ equal to 1.01 and a cov equal to 0.16) as given in Table 3.1. Other investigators using different collections of pile load test data have found the scatter to be greater.

Long and Anderson (2012) compared the capacity of piles predicted using the computer program DRIVEN with estimates of capacity based on CAPWAP. All CAPWAP estimates were based on restrike behavior of the pile. Typical setup times were greater than 3 days, and often greater than 7 days. The results of comparing pile capacities with DRIVEN indicate a μ of 0.88 with a cov of 0.60 as shown in Table 3.1.

Several different methods have been investigated, reported, and quantified by several different investigators. A common finding is that most of the static methods exhibit a cov between 0.5 and 0.66. A value of cov above 0.5 is considered to represent a high degree of scatter and there are other methods, such as those that estimate capacity based on driving behavior, that typically exhibit less scatter and lower cov.

3.3 DYNAMIC FORMULAE

Dynamic formulae have been developed to account for the relationship between static pile capacity and the resistance a pile exhibits during driving. Dynamic formulae relate the energy being delivered to the pile and its corresponding resistance to penetration to estimate axial pile capacity for a static load. Some dynamic formulae are be based on a simplified model for the pile, pile hammer and energy delivery; however, other dynamic formulae may simply be based on correlation and without theoretical basis. Regardless of their origin, dynamic formulae are characteristically simple to calculate and use simple to record observations necessary to calculate capacity. Over 100 dynamic formulae have been developed, but only a few methods are commonly used. A common dynamic formula used by DOT's in the U.S. is the FHWA-modified Gates formula. Wisconsin DOT currently (2013) uses the FHWA-modified Gates formula. Previously, Wisconsin DOT used a dynamic formula based on the Engineering News Formula.

Flaate (1964) and then later Olson and Flaate (1967) collected static load tests on timber, concrete and steel piles along with information on resistance during pile driving. They investigated seven different dynamic formulae, one of which was the original Gates (1957) method. Capacities predicted using the dynamic formulae were compared with results of static load tests and the original Gates dynamic formulae was determined to be one of the better performing methods. Further improvement to the method was recommended by Olson and Flaate by modifying the original Gates equation by applying a slope and intercept. The FHWA-modified Gates formula is very similar to the Gates equation modified by Olson and Flaate. The original Gates formula exhibited a mean of 0.86 and a cov of 0.45 and these values are shown in Table 3.2. The FHWA-modified Gates applied to this dataset results in a mean of 1.2 and a cov of 0.34 showing significant reduction in scatter compared with the original Gates method. Furthermore, the cov of 0.36 is significantly smaller than cov's determined in previous studies for static methods mentioned in section 3.2.

Fragaszy et al (1989) collected results of 63 pile load tests in which measurements of pile driving resistance were also recorded. They investigated several different methods, of which one was the original Gates (1957) formula. The resulting statistics were a mean of 0.67 with a cov equal to 0.33 and are given in Table 3.2.

The NCHRP-507 report by Paikowski studied a number of dynamic methods including the FHWA-modified Gates formula. Using the results of 135 piles, the resulting mean was found to be 1.20 with a cov equal to 0.53.

Long et al (2009) conducted a study for the Wisconsin DOT in which they collected 156 cases from several different sources and compared static load test capacity with the capacity predicted using several different dynamic formulae. The study found that the FHWA-Gates method predicted capacity with a mean of 1.13 and a cov of 0.42.

Long and Anderson (2012) conducted 37 dynamic load tests in Illinois on driven steel piling. Static load capacity was determined from CAPWAP interpretation of restrike data for each pile. The resulting statistics were a mean of 1.31 and a cov of 0.25 as shown in Table 3.2.

3.4 AGREEMENT BETWEEN DYNAMIC FORMULAE AND STATIC METHOD

Few studies have been conducted to determine the agreement between axial pile capacities estimated using static methods with the axial capacities estimated using dynamic formulae. This is because most comparative efforts have been to take the direct approach and compare predicted capacity with measured capacity. The idea would be to compare static pile capacity with estimates based on static methods, and to independently compare static pile capacity with estimates from dynamic formulae. However, comparing and quantifying the agreement between estimates of capacity based on the static method and the dynamic formula does have merit because it allows the engineer to develop realistic expectations of how accurately driving behavior in the field will be predicted using static methods.

Long, et al (2009) conducted a study for the Illinois DOT in which comparisons were made between estimates of capacity using the computer program DRIVEN and different dynamic formulae. The statistics were developed for 4 distinct datasets: H-piles in sand, H-piles in clay, CIP piles in sand, and CIP piles in clay. Approximately 25 piles were used in each of the 4 datasets to determine the statistics which are given in Table 3.3. Summary statistics were also determined for all the cases considered as one dataset, which resulted in a mean of 0.6 and a cov of 0.6.

The scatter for agreement between DRIVEN and the FHWA-modified gates method is high (cov values around 0.6). For comparison, the cov for estimated capacity using DRIVEN and measured pile capacity was presented in section 3.2 and shown to be between 0.5 and 0.66. The cov for estimates of pile capacity using FHWA-modified Gates and measured pile capacity was presented in section 3.3 and shown to be between 0.33 and 0.42.

Table 3.1 Statistics for Static Methods

Reference	Mean	cov	n	Predictive Method
Briaud and Tucker	1.19	0.66	77	Coyle and Castello (1981)
Briaud and Tucker	0.92	0.58	77	API(1986)
Dennis (1981)	0.61	0.53	72	Tomlinson (1957)
Dennis (1981)	0.97	0.45	72	Tomlinson (1971)
Dennis (1981)	0.99	0.55	87	API (1986)
Dennis (1981)	1.00	0.66	87	Coyle and Castello (1981)
NCHRP-507 Pipe Piles in Clay	1.95	0.50	18	Tomlinson (1971)
NCHRP-507 Pipe Piles in Sand	0.86	0.52	19	Nordlund (1963)
NCHRP-507 Pipe Piles in Mixed	1.83	0.59	13	Tomlinson (1971)/ Nordlund (1963)
Coyle and Castello(1981)	1.01	0.16	22	Coyle and Castello (1981)
Long and Anderson (2012)	0.88	0.60	37	DRIVEN

Table 3.2 Statistics for dynamic formulae

Reference	Mean	cov	n	Soil and Pile
Flaate(1964) Olson and Flaate(1967)	0.86	0.45	116	Original Gates (1957)
Flaate(1964) Olson and Flaate(1967)	1.2	0.34	116	FHWA-modified Gates
Fragaszy et al (1989)	0.67	0.33	63	Original Gates (1957)
NCHRP-507	1.20	0.53	135	FHWA-modified Gates
Long et al (2009)	1.13	0.42	156	FHWA-modified Gates
Long and Anderson (2012)	1.31	0.25	37	FHWA-modified Gates

Table 3.3 Agreement between static method/dynamic formulae
(DRIVEN/FHWA-modified Gates)

Reference	Mean	cov	n	Predictive Method
Long, et al (2009)	0.80	0.70	21	H-piles in sand
Long, et al (2009)	0.40	0.50	25	H-piles in clay
Long, et al (2009)	0.50	0.40	21	CIP piles in sand
Long, et al (2009)	0.60	0.30	25	CIP piles in clay
Long, et al (2009)	0.60	0.60	92	All piles

4.0 DESCRIPTION OF PILE CAPACITY METHODS

4.1 INTRODUCTION

Descriptions for the methods used to estimate driven pile capacity are given herein. The method used to determine capacity based on soil properties (static method) is automated in the computer program DRIVEN, which uses Tomlinson's (1971) method for clays, and Nordlund's (1963) and Thurman's (1964) method for piles in sand. Dynamic formulae, specifically the FHWA-modified Gates and the Engineering News formula are described next, and then a brief description is given for determining capacity using the wave equation (WEAP).

4.2 STATIC METHODS - DRIVEN

Static methods calculate pile capacity based on soil strength and soil type. Strength of the soil may be assessed from laboratory or field tests. Strength for fine-grained soils are typically determined from laboratory compression tests and strength for coarse-grained soils are typically determined from the results of tests conducted in the field, such as the Standard Penetration Test (SPT)

DRIVEN is a computer program available through the FHWA that allows the user to estimate conveniently the axial capacity of a pile. The user inputs a soil profile along with soil properties such as unit weight, friction angle or undrained shear strength, and position of the water table. The pile geometry is also input. DRIVEN estimates the capacity of the pile. The user can select from several options to relate soil properties to unit side resistance and end bearing. It is typical to select the Tomlinson method for fine-grained soil and Nordlund/Thurman option for coarse-grained soil.

The method used to estimate base capacity of a pile depends on whether the soil is a sand or clay. If a soil is coarse grained, it is considered cohesionless, and DRIVEN determines the base capacity using the following formula, after Thurman (1964):

$$Q_b = A_p \sigma'_{vo} \alpha N'_q \tag{4.1}$$

where A_p is the area of the base of the pile, σ_{vo}' is the effective vertical stress at the tip of the pile, α is a correction factor based on ϕ and the depth/width ratio of the pile (Fig. 4.1), and N_q' is a bearing capacity factor based on ϕ (Fig. 4.1). There is a maximum value for the unit base resistance which is based on Meyerhof's (1976) recommendations (Fig. 4.2).

If the tip of the pile bears on a cohesive layer, the base capacity is determined as:

$$Q_b = 9s_u \cdot A_p \tag{4.2}$$

where s_u is the undrained shear strength of the soil at the pile tip.

The unit side resistance is determined on a layer-by-layer basis, and different formulae are used depending on whether the layer is cohesive or cohesionless. For a cohesionless soil, DRIVEN uses a formula based on Nordlund (1963, 1979). The unit side capacity of the pile is determined by:

$$f_s = K_\delta C_f \sigma'_{vo} \sin\delta \tag{4.3}$$

Where δ is the pile-soil interface friction angle, K_δ is the coefficient of lateral earth pressure against the side of the pile and is determined as a function of pile size and ϕ (Fig. 4.3). The term, C_f, is a correction to K_δ when ϕ is not equal to δ (Figs. 4.4 and 4.5). The total side capacity is then determined by integrating f_s along the surface area of the pile.

There is no maximum value of skin friction applied when computing pile capacity, and the unit side capacity becomes unreasonably large for high ϕ values. Accordingly, recommendations in the DRIVEN user's manual recommend the friction angle for granular soils be limited to 36 degrees or less. DRIVEN will allow the user to override the limit and use friction angles that exceed 36 degrees when the user determines higher strengths are necessary.

The unit side resistance is determined using Tomlinson's (1971) α-Method when a cohesive layer is in contact with the pile sides. The unit side resistance is estimated as a proportion of the undrained strength,

$$f_s = \alpha \cdot s_u \tag{4.4}$$

where α is an empirical coefficient that varies with undrained soil strength and with relative depth (Fig 4.6).

4.3 DYNAMIC METHODS

Two dynamic methods were used for predicting pile capacity. These methods use data recorded during the driving of a pile to determine its capacity. The most important parameters for these methods are the energy delivered to the pile due to the weight and drop of the pile hammer and the number of blows to drive the pile a given distance at the end-of-driving. Two dynamic methods are considered in this study: the

Wisconsin DOT-Modified Engineering News Formula (EN), and the FHWA-modified Gates Formula.

4.3.1 Original and FHWA-modified Gates Method

The original dynamic formula was developed by Gates in 1957 and is as follows:

$$Q_u = \left({}^{6}/_{7}\right)\sqrt{eE}\ \log\left({}^{10}/_{s}\right) \tag{4.5}$$

where Q_u is the ultimate pile capacity (tons), E is the energy of pile driving hammer (ft-lb), e is the efficiency of hammer (0.75 for drop hammers, and 0.85 for all other hammers, or efficiency given by manufacturer), and s is the pile set per blow (inches). A factor of safety equal to 3 was recommended by Gates to determine the allowable bearing capacity.

The Federal Highway Administration has modified Gates' original equation and recommends the following:

$$Q_u = 1.75\sqrt{WH}\ \log(10N) - 100 \tag{4.6}$$

where Q_u is the ultimate pile capacity in kips, W is the weight of hammer in pounds, H is the drop of hammer in feet, and N is the driving resistance in blows/in. This equation is currently used by Wisconsin DOT.

4.3.2 EN Formula

Although Wisconsin DOT no longer uses the EN formula, a number of cases investigated in this study were installed years earlier at a time when the EN was used by Wisconsin DOT to control pile installation in the field. Accordingly, some discussion is given for the EN formula.

The original Engineering News formula was developed by Wellington in 1892 for timber pile driven with drop hammers. Wellington developed a simple energy balance equation and expressed it as:

$$Q_u = \frac{WH}{s+c} \tag{4.7}$$

where Q_u is the ultimate static pile capacity, W is the weight of hammer, H is the drop of hammer, s is the pile penetration for the last blow and c is a constant (with units of length). Specific values for c depend on the hammer type and may also depend upon the ratio of the weight of the pile to the weight of the hammer ram. However, the original method tends to overpredict capacity.

Most forms of the EN formula used today express the capacity in terms of a safe bearing load, which means there is an implicit factor of safety applied to the estimate. Before 2009, Wisconsin DOT used the following to determine the allowable bearing capacity of a pile:

$$Q_a = \frac{2WH}{s+c} \quad (4.8)$$

where Q_a is the the allowable bearing capacity in kips, W = weight of the hammer in pounds, H = drop of the hammer in feet, s = pile penetration for the last blow and c = 0.2 inches for air/steam and diesel hammers. There is a built-in reduction factor of six in the formula, which means the EN formula predicts an allowable capacity instead of an ultimate capacity.

4.4 WAVE EQUATION ANALYSIS

Wave equation analyses use the one-dimensional wave equation to estimate pile stresses and pile capacity during driving (Goble and Rausche, 1986). Isaacs (1931) first suggested that a one-dimensional wave equation analysis can model the hammer-pile-soil system more accurately than dynamic formulae based on Newtonian mechanics.

Wave equation analyses model the pile hammer, pile, and soil resistance as a discrete set of masses, springs, and viscous dashpots. A finite difference method is used to model the stress-wave through the hammer-pile-soil system. The basic wave equation is:

$$E_p \frac{\partial^2 u}{\partial x^2} - \frac{S_p}{A_p} f_s = \rho_b \frac{\partial^2 u}{\partial t^2} \quad (4.9)$$

Where E_p is the modulus of elasticity of the pile, u is the axial displacement of the pile, x is the distance along axis of pile, S_p is the pile circumference, A_p is the pile area, f_s is the frictional stress along the pile, ρ_b is the unit density of the pile material, and t is time.

Wave equation analyses may be conducted before piles are driven to assess the behavior expected for the hammer-pile selection. Wave equation analyses provide a rational means to evaluate the effect of changes in pile properties or pile driving systems on pile driving behavior and driving stresses (FHWA, 1995). Furthermore, better estimates of pile capacity and pile behavior have been reported if the field measurement of energy delivered to the pile is used as a direct input into the analyses (FHWA, 1995).

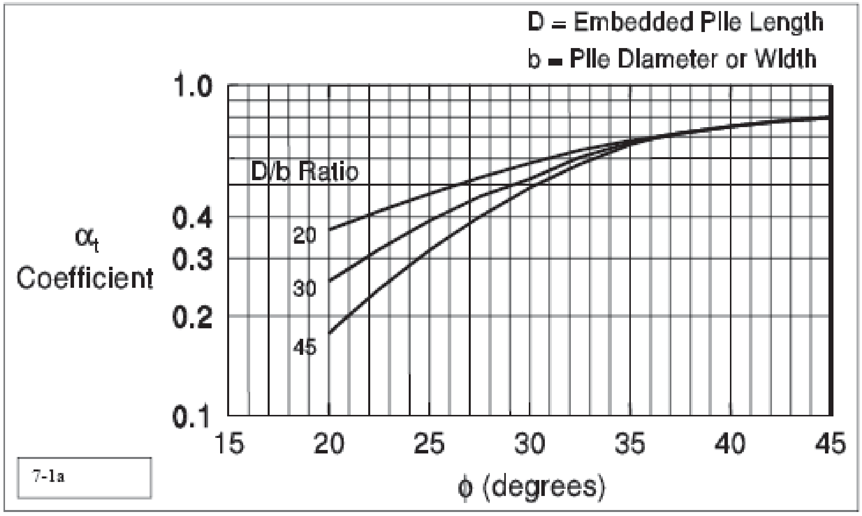

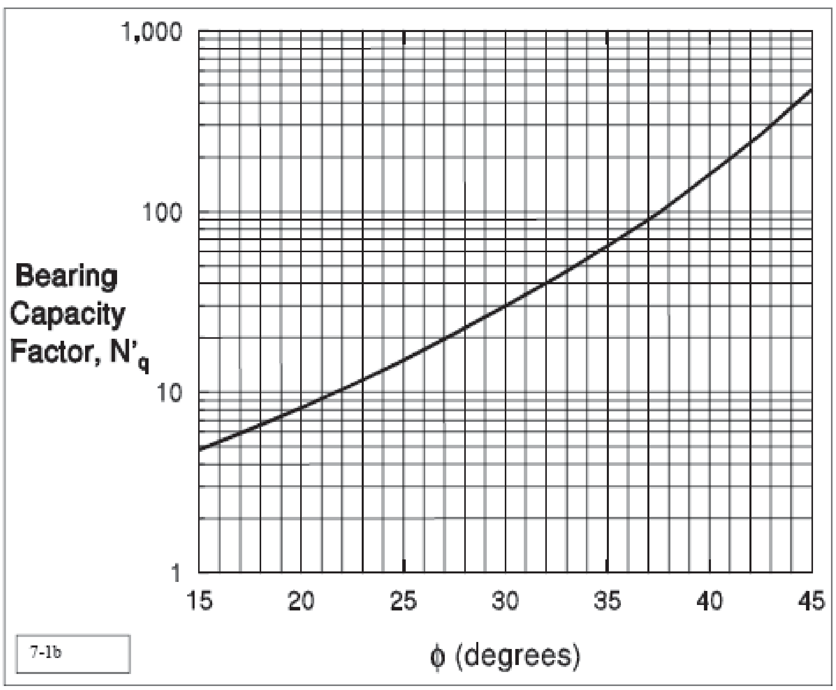

Figure 4.1. Charts for determining α_t and N_q' for DRIVEN (DRIVEN Manual).

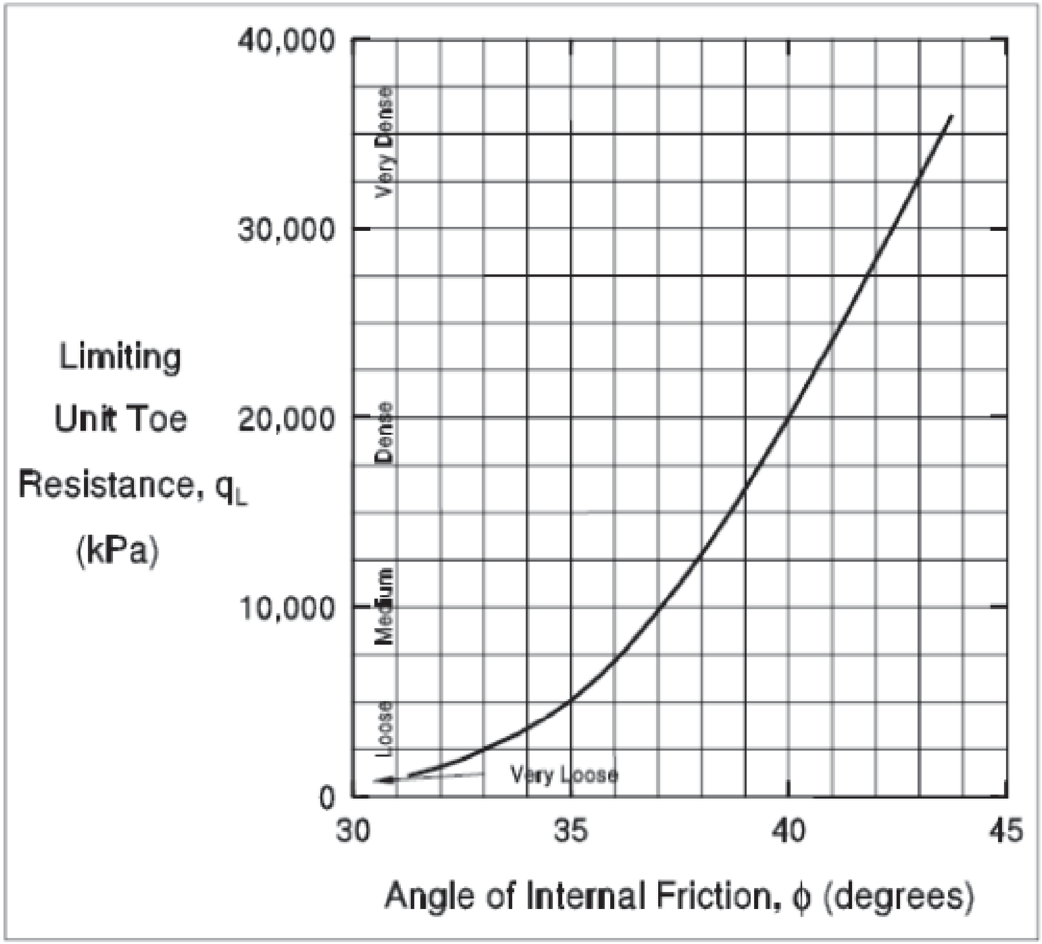

Figure 4.2. Limiting values of unit base capacity for DRIVEN.

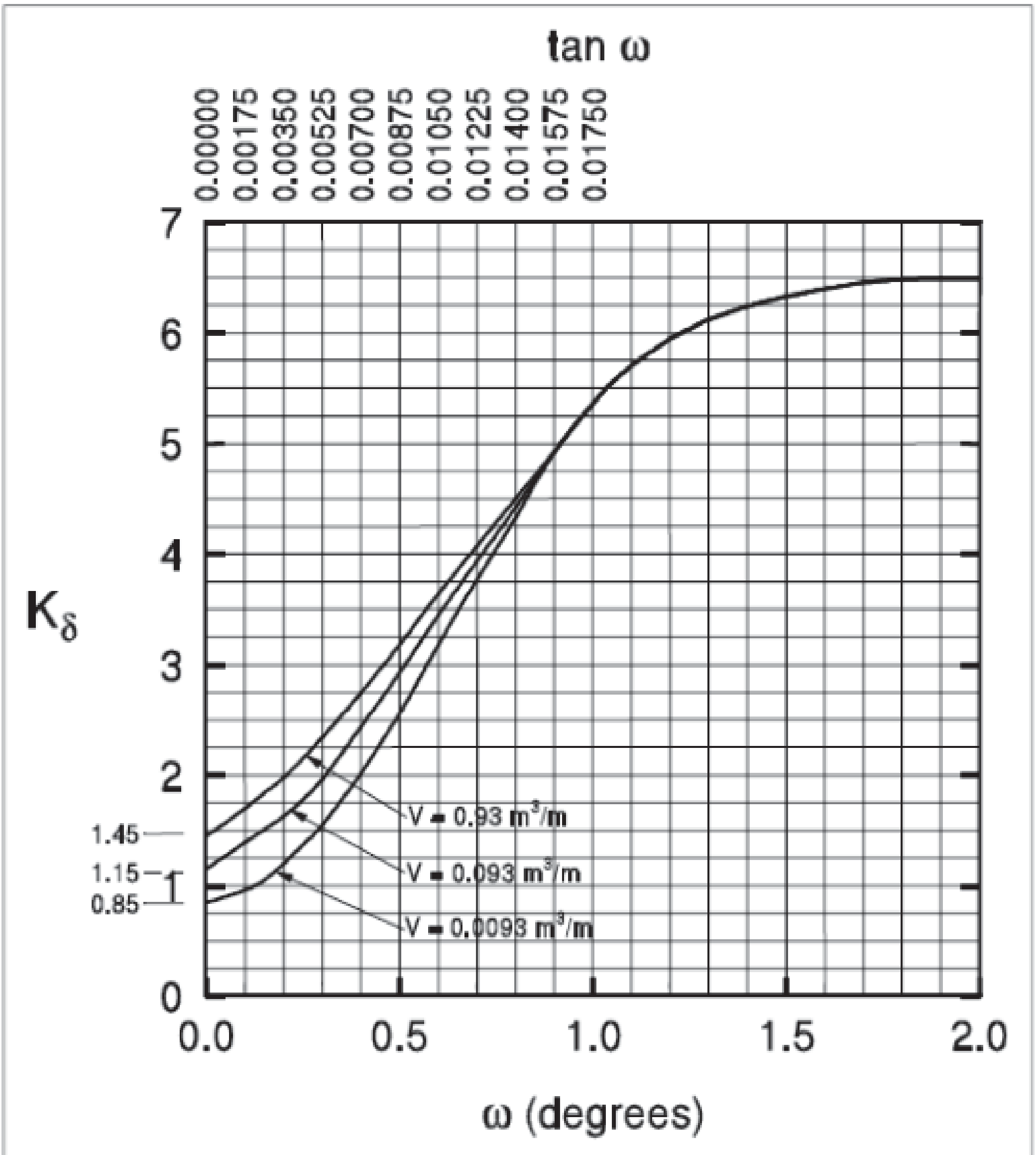

*Note that this applies only to soil where ϕ = 30°, other charts are available for different values of ϕ, and ω is the taper of the pile ($\omega = 0$ for straight piles).

Figure 4.3. Design Curves for determining K_δ (DRIVEN Manual).

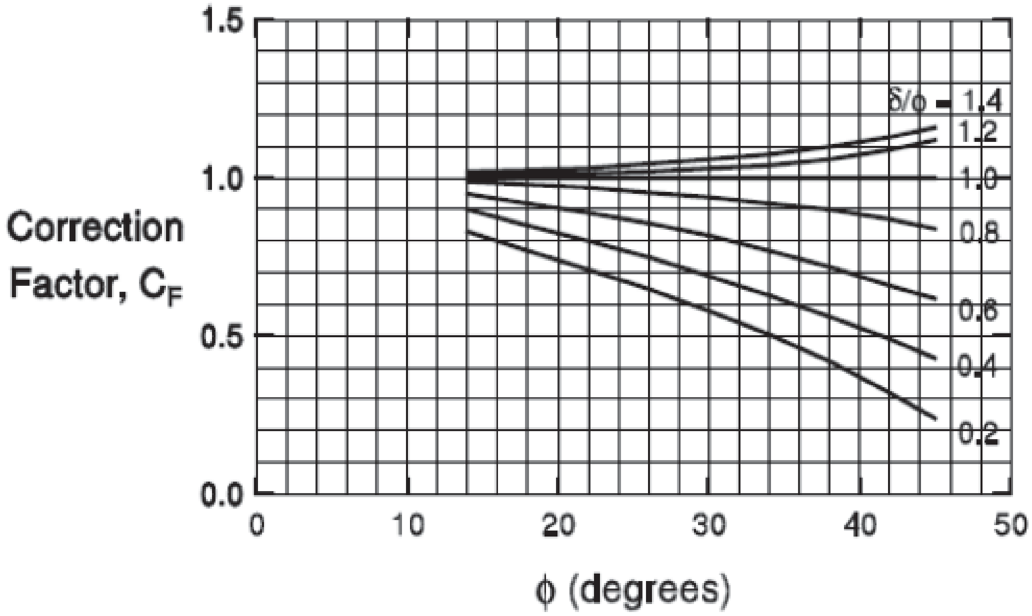

Figure 4.4. Correction Factor for $\delta \neq \phi$ (DRIVEN Manual).

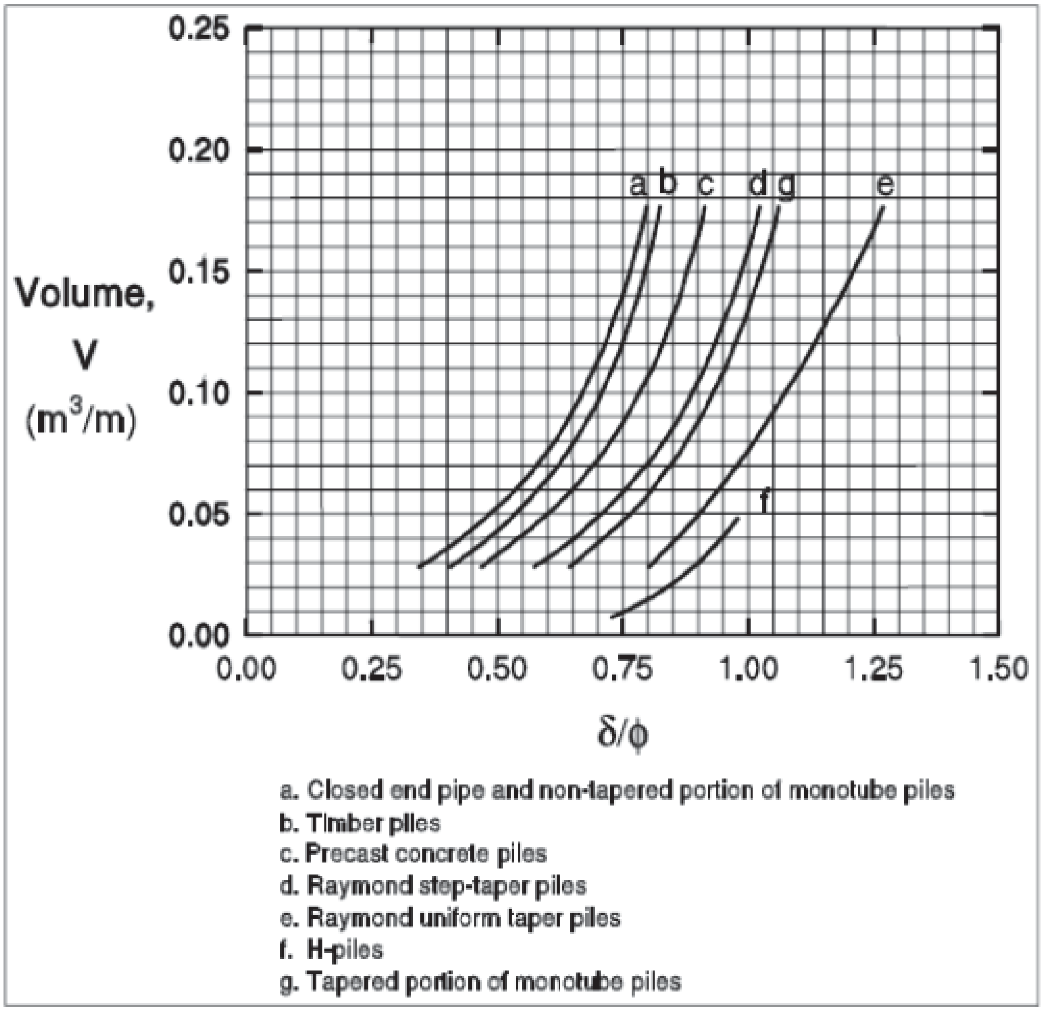

Figure 4.5. Chart for determining δ/ϕ (DRIVEN Manual).

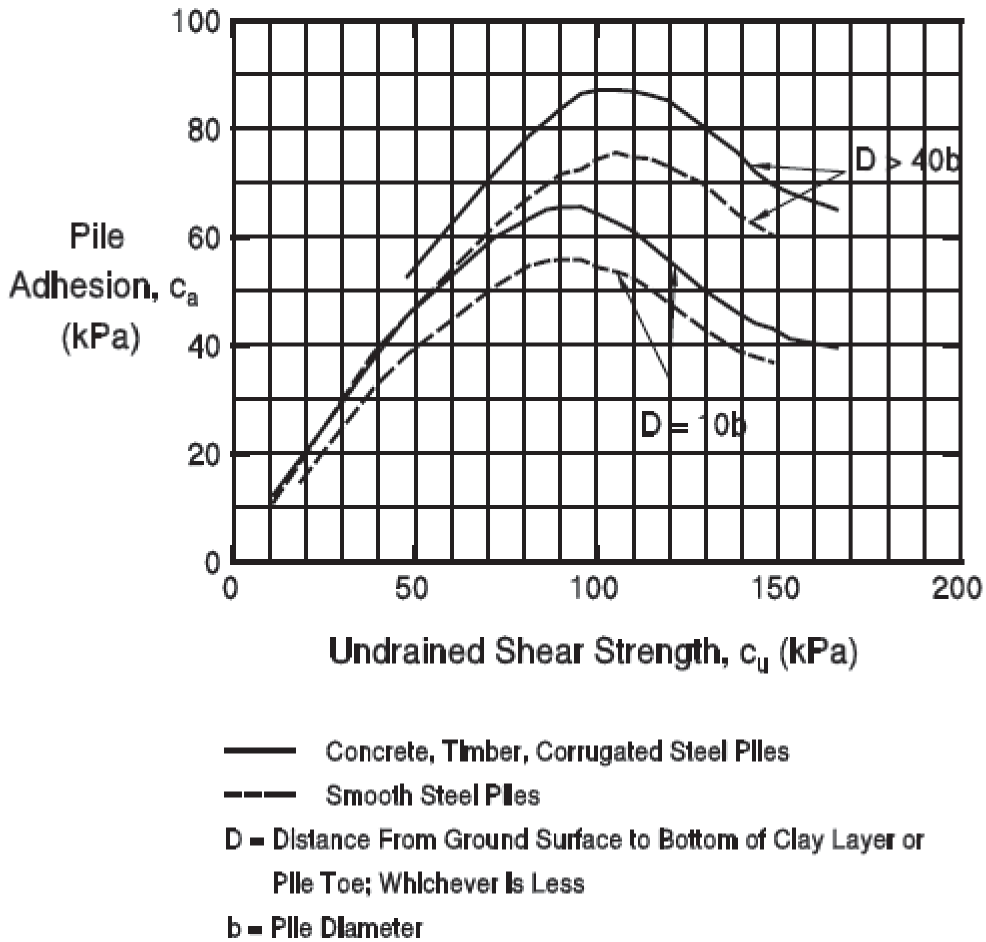

Figure 4.6. Adhesion values for Tomlinson's α-method (1979) (DRIVEN Manual).

5.0 DATA COLLECTION

5.1 INTRODUCTION

Information was collected and interpreted for 182 cases from the bridge files of the Wisconsin Department of Transportation. Information for each case typically included the bridge design plans, soil boring logs, pile driving logs, and a site Investigation Report. Information collected for each case included detail for the soil profile, pile, hammer, and pile driving resistance, from which estimates were made of the capacity of the pile from dynamic and static methods. Penetration lengths of the pile in the field were recorded as well as lengths necessary to develop capacity according to the static method used in the computer program, DRIVEN.

5.2 CHARACTERISTICS OF THE COLLECTION

Characteristics for 182 driven pile cases at 63 different sites in Wisconsin are presented herein. Given in Table 5.1 are details of the location, bridge structure number, location of the substructure, and pile number for each case. Table 5.2 provides summary details of for the soil encountered at each site, with information on the primary soil along the side of the pile, the soil at the tip of the pile, the soil strength at the tip of the driven pile, and the vertical effective stress at the tip of the pile. Pile and Pile hammer details for each case are given in Table 5.3. Information about the pile geometry such as diameter, thickness, and driven length are provided. The model and manufacturer of the pile hammer used at the site is given, along with details such as the ram weight, and the stroke height of the hammer at the end of driving. Also provided is the resistance of the pile at the end of driving. Table 5.4 summarizes the capacity estimated with the static method used in the computer program DRIVEN assuming the soil profile as determined from the soil exploration, the capacity estimated with DRIVEN, but assuming a limiting value of 36 degrees for the soil profile. Also included are estimates of capacity using different dynamic formulae, such as the EN formula historically used by Wisconsin DOT, the FHWA-modified Gates method that is currently used by Wisconsin DOT, and estimates of capacity based on the wave equation (WEAP). Included on the last column of Table 5.4 are estimates of pile capacity after applying a correction factor for overburden stress that is described in detail in the next chapter.

All of the piles in the collection were cast-in-place (CIP) piles. These piles are closed-ended pipe sections with a wall thickness of 0.5 inch or less. They are driven as steel sections, and then filled with concrete to improve their structural stiffness and capacity. Most of the piles had an outside diameter of 14 inches, but diameters ranged from 10.75 to 16 inches (Table 5.5). The driven length of piles varied from about 6 ft to about 144 ft. A cumulative distribution plot for pile length is shown in Fig. 5.1. The median depth of penetration is about 80 ft. and approximately 75 percent of the piles were driven to lengths between 20 and 100 ft.

All piles in this collection were driven with open-ended diesel hammers. Table 5.6 lists all the pile hammers used in the collection, and the number of times it was used. The smallest hammer used was a Delmag D-12 and the largest hammer used was a Delmag D30-32. The Delmag D30-32 was used for 113 cases, making it the most used hammer in the collection.

Piles were driven until the requirements for pile capacity were met. Piles driven before 2009 typically followed the EN pile driving formula, whereas piles driven after 2009 were driven using the FHWA-modified Gates formula. The FHWA-modified Gates method is used herein as a metric for identifying pile capacity in the field because it is currently being used by Wisconsin DOT. Shown in Fig. 5.2 is a cumulative distribution plot for pile capacity. The median pile capacity is about 620 kips but varies from about 240 kips to 800 kips. Seventy percent of the piles exhibit a capacity between 400 and 700 kips, and 46 percent of the piles were driven to capacities between 600 and 720 kips.

Seventy-five percent of the piles developed less than 30 percent of their total load in end bearing (Fig. 5.3) as determined from the computer program DRIVEN (with 36 degree limit imposed). This means the 70 percent the piles develop a significant portion of their capacity from side resistance. Less than five percent of the piles develop more than 70 percent of their capacity from end bearing (according to the computer program, DRIVEN). Therefore, the majority of the piles in this collection are classified as friction piles.

A higher percentage of pile capacity in this collection is developed in sand, or coarse-grained soil (Fig. 5.4). Thirty-two percent of the piles in the collection developed more than 70 percent of pile capacity in sand, whereas only 10 percent of the piles developed 70 percent or more of it capacity in clay. Overall, 40 percent of capacity was developed in fine-grained soil while 60 percent of pile capacity was developed in coarse-grained soil. About 25 percent of the piles developed all their capacity in sand.

5.3 SOIL PROPERTIES

Soil properties were determined using methods consistent with current Wisconson DOT practice and with the computer program DRIVEN. Coarse-grained soils were assigned a friction angle based on the standard penetration test (SPT) result, and the effective stress of the soil at the position of the SPT.

The friction angle was determined from results of the standard penetration test. The standard penetration test value (N_{spt}) is determined as the number of blows required to penetrate a standard split spoon sampler between a penetration of 6 inches and a penetration of 18 inches. Typical dimension for Nspt is blows per foot (bpf). However, the effective stress in the ground at the level of the test also influences N_{spt}, therefore, the N_{spt} value is corrected for the effect of overburden stress.

$$N_{spt}^{corr} = C_N N_{spt} \tag{5.1}$$

Where N_{spt}^{corr} is the corrected standard penetration value, C_N is the correction factor for overburden stress (Fig. 5.5), and N_{spt} is the field value for the standard penetration test. Friction angle for a granular soil is determined from the corrected Nspt value and Table 5.7.

Fine-grained soil was assigned an undrained shear strength based on results of unconfined compression tests, and/or pocket penetrometer tests. Shear strength in very stiff soils were also compared with estimates of shear strength based on standard penetration test results if available.

The unit weight for a soil was determined from information in the soil borings and/or from information provided in the soil reports. For fine grained soil, unit weights were determined by interpreting the results of water content, or from reported values in soil reports. Unit weights for granular soils were determined from soil reports, or from Nspt values (Table 5.8).

Position of the groundwater table were commonly reported in the soil boring logs, and also in the soil reports. The bridge structures commonly were crossing over water, and the groundwater table was near the ground surface.

Table 1. Pile Data - Location and Soil Characteristics

RefNo	Site	Structure Number	Location	Pile #
1	Dodgeville	B-56-165	S. Abutment	1
2	Dodgeville	B-56-165	N. Abutment	1
3	Dodgeville	B-56-165	Pier 1	3
4	Dodgeville	B-56-165	Pier 2	5
5	Dodgeville	B-56-165	Pier 3	9
6	Dodgeville	B-56-165	Pier 4	4
7	Dodgeville	B-56-165	Pier 5-6	3-4
8	Dodgeville	B-56-165	Pier 1	4
9	Dodgeville	B-56-165	Pier 5-6	5
10	Dane Co. 534	B-13-534	N. Abutment	3
11	Dane Co. 534	B-13-534	S. Abutment	1
12	Dane Co. 533	B-13-533	W. Abutment	8
13	Dane Co. 533	B-13-533	E. Abutment	8
14	Eau Claire - 177	B-18-177	W. Abutment	5
15	Eau Claire - 177	B-18-177	E. Abutment	10
16	Eau Clare - 177	B-18-177	E. Abutment	11
17	Dane 520/521	B-13-520/521	N. Abutment	2
18	Dane 520/521	B-13-520/521	N. Abutment	1
19	Dane 520/521	B-13-520/521	S. Abutment	6
20	Dane 520/521	B-13-520/521	S. Abutment	4
21	Dane 531/532	B-13-531/532	N. Abut (531)	33
22	Dane 531/532	B-13-531/532	N. Abut (532)	23
23	Dane 531/532	B-13-531/532	S. Abut (531)	34
24	Dane 531/532	B-13-531/532	S. Abut (532)	32
25	Eau Claire - 176	B-18-176	Pier	2
26	Eau Claire - 176	B-18-176	E. Abutment	4
27	Dane 529/530	B-13-529-530	N. Abutment	37
28	Dane 529/530	B-13-529-530	N. Abutment	22
29	Dane 529/530	B-13-529-530	S. Abutment	33
30	Dane 529/530	B-13-529-530	S. Abutment	24
31	Dane 529/530	B-13-529-530	S. Abutment	36
32	Jacksonville	B-28-152	Pier 1	3
33	Jacksonville	B-28-152	Pier 1	5
34	Jacksonville	B-28-152	Pier 1	6
35	Jacksonville	B-28-152	Pier 1	7
36	Jacksonville	B-28-152	Pier 1	12
37	Jacksonville	B-28-152	Pier 2	1
38	Jacksonville	B-28-152	Pier 2	5
39	Jacksonville	B-28-152	Pier 2	10
40	Jacksonville	B-28-152	Pier 2	26

Table 5.1 Pile Data - Location

RefNo	Site	Structure Number	Location	Pile #
41	Jacksonville	B-28-152	Pier 2	33
42	Jacksonville	B-28-152	Pier 3	1
43	Jacksonville	B-28-152	Pier 3	2
44	Jacksonville	B-28-152	Pier 3	13
45	Jacksonville	B-28-152	Pier 3	25
46	Jacksonville	B-28-152	Pier 3	36
47	Jacksonville	B-28-152	Pier 4	8
48	Jacksonville	B-28-152	Pier 4	10
49	Jacksonville	B-28-152	Pier 4	19
50	Jacksonville	B-28-152	Pier 4	25
51	Jacksonville	B-28-152	Pier 4	39
52	Jacksonville	B-28-152	Pier 5	1
53	Jacksonville	B-28-152	Pier 5	12
54	Jacksonville	B-28-152	Pier 5	27
55	Jacksonville	B-28-152	Pier 5	29
56	Jacksonville	B-28-152	Pier 5	19
57	Jacksonville	B-28-152	N. Abutment	2
58	Jacksonville	B-28-152	N. Abutment	3
59	Jacksonville	B-28-152	N. Abutment	16
60	Jacksonville	B-28-152	S. Abutment	3
61	Jacksonville	B-28-152	S. Abutment	10
62	Jacksonville	B-28-152	S. Abutment	11
63	Lacy Road	B-13-615	E. Abutment	5
64	Lacy Road	B-13-615	Pier	3
65	Lacy Road	B-13-615	W. Abutment	19
66	Manitowoc	B-36-187	N. Abutment	1
67	Manitowoc	B-36-188	S. Abutment	1
68	Jefferson	B-28-138	N. Abutment	5
69	Jefferson	B-28-138	N. Abutment	6
70	Jefferson	B-28-138	Pier	5
71	Jefferson	B-28-138	Pier	5
72	Jefferson	B-28-138	S. Abutment	5
73	Jefferson	B-28-138	S. Abutment	6
74	Jefferson	B-28-138	S. Abutment	7
75	Dane	B-13-605	Pier 1	1
76	Dane	B-13-605	Pier 2	4
77	Racine	B-51-102	N. Abutment	4
78	Racine	B-51-102	N. Abutment	10
79	Racine	B-51-102	Pier 1	2
80	Racine	B-51-102	Pier 1	3

Table 5.1 (continued). Pile Data - Location and Soil Characteristics

RefNo	Site	Structure Number	Location	Pile #
81	Racine	B-51-102	Pier 2	2
82	Racine	B-51-102	Pier 2	9
83	Racine	B-51-102	Pier 3	10
84	Racine	B-51-102	Pier 3	11
85	Racine	B-51-102	S. Abutment	1
86	Racine	B-51-102	S. Abutment	6
87	Racine	B-51-103	N. Abutment	8
88	Racine	B-51-103	N. Abutment	12
89	Racine	B-51-103	Pier 1	1
90	Racine	B-51-103	Pier 1	6
91	Racine	B-51-103	Pier 2	3
92	Racine	B-51-103	Pier 2	7
93	Racine	B-51-103	S. Abutment	6
94	Racine	B-51-103	S. Abutment	11
95	Jefferson CoNB STH 26	B-28-146	S. Abut	1
96	Jefferson CoNB STH 26	B-28-146	S. Abut	2
97	Jefferson CoNB STH 26	B-28-146	S. Abut	3
98	Jefferson CoNB STH 26	B-28-146	S. Abut	4
99	Jefferson CoNB STH 26	B-28-146	S. Abut	5
100	Jefferson CoNB STH 26	B-28-146	S. Abut	6
101	Jefferson CoNB STH 26	B-28-146	S. Abut	7
102	Jefferson CoNB STH 26	B-28-146	S. Abut	8
103	Jefferson CoNB STH 26	B-28-146	S. Abut	9
104	Jefferson CoNB STH 26	B-28-146	S. Abut	10
105	Jefferson CoNB STH 26	B-28-146	S. Abut	11
106	Jefferson CoNB STH 26	B-28-146	S. Abut	12
107	Jefferson CoNB STH 26	B-28-146	S. Abut	13
108	Jefferson CoNB STH 26	B-28-146	S. Abut	14
109	Jefferson CoNB STH 26	B-28-146	S. Abut	15
110	Jefferson CoNB STH 26	B-28-146	S. Abut	16
111	Jefferson CoNB STH 26	B-28-146	S. Abut	17
112	Jefferson CoNB STH 26	B-28-146	S. Abut	18
113	Jefferson CoNB STH 26	B-28-146	S. Abut	19
114	Jefferson CoNB STH 26	B-28-146	S. Abut	20
115	Jefferson CoSB STH 26	B-28-147	S. Abut	1
116	Jefferson CoSB STH 26	B-28-147	S. Abut	2
117	Jefferson CoSB STH 26	B-28-147	S. Abut	3
118	Jefferson CoSB STH 26	B-28-147	S. Abut	4
119	Jefferson CoSB STH 26	B-28-147	S. Abut	5
120	Jefferson CoSB STH 26	B-28-147	S. Abut	6

Table 5.1 (continued) Pile Data - Location

RefNo	Site	Structure Number	Location	Pile #
121	Jefferson CoSB STH 26	B-28-147	S. Abut	7
122	Jefferson CoSB STH 26	B-28-147	S. Abut	8
123	Jefferson CoSB STH 26	B-28-147	S. Abut	9
124	Jefferson CoSB STH 26	B-28-147	S. Abut	10
125	Jefferson CoSB STH 26	B-28-147	S. Abut	11
126	Jefferson CoSB STH 26	B-28-147	S. Abut	12
127	Jefferson CoSB STH 26	B-28-147	S. Abut	13
128	Jefferson CoSB STH 26	B-28-147	S. Abut	14
129	Jefferson CoSB STH 26	B-28-147	S. Abut	15
130	Jefferson CoSB STH 26	B-28-147	S. Abut	16
131	Jefferson CoSB STH 26	B-28-147	S. Abut	17
132	Jefferson CoSB STH 26	B-28-147	S. Abut	18
133	Jefferson CoSB STH 26	B-28-147	S. Abut	W1
134	Jefferson CoSB STH 26	B-28-147	S. Abut	W2
135	Jefferson CoSB STH 26	B-28-146	Pier 2	1
136	Jefferson CoSB STH 26	B-28-146	Pier 2	2
137	Jefferson CoSB STH 26	B-28-146	Pier 2	4
138	Jefferson CoSB STH 26	B-28-146	Pier 2	5
139	Jefferson CoSB STH 26	B-28-146	Pier 2	6
140	Jefferson CoSB STH 26	B-28-146	Pier 2	7
141	Jefferson CoSB STH 26	B-28-146	Pier 2	8
142	Jefferson CoSB STH 26	B-28-146	Pier 2	9
143	Jefferson CoSB STH 26	B-28-146	Pier 2	10
144	Jefferson CoSB STH 26	B-28-146	Pier 2	11
145	Jefferson CoSB STH 26	B-28-146	Pier 2	12
146	Jefferson CoSB STH 26	B-28-146	Pier 2	13
147	Jefferson CoSB STH 26	B-28-146	Pier 2	14
148	Jefferson CoSB STH 26	B-28-146	Pier 2	15
149	Jefferson CoSB STH 26	B-28-146	Pier 2	16
150	Jefferson CoSB STH 26	B-28-146	Pier 2	17
151	Jefferson CoSB STH 26	B-28-146	Pier 2	18
152	Jefferson CoSB STH 26	B-28-146	Pier 2	19
153	Jefferson CoSB STH 26	B-28-146	Pier 2	20
154	Jefferson CoSB STH 26	B-28-146	Pier 2	21
155	Jefferson CoSB STH 26	B-28-146	Pier 2	22
156	Jefferson CoSB STH 26	B-28-146	Pier 2	23
157	Jefferson CoSB STH 26	B-28-146	Pier 2	24
158	Jefferson CoSB STH 26	B-28-146	Pier 2	25
159	Jefferson CoSB STH 26	B-28-146	Pier 2	26
160	Jefferson CoSB STH 26	B-28-146	Pier 2	27

Table 5.1 (continued) Pile Data - Location

RefNo	Site	Structure Number	Location	Pile #
161	Jefferson CoSB STH 26	B-28-146	Pier 2	28
162	Jefferson CoSB STH 26	B-28-146	Pier 2	29
163	Sauk and Iowa Co.	B-56-181	East Abut	14
164	Sauk and Iowa Co.	B-56-181	Pier 1	11
165	Sauk and Iowa Co.	B-56-181	Pier 2	11
166	Sauk and Iowa Co.	B-56-181	Pier 3	20
167	Sauk and Iowa Co.	B-56-181	Pier 4	33
168	Sauk and Iowa Co.	B-56-181	Pier 5	22
169	Sauk and Iowa Co.	B-56-181	Pier 6	7
170	Sauk and Iowa Co.	B-56-181	Pier 7	11
171	Sauk and Iowa Co.	B-56-181	Pier 8	17
172	Sauk and Iowa Co.	B-56-181	Pier 9	10
173	Sauk and Iowa Co.	B-56-181	West Abut	13
174	Sauk and Iowa Co.	B-56-181	East Abut	14
175	Sauk and Iowa Co.	B-56-181	Pier 1	11
176	Sauk and Iowa Co.	B-56-181	Pier 2	11
177	Sauk and Iowa Co.	B-56-181	Pier 3	20
178	Sauk and Iowa Co.	B-56-181	Pier 4	33
179	Sauk and Iowa Co.	B-56-181	Pier 5	22
180	Sauk and Iowa Co.	B-56-181	Pier 6	7
181	Sauk and Iowa Co.	B-56-181	Pier 7	11
182	Sauk and Iowa Co.	B-56-181	Pier 8	17

Table 5.2. Pile Data – Soil Characteristics

Ref No.	Primary Side Soil	Primary Tip Soil	Soil Strength (degrees or psf)	Vertical Effective Stress at Tip (psf)
1	Sand	Sand	36	2968
2	Sand	Sand	36	2307
3	Sand	Sand	36	3646
4	Sand	Sand	34	3254
5	Sand	Sand	33	4021
6	Sand	Sand	39	3983
7	Sand	Sand	32	4311
8	Sand	Sand	36	3617
9	Sand	Sand	32	4134
10	Sand	Clay	Su=1700psf	2217
11	Sand	Clay	Su=1700psf	2421
12	Sand	Sand	32	2238
13	Sand	Sand	32	2585
14	Sand	Sand	36	1305
15	Sand	Sand	39	1600
16	Sand	Sand	31	2819
17	Sand	Sand	35	2629
18	Sand	Sand	35	2763
19	Sand	Sand	37	2527
20	Sand	Sand	37	2459
21	Sand	sand	30	2444
22	Sand	Clay	Su=1000psf	3252
23	Sand	Clay	Su=1500psf	2134
24	Sand	sand	30	2119
25	Sand	Sand	32	1245
26	Sand	Sand	32	1082
27	Mix	Clay	Su=1700psf	2060
28	Mix	Clay	Su=1700psf	2123
29	Mix	Clay	Su=1250psf	3776
30	Mix	Clay	Su=2000psf	1788
31	Mix	Clay	Su=1250psf	2167
32	Clay	Sand	33	6099
33	Clay	Sand	33	5928
34	Clay	Sand	33	5984
35	Clay	Sand	33	5984
36	Clay	Sand	33	5665
37	Clay	Sand	39	4756
38	Clay	Sand	39	4569
39	Clay	Sand	39	4756
40	Clay	Sand	39	4819

Table 5.2 (continued) Pile Data - Soil Characteristics

Ref No.	Primary Side Soil	Primary Tip Soil	Soil Strength (degrees or psf)	Vertical Effective Stress at Tip (psf)
41	Clay	Sand	39	5195
42	Clay	Sand	39	4869
43	Clay	Sand	39	4907
44	Clay	Sand	39	4869
45	Clay	Sand	39	4270
46	Clay	Sand	39	4794
47	Clay	Sand	39	4846
48	Clay	Sand	36	4402
49	Clay	Sand	36	4402
50	Clay	Sand	36	3820
51	Clay	Sand	36	4527
52	Clay	Sand	39	4885
53	Clay	Sand	39	5076
54	Clay	Sand	39	3832
55	Clay	Sand	39	3948
56	Clay	Sand	39	4063
57	Sand	Sand	40	2515
58	Sand	Sand	40	3216
59	Sand	Sand	40	3216
60	Clay	Sand	40	6597
61	Clay	Sand	40	6697
62	Clay	Sand	40	6754
63	Sand (IGM)	Sand (IGM)	40	1335
64	Sand (IGM)	Sand (IGM)	40	1375
65	Sand (IGM)	Sand (IGM)	40	1430
66	Clay	Sand	40	1745
67	Clay	Sand	40	1621
68	Sand	Sand	39	3873
69	Sand	Sand	39	4791
70	Sand	Sand	40	2002
71	Sand	Sand	40	1543
72	Sand	Sand	40	2887
73	Sand	Sand	40	2887
74	Sand	Sand	40	2887
75	Sand	Sand	40	2663
76	Sand	Sand	40	2008
77	Sand	Sand	40	2612
78	Sand	Sand	40	2378
79	Sand/Clay mix	Clay	Su=3000psf	2286
80	Sand/Clay mix	Clay	Su=3000psf	2229

Table 5.2 (continued) Pile Data - Soil Characteristics

Ref No.	Primary Side Soil	Primary Tip Soil	Soil Strength (degrees or psf)	Vertical Effective Stress at Tip (psf)
81	Sand	Sand	38	2197
82	Sand	Sand	36	1839
83	Sand	Sand	40	2924
84	Sand	Sand	40	2862
85	Sand	Sand	40	2688
86	Sand	Sand	40	2751
87	Sand	Sand	40	3124
88	Sand	Sand	40	3057
89	Sand	Sand	40	2638
90	Sand	Sand	40	2450
91	Sand	Sand	40	2872
92	Sand	Sand	40	2816
93	Sand	Sand	40	2760
94	Sand	Sand	40	2510
95	Clay	sand	45	6432
96	Clay	sand	45	6510
97	Clay	sand	45	6665
98	Clay	sand	45	6665
99	Clay	sand	45	6665
100	Clay	sand	45	6742
101	Clay	sand	45	6587
102	Clay	sand	45	6587
103	Clay	sand	45	6587
104	Clay	sand	45	6665
105	Clay	sand	45	6665
106	Clay	sand	45	6665
107	Clay	sand	45	6898
108	Clay	sand	45	6820
109	Clay	sand	45	6665
110	Clay	sand	45	6665
111	Clay	sand	45	6820
112	Clay	sand	45	6742
113	Clay	sand	45	6820
114	Clay	sand	45	6975
115	Clay	sand	45	6384
116	Clay	sand	45	6384
117	Clay	sand	45	6384
118	Clay	sand	45	6384
119	Clay	sand	45	6229
120	Clay	sand	45	6229

Table 5.2 (continued) Pile Data - Soil Characteristics

Ref No.	Primary Side Soil	Primary Tip Soil	Soil Strength (degrees or psf)	Vertical Effective Stress at Tip (psf)
121	Clay	sand	45	6229
122	Clay	sand	45	6229
123	Clay	sand	45	6462
124	Clay	sand	45	6462
125	Clay	sand	45	6462
126	Clay	sand	45	6462
127	Clay	sand	45	6462
128	Clay	sand	45	6384
129	Clay	sand	45	6462
130	Clay	sand	45	6384
131	Clay	sand	45	6307
132	Clay	sand	45	6384
133	Clay	sand	45	6617
134	Clay	sand	45	6462
135	Clay	sand	45	5262
136	Clay	sand	45	5332
137	Clay	sand	45	4649
138	Clay	sand	45	4385
139	Clay	sand	45	4019
140	Clay	sand	45	4587
141	Clay	sand	45	5386
142	Clay	sand	45	5394
143	Clay	sand	45	4750
144	Clay	sand	45	4331
145	Clay	sand	45	4120
146	Clay	sand	45	3974
147	Clay	sand	45	4181
148	Clay	sand	45	5138
149	Clay	sand	45	4804
150	Clay	sand	45	4548
151	Clay	sand	45	4354
152	Clay	sand	45	4377
153	Clay	sand	45	3998
154	Clay	sand	45	4046
155	Clay	sand	45	4913
156	Clay	sand	45	4657
157	Clay	sand	45	4478
158	Clay	sand	45	4556
159	Clay	sand	45	4107
160	Clay	sand	45	4066

Table 5.2 (continued) Pile Data - Soil Characteristics

Ref No.	Primary Side Soil	Primary Tip Soil	Soil Strength (degrees or psf)	Vertical Effective Stress at Tip (psf)
161	Clay	sand	45	4127
162	Clay	sand	45	5006
163	Clay	sand, some gravel	39	5006
164	Clay	sand, some gravel	38	7524
165	Clay	sand, some gravel	36	7524
166	Clay	sand, some gravel	34	7524
167	Clay	sand, some gravel	37	7524
168	Clay	sand, some gravel	36	7524
169	Clay	sand, some gravel	36	7524
170	Clay	sand, some gravel	40	7749
171	Clay	sand, some gravel	38	7749
172	Clay	sand, some gravel	36	6433
173	Clay	sand, some gravel	33	5294
174	Clay	sand, tr gravel	39	7442
175	Clay	sand, tr gravel	38	4900
176	Clay	sand, tr gravel	36	6150
177	Clay	sand, tr gravel	34	6625
178	Clay	sand, tr gravel	37	6376
179	Clay	sand, tr gravel	36	6229
180	Clay	sand, tr gravel	36	6129
181	Clay	sand, tr gravel	40	4801
182	Clay	sand, tr gravel	38	5610

Table 5.3 Pile Data - Pile and Hammer Characteristics

Ref No.	Pile Diameter (in)	Pile Thickness (in)	Hammer	Ram Weight (kips)	Stroke Height (ft)	BPF	Driven Penetration (ft)
1	10.75	0.209	D12	2.750	7.0	80	66
2	10.75	0.209	D12	2.750	7.0	80	54
3	16.00	0.500	D30-32	6.615	8.0	45	80
4	16.00	0.500	D30-32	6.615	7.5	48	70
5	16.00	0.500	D30-32	6.615	8.0	45	84
6	16.00	0.500	D30-32	6.615	8.0	44	81
7	16.00	0.500	D30-32	6.615	8.0	45	90
8	16.00	0.500	D30-32	6.615	8.0	45	80
9	16.00	0.500	D30-32	6.615	8.0	43	87
10	10.75	0.219	D19-32	4.190	7.0	21	49
11	10.75	0.219	D19-32	4.190	6.0	21	51
12	10.75	0.219	D19-32	4.190	6.0	40	46
13	10.75	0.219	D19-32	4.190	6.0	39	47
14	10.75	0.219	D16-32	3.520	7.5	43	23
15	10.75	0.219	D16-32	3.520	8.5	40	34
16	10.75	0.219	D16-32	3.520	7.5	45	55
17	10.75	0.365	Ape D19-42	4.190	7.0	38	44
18	10.75	0.365	Ape D19-42	4.190	7.0	36	46
19	10.75	0.365	Ape D19-42	4.190	7.0	37	47
20	10.75	0.365	Ape D19-42	4.190	7.0	42	46
21	10.75	0.219	D19-32	4.190	6.0	50	51
22	10.75	0.219	D19-32	4.190	6.5	40	55
23	10.75	0.219	D19-32	4.190	6.5	56	40
24	10.75	0.219	D19-32	4.190	6.5	40	44
25	12.75	0.219	D19-32	4.190	7.5	32	23
26	12.75	0.219	D19-32	4.190	7.0	48	20
27	10.75	0.219	D19-32	4.190	7.5	44	54
28	10.75	0.219	D19-32	4.190	7.5	44	58
29	10.75	0.219	D19-32	4.190	6.5	60	76
30	10.75	0.219	D19-32	4.190	7.0	40	34
31	10.75	0.219	D19-32	4.190	7.0	55	42
32	14.00	0.375	D30-32	6.600	8.5	80	137
33	14.00	0.375	D30-32	6.600	8.0	69	134
34	14.00	0.375	D30-32	6.600	8.0	69	135
35	14.00	0.375	D30-32	6.600	8.5	60	135
36	14.00	0.375	D30-32	6.600	8.0	69	129
37	14.00	0.375	D30-32	6.600	9.5	69	92
38	14.00	0.375	D30-32	6.600	9.5	60	89
39	14.00	0.375	D30-32	6.600	9.5	80	92
40	14.00	0.375	D30-32	6.600	9.5	69	93

Table 5.3 (continued) Pile Data - Pile and Hammer Characteristics

Ref No.	Pile Diameter (in)	Pile Thickness (in)	Hammer	Ram Weight (kips)	Stroke Height (ft)	BPF	Driven Penetration (ft)
41	14.00	0.375	D30-32	6.600	9.0	96	99
42	14.00	0.375	D30-32	6.600	10.0	69	96
43	14.00	0.375	D30-32	6.600	9.0	69	97
44	14.00	0.375	D30-32	6.600	9.0	80	96
45	14.00	0.375	D30-32	6.600	9.0	69	84
46	14.00	0.375	D30-32	6.600	10.0	96	94
47	14.00	0.375	D30-32	6.600	9.0	69	94
48	14.00	0.375	D30-32	6.600	10.0	60	87
49	14.00	0.375	D30-32	6.600	9.5	60	87
50	14.00	0.375	D30-32	6.600	9.0	69	77
51	14.00	0.375	D30-32	6.600	9.0	69	89
52	14.00	0.375	D30-32	6.600	10.0	69	95
53	14.00	0.375	D30-32	6.600	9.0	96	98
54	14.00	0.375	D30-32	6.600	10.0	69	77
55	14.00	0.375	D30-32	6.600	9.5	69	79
56	14.00	0.375	D30-32	6.600	9.5	64	81
57	14.00	0.375	D30-32	6.600	10.0	32	50
58	14.00	0.375	D30-32	6.600	10.5	53	62
59	14.00	0.375	D30-32	6.600	9.5	48	62
60	14.00	0.375	D30-32	6.600	8.5	48	141
61	14.00	0.375	D30-32	6.600	9.5	44	143
62	14.00	0.375	D30-32	6.600	9.0	44	144
63	12.75	0.375	D19-32	4.190	8.5	87	11
64	12.75	0.375	D19-32	4.190	9.0	72	7
65	12.75	0.375	D19-32	4.190	8.0	60	15
66	10.75	0.219	D16-32	3.300	6.5	44	24
67	10.75	0.219	D16-32	3.300	6.5	42	26
68	12.75	0.375	D30-32	6.600	8.0	42	43
69	12.75	0.375	D30-32	6.600	7.0	46	57
70	12.75	0.375	D30-32	6.600	7.5	46	33
71	12.75	0.375	D30-32	6.600	8.0	46	26
72	12.75	0.375	D30-32	6.600	8.0	32	46
73	12.75	0.375	D30-32	6.600	8.0	38	46
74	12.75	0.375	D30-32	6.600	8.0	32	46
75	10.75	0.250	D19-32	2.750	7.5	49	47
76	10.75	0.250	D19-32	2.750	6.5	103	35
77	10.75	0.250	D25-32	5.510	8.5	19	50
78	10.75	0.250	D25-32	5.510	9.0	18	46
79	12.75	0.500	D25-32	5.510	8.5	47	41
80	12.75	0.500	D25-32	5.510	9.0	42	40

Table 5.3 (continued) Pile Data - Pile and Hammer Characteristics

Ref No.	Pile Diameter (in)	Pile Thickness (in)	Hammer	Ram Weight (kips)	Stroke Height (ft)	BPF	Driven Penetration (ft)
81	12.75	0.500	D25-32	5.510	9.5	39	43
82	12.75	0.500	D25-32	5.510	9.0	42	37
83	12.75	0.500	D25-32	5.510	9.0	60	53
84	12.75	0.500	D25-32	5.510	9.0	60	52
85	10.75	0.250	D25-32	5.510	9.5	28	49
86	10.75	0.250	D25-32	5.510	9.0	38	50
87	10.75	0.250	D25-32	5.510	9.0	18	54
88	10.75	0.250	D25-32	5.510	8.5	19	53
89	12.75	0.500	D25-32	5.510	8.5	50	50
90	12.75	0.500	D25-32	5.510	8.0	44	47
91	12.75	0.500	D25-32	5.510	8.0	60	51
92	12.75	0.500	D25-32	5.510	8.0	70	50
93	10.75	0.250	D25-32	5.510	8.0	25	51
94	10.75	0.250	D25-32	5.510	7.0	24	47
95	14.00	0.375	D30-32	6.600	9.0	69	97
96	14.00	0.375	D30-32	6.600	10.0	80	98
97	14.00	0.375	D30-32	6.600	8.5	69	100
98	14.00	0.375	D30-32	6.600	9.0	80	100
99	14.00	0.375	D30-32	6.600	9.0	80	100
100	14.00	0.375	D30-32	6.600	9.0	69	101
101	14.00	0.375	D30-32	6.600	10.0	60	99
102	14.00	0.375	D30-32	6.600	10.0	80	99
103	14.00	0.375	D30-32	6.600	9.5	69	99
104	14.00	0.375	D30-32	6.600	9.5	60	100
105	14.00	0.375	D30-32	6.600	9.5	80	100
106	14.00	0.375	D30-32	6.600	9.5	60	100
107	14.00	0.375	D30-32	6.600	9.0	69	103
108	14.00	0.375	D30-32	6.600	9.0	69	102
109	14.00	0.375	D30-32	6.600	9.0	80	100
110	14.00	0.375	D30-32	6.600	9.5	69	100
111	14.00	0.375	D30-32	6.600	9.0	120	102
112	14.00	0.375	D30-32	6.600	9.0	69	101
113	14.00	0.375	D30-32	6.600	9.0	69	102
114	14.00	0.375	D30-32	6.600	9.5	69	104
115	14.00	0.375	D30-32	6.600	10.0	60	101
116	14.00	0.375	D30-32	6.600	10.0	60	101
117	14.00	0.375	D30-32	6.600	9.5	80	101
118	14.00	0.375	D30-32	6.600	10.0	69	101
119	14.00	0.375	D30-32	6.600	10.0	69	99
120	14.00	0.375	D30-32	6.600	9.0	69	99

Table 5.3 (continued) Pile Data - Pile and Hammer Characteristics

Ref No.	Pile Diameter (in)	Pile Thickness (in)	Hammer	Ram Weight (kips)	Stroke Height (ft)	BPF	Driven Penetration (ft)
121	14.00	0.375	D30-32	6.600	9.5	69	99
122	14.00	0.375	D30-32	6.600	10.0	60	99
123	14.00	0.375	D30-32	6.600	9.5	80	102
124	14.00	0.375	D30-32	6.600	9.5	80	102
125	14.00	0.375	D30-32	6.600	10.0	80	102
126	14.00	0.375	D30-32	6.600	9.0	60	102
127	14.00	0.375	D30-32	6.600	10.0	80	102
128	14.00	0.375	D30-32	6.600	9.5	80	101
129	14.00	0.375	D30-32	6.600	9.5	60	102
130	14.00	0.375	D30-32	6.600	9.5	69	101
131	14.00	0.375	D30-32	6.600	9.5	80	100
132	14.00	0.375	D30-32	6.600	10.0	69	101
133	14.00	0.375	D30-32	6.600	10.0	53	104
134	14.00	0.375	D30-32	6.600	10.0	120	102
135	14.00	0.375	D30-32	6.600	8.5	69	81
136	14.00	0.375	D30-32	6.600	9.5	60	82
137	14.00	0.375	D30-32	6.600	8.5	96	73
138	14.00	0.375	D30-32	6.600	9.5	69	70
139	14.00	0.375	D30-32	6.600	9.5	60	64
140	14.00	0.375	D30-32	6.600	9.5	80	72
141	14.00	0.375	D30-32	6.600	8.5	80	82
142	14.00	0.375	D30-32	6.600	9.0	60	83
143	14.00	0.375	D30-32	6.600	8.5	69	74
144	14.00	0.375	D30-32	6.600	9.0	60	69
145	14.00	0.375	D30-32	6.600	9.0	69	66
146	14.00	0.375	D30-32	6.600	9.5	60	64
147	14.00	0.375	D30-32	6.600	9.0	69	67
148	14.00	0.375	D30-32	6.600	9.0	80	79
149	14.00	0.375	D30-32	6.600	8.5	69	75
150	14.00	0.375	D30-32	6.600	9.0	69	72
151	14.00	0.375	D30-32	6.600	9.0	60	69
152	14.00	0.375	D30-32	6.600	9.5	60	69
153	14.00	0.375	D30-32	6.600	10.0	80	64
154	14.00	0.375	D30-32	6.600	8.5	69	65
155	14.00	0.375	D30-32	6.600	8.5	80	76
156	14.00	0.375	D30-32	6.600	8.5	69	73
157	14.00	0.375	D30-32	6.600	9.0	60	71
158	14.00	0.375	D30-32	6.600	8.5	69	72
159	14.00	0.375	D30-32	6.600	9.5	60	66
160	14.00	0.375	D30-32	6.600	8.5	69	65

Table 5.3 (continued) Pile Data - Pile and Hammer Characteristics

Ref No.	Pile Diameter (in)	Pile Thickness (in)	Hammer	Ram Weight (kips)	Stroke Height (ft)	BPF	Driven Penetration (ft)
161	14.00	0.375	D30-32	6.600	9.0	60	66
162	14.00	0.375	D30-32	6.600	8.5	69	78
163	12.75	0.375	D19-32	4.190	7.0	78	130
164	12.75	0.375	D19-32	4.190	6.5	120	122
165	12.75	0.375	D19-32	4.190	6.5	120	117
166	12.75	0.375	D19-32	4.190	6.5	130	116
167	12.75	0.375	D19-32	4.190	6.5	120	117
168	12.75	0.375	D19-32	4.190	6.5	137	119
169	12.75	0.375	D19-32	4.190	6.5	160	119
170	12.75	0.375	D19-32	4.190	6.0	117	116
171	12.75	0.375	D19-32	4.190	6.5	96	111
172	12.75	0.375	D19-32	4.190	6.5	91	110
173	12.75	0.375	D19-32	4.190	7.0	74	89
174	12.75	0.375	D19-32	4.190	6.0	69	122
175	12.75	0.375	D19-32	4.190	6.0	43	83
176	12.75	0.375	D19-32	4.190	6.0	38	105
177	12.75	0.375	D19-32	4.190	6.5	70	113
178	12.75	0.375	D19-32	4.190	6.5	44	108
179	12.75	0.375	D19-32	4.190	6.0	43	99
180	12.75	0.375	D19-32	4.190	6.0	37	98
181	12.75	0.375	D19-32	4.190	5.5	32	78
182	12.75	0.375	D19-32	4.190	6.5	30	88

Table 5.4 Pile Capacity Estimates

Ref No.	Eng. News (kips)	FHWA-modifiedGates (kips)	GRL WEAP (kips)	DRIVEN Original (kips)	DRIVEN Limit 36° (kips)	Correction Factor*DRIVEN (kips)
1	110	343	220	161	161	317
2	110	343	236	56	56	203
3	227	534	430	457	389	572
4	221	524	425	235	235	427
5	220	533	370	393	393	501
6	220	526	409	405	405	523
7	227	534	446	425	414	477
8	220	526	420	306	306	463
9	220	526	430	396	386	473
10	76	273	213	69	69	294
11	65	245	180	80	80	270
12	101	322	248	62	62	231
13	99	320	240	82	82	220
14	110	342	225	84	84	419
15	120	361	245	53	49	233
16	113	248	225	92	74	174
17	114	350	290	122	122	302
18	110	343	280	130	130	293
19	112	346	280	163	136	352
20	121	363	295	157	131	357
21	114	349	245	115	49	160
22	109	340	245	152	102	188
23	131	382	265	72	58	273
24	109	340	245	87	39	178
25	104	332	220	53	53	263
26	124	369	260	43	43	215
27	133	385	260	130	130	630
28	133	385	260	146	146	708
29	136	391	245	205	177	252
30	117	356	240	40	40	185
31	140	400	260	73	72	330
32	321	656	373	827	827	689
33	282	606	350	742	742	618
34	282	606	350	803	803	669
35	281	604	353	803	803	669
36	282	607	353	722	722	601
37	334	669	445	866	646	645
38	314	665	430	819	612	646
39	358	699	460	866	646	645
40	334	670	445	883	657	644

Table 5.4 (continued) Pile Capacity Estimates

Ref No.	Eng. News (kips)	FHWA-modifiedGates (kips)	GRL WEAP (kips)	DRIVEN Original (kips)	DRIVEN Limit 36^o (kips)	Correction Factor*DRIVEN (kips)
41	366	711	460	984	730	645
42	352	690	450	847	672	649
43	317	650	420	862	684	653
44	339	678	430	847	672	649
45	317	649	420	439	439	514
46	406	755	474	818	648	640
47	317	649	450	1000	678	659
48	330	664	470	600	600	668
49	314	645	455	600	600	668
50	317	649	455	433	433	599
51	317	649	450	622	622	665
52	352	690	483	848	703	676
53	366	711	473	892	739	674
54	352	690	490	463	463	638
55	334	670	472	477	477	628
56	324	656	467	492	492	620
57	230	541	430	240	240	697
58	326	659	530	671	671	1158
59	279	602	480	671	671	1158
60	249	564	335	766	766	639
61	264	584	350	785	785	655
62	250	566	335	938	938	781
63	211	515	490	252	158	788
64	206	504	366	256	256	1280
65	86	444	330	259	258	1290
66	91	301	220	70	69	329
67	88	296	195	127	127	611
68	217	521	415	538	316	421
69	200	495	380	676	433	428
70	215	516	380	302	145	586
71	229	536	400	220	108	541
72	184	474	370	520	490	1003
73	207	506	388	520	490	1003
74	184	474	370	520	490	1003
75	135	388	275	207	207	475
76	113	352	300	70	42	189
77	113	354	275	220	220	546
78	114	358	280	148	148	461
79	206	503	395	215	150	582
80	204	502	400	214	151	622

Table 5.4 (continued) Pile Capacity Estimates

Ref No.	Eng. News (kips)	FHWA-modifiedGates (kips)	GRL WEAP (kips)	DRIVEN Original (kips)	DRIVEN Limit 36^o (kips)	Correction Factor*DRIVEN (kips)
81	206	505	389	228	228	766
82	204	502	384	135	134	554
83	248	562	414	460	267	550
84	248	562	415	450	262	558
85	167	448	350	272	153	358
86	192	485	360	272	158	356
87	114	358	288	560	174	319
88	113	354	280	555	170	322
89	213	513	391	311	216	528
90	186	475	360	272	195	542
91	220	524	393	164	164	363
92	237	549	405	160	160	367
93	130	385	283	300	177	403
94	110	347	260	265	159	430
95	317	649	380	1372	737	614
96	377	720	427	1398	753	628
97	299	628	362	1449	786	655
98	339	678	397	1449	786	655
99	339	678	397	1449	786	655
100	317	649	380	1475	802	668
101	330	664	403	1424	770	641
102	377	720	427	1424	770	641
103	334	670	400	1424	770	641
104	314	644	384	1449	786	655
105	358	699	410	1449	786	655
106	314	644	384	1449	786	655
107	317	649	380	1526	834	695
108	317	649	380	1501	818	682
109	339	678	397	1449	786	655
110	334	670	400	1449	786	655
111	396	753	421	1501	818	682
112	317	649	380	1475	802	668
113	317	649	380	1501	818	682
114	334	670	400	1552	850	709
115	330	664	403	1475	735	613
116	330	664	403	1475	735	613
117	358	699	410	1475	735	613
118	352	690	413	1475	735	613
119	352	690	413	1424	680	567
120	317	649	380	1424	680	567

Table 5.4 (continued) Pile Capacity Estimates

Ref No.	Eng. News (kips)	FHWA-modifiedGates (kips)	GRL WEAP (kips)	DRIVEN Original (kips)	DRIVEN Limit 36° (kips)	Correction Factor*DRIVEN (kips)
121	334	670	400	1424	680	567
122	330	664	403	1424	680	567
123	358	699	410	1501	751	626
124	358	699	410	1501	751	626
125	377	720	427	1501	751	626
126	297	625	367	1501	751	626
127	377	720	427	1501	751	626
128	358	699	410	1475	735	613
129	314	644	384	1501	751	626
130	334	670	400	1475	735	613
131	358	699	410	1449	719	599
132	352	690	413	1475	735	613
133	311	641	390	1552	783	652
134	440	799	458	1501	751	626
135	299	628	360	1438	723	628
136	314	644	379	1456	734	627
137	345	689	391	1288	629	649
138	334	670	395	1227	592	662
139	314	644	379	538	538	683
140	358	699	408	1274	621	652
141	321	656	373	1470	743	626
142	297	625	363	1472	744	625
143	299	628	360	1311	644	644
144	297	625	363	1215	584	665
145	317	649	376	553	553	677
146	314	644	379	449	449	584
147	317	649	376	562	562	674
148	339	678	393	1405	703	631
149	299	628	360	1323	652	642
150	317	649	376	1265	615	654
151	297	625	363	1220	587	664
152	314	644	379	1226	591	663
153	377	720	425	494	493	633
154	299	628	360	542	542	682
155	321	656	373	1348	667	637
156	299	628	360	1290	631	648
157	297	625	363	1249	605	657
158	299	628	360	1267	616	653
159	314	644	379	551	551	678
160	299	628	360	545	545	681

Table 5.4 (continued) Pile Capacity Estimates

Ref No.	Eng. News (kips)	FHWA-modifiedGates (kips)	GRL WEAP (kips)	DRIVEN Original (kips)	DRIVEN Limit 36° (kips)	Correction Factor*DRIVEN (kips)
161	297	625	363	554	554	677
162	299	628	360	1371	681	634
163	166	443	354	n/a	n/a	634
164	182	478	348	719	719	599
165	182	478	348	n/a	n/a	599
166	186	488	353	n/a	n/a	599
167	182	478	347	n/a	n/a	599
168	189	494	356	n/a	n/a	599
169	198	514	366	n/a	n/a	599
170	166	452	326	886	886	738
171	168	450	332	n/a	n/a	738
172	164	443	328	628	628	523
173	162	436	336	341	341	292
174	134	388	305	727	701	584
175	105	331	255	368	342	327
176	97	316	248	505	500	417
177	147	410	308	646	638	532
178	115	352	282	532	522	435
179	105	331	255	622	608	507
180	96	313	240	588	586	488
181	80	279	195	565	420	414
182	91	304	227	661	517	431

Table 5.5. Distribution of CIP Pile sizes in case history database.

Diameter (in)	number of cases
10.75	34
12.75	42
14	99
16	7

Table 5.6. Types of Open Ended Diesel Hammers employed in case history database

Hammer	number of cases
Delmag D12	2
Delmag D16-32	5
Delmag D19-32	40
Ape D19-42	4
Delmag D25-32	18
Delmag D30-32	113

Table 5.7. Relationship between friction angle and corrected standard penetration test value

N_{spt}^{corr}	ϕ (deg)
5	28.1
10	30.0
15	31.5
20	33.0
25	34.5
30	36.0
35	37.5
40	38.8
45	40.0
50	41.0
55	42.0
60	43.0

Table 5.8. Relationship between standard penetration test value and Unit Weight

N_{spt}	**Unit Weight (pcf)**
0-4	70-100
4-10	90-115
10-30	110-130
30-50	110-140
50+	130-150

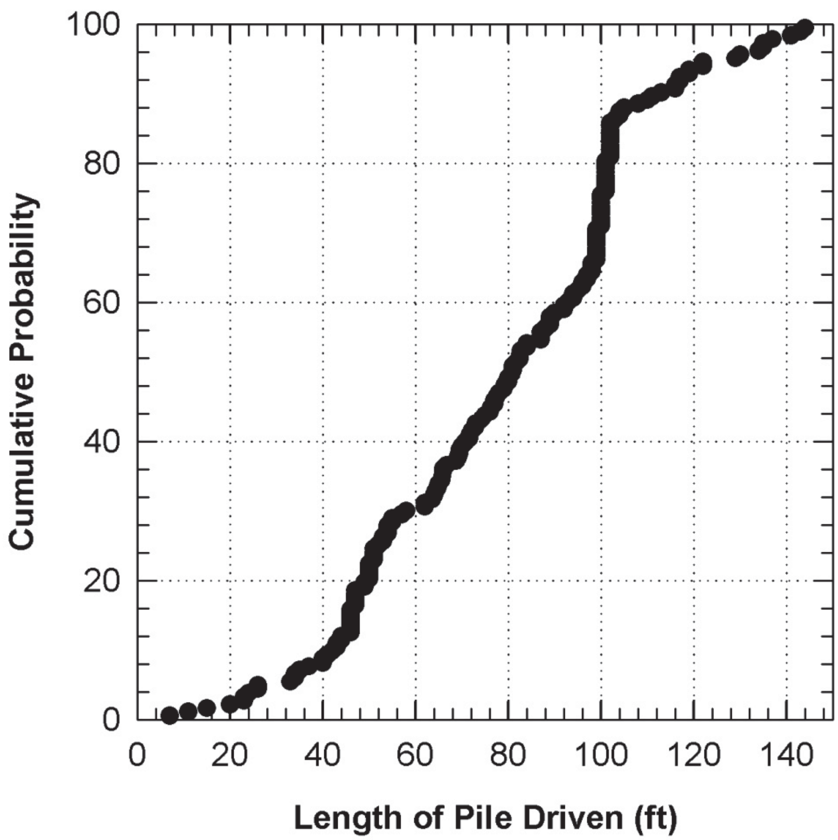

Figure 5.1 Cumulative distribution for driven length of piling.

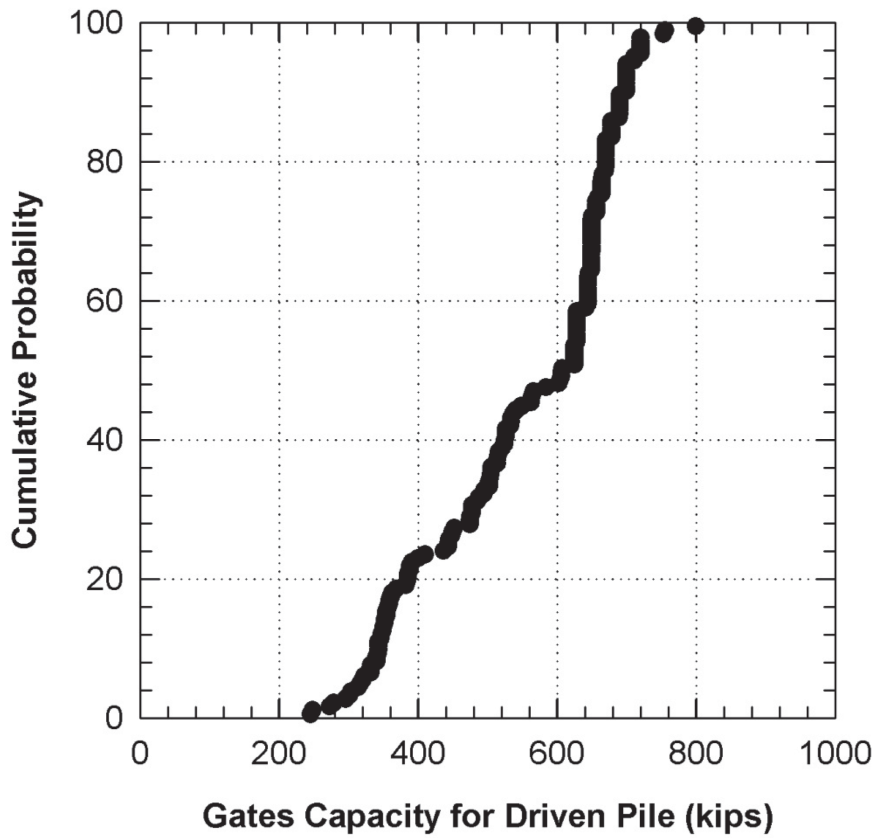

Figure 5.2 Cumulative distribution for capacity of piling using FHWA-modified Gates formula.

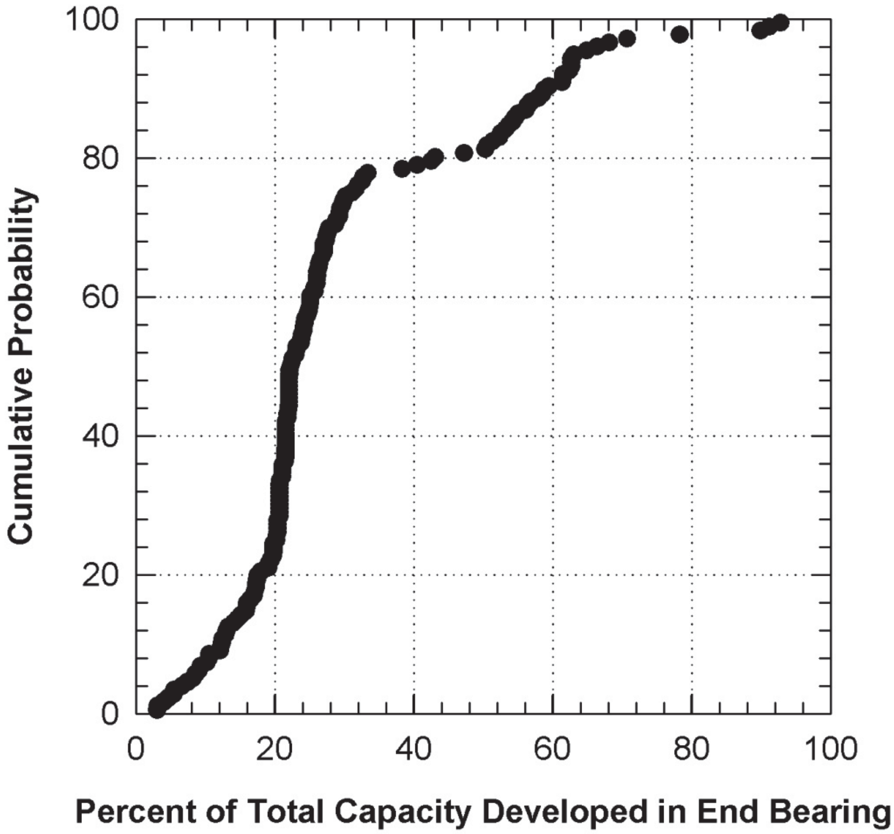

Figure 5.3 Cumulative distribution for percent of total pile capacity developed in end bearing.

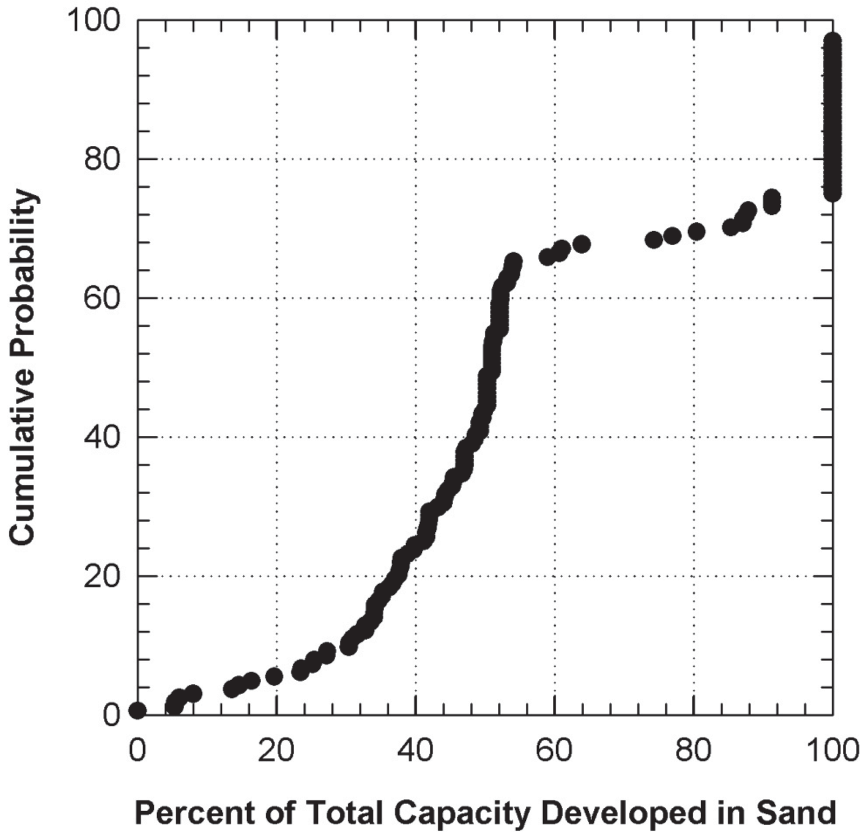

Figure 5.4 Cumulative distribution for percent of total pile capacity developed in coarse-grained soil.

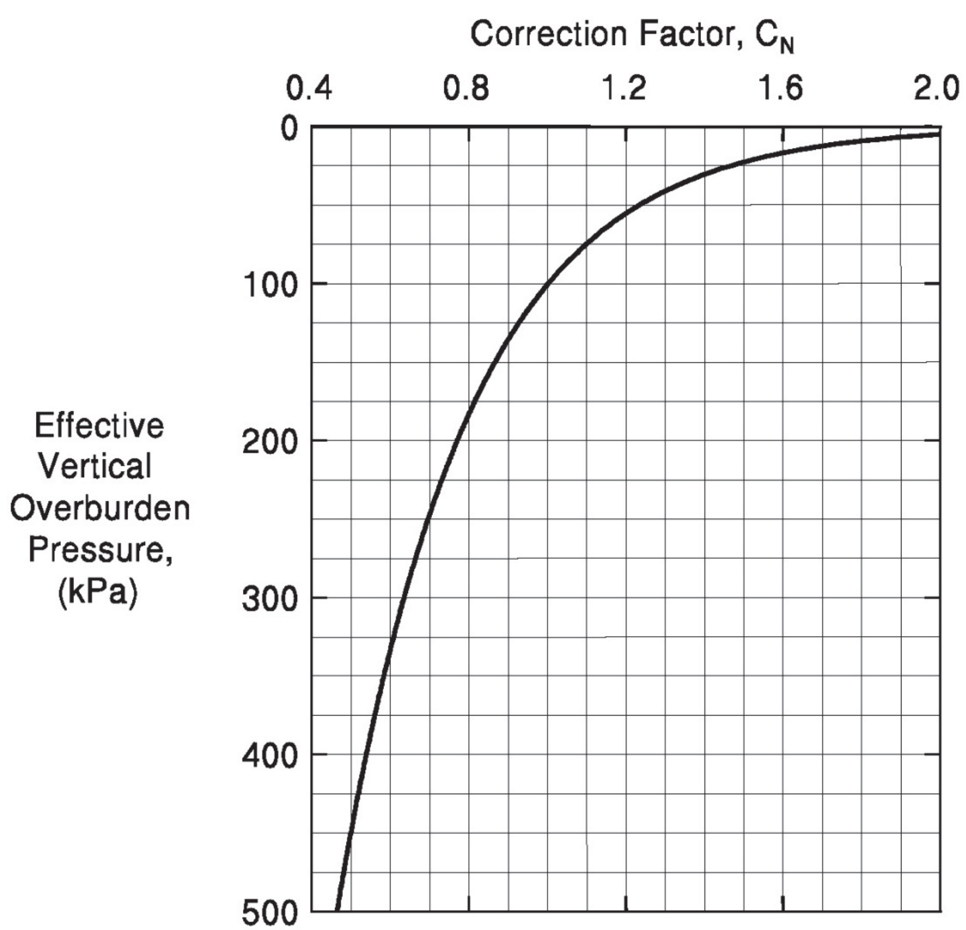

Figure 5.5 Standard Penetration test correction factor for overburden stress.

6.0 AGREEMENT BETWEEN FHWA-MODIFIED GATES AND DRIVEN – NO LIMITING VALUE FOR SOIL FRICTION ANGLE

6.1 INTRODUCTION

All cases were analyzed with a static method (DRIVEN), two dynamic formulae (EN formula, FHWA-modified Gates), and wave equation analysis (WEAP) to determine the agreement between these methods. The statistical metrics and graphs used to quantify and illustrate agreement between methods is discussed first, followed by the results of comparisons. While all four estimates were determined for each case, particular emphasis is placed on the two methods commonly used by Wisconsin DOT (DRIVEN and FHWA-modified Gates).

6.2 TOOLS FOR ASSESSING AGREEMENT

6.2.1 Plots

A plot of capacity determined from the dynamic formula, EN, versus capacity determined from the static method , DRIVEN, is shown in Fig. 6.1. The graph includes a 45 degree solid line that identifies perfect agreement between the two methods ($Q_{EN} = Q_{DRIVEN}$). Data points close to the 45 degree solid line indicate cases where the capacities predicted by both methods closely agree. Data points that plot above the 45 degree line indicate that the EN formula estimated greater capacity than DRIVEN, and data points below the 45 degree line indicate cases where EN estimated less capacity than DRIVEN.

Visual inspection of Fig. 6.1 provides the reader with a subjective assessment of the agreement between the methods. These plots can be used to visually determine trends in agreement, such as one method's tendency to over- or under-predict capacity compared to another method. For example, Fig. 6.1 indicates the EN formula estimates capacities higher than capacities estimated with DRIVEN for DRIVEN capacities less than 100 kips. Furthermore, there seems to be a trend that the EN formula estimates capacities lower than DRIVEN when the DRIVEN capacity is estimated to be greater than 100 kips.

The scatter exhibited by the plot allows assessment of the precision of agreement between the two methods. For example, a plot exhibiting considerable scatter indicates poor agreement. Plots that exhibits smaller scatter indicate methods that agree with greater precision.

While Fig. 6.1 is a useful visual tool for comparing the agreement between methods, there is also a need to quantify the accuracy and precision between methods to allow comparisons to be made objectively. Means to quantify accuracy and precision are discussed in the following section.

6.2.2 Statistics

Agreement (accuracy and precision) between two methods was assessed visually in the previous section. Accuracy is defined as how well, on the average, the methods agree. In statistics, this is defined as the average, mean, or bias. The scatter in the plot is a measure of how consistently the method agree, and this is referred to as precision.

Bias and precision will be used herein as two simple statistical parameters for defining how well two methods agree. Bias is a systematic error between the average ratio of estimate from method 1 divided by the estimate from method 2 and the ideal ratio of unity. Statistically, the bias can be estimated with a sample mean. Precision is a measure of scatter and can be estimated with a sample standard deviation. A normalized measure of scatter is termed the coefficient of variation. The three terms, mean (μ), standard deviation (σ), and coefficient of variation (cov), are defined in detail below. While the distribution for a ratio (estimate from method 1/estimate from method 2) is typically log-normal (Cornell, 1969), mean, standard deviation, and coefficient of variation are determined using a normal distribution for simplicity.

The mean (μ) is calculated as

$$\mu = \frac{1}{n}\sum_{i=1}^{n}\frac{estimate\ from\ method\ 1}{estimate\ from\ method\ 2} \tag{6.1}$$

where n is the number of observations. A mean value equal to 1.0 represents that, on the average, predicted capacity equals measured capacity. For $\mu < 1$, method 1, on the average, predicts capacity smaller than method 2. Method 1 predicts capacity greater than method 2, on the average, when $\mu > 1$.

A measure for scatter can be quantified with a standard deviation (σ). The equation for standard deviation is as follows:

$$\sigma^2 = \frac{1}{n-1}\sum_{i-1}^{n}\left(\left\{\frac{estimate\ from\ method\ 1}{estimate\ from\ method\ 2}\right\}_i - \mu\right)^2 \tag{6.2}$$

where σ is the standard deviation, μ is the mean, and n is the number of cases.

The coefficient of variation (cov) is a normalized measure of scatter and is determined as follows:

$$cov = \frac{\sigma}{\mu} \tag{6.3}$$

A cumulative distribution plot is used to identify the distribution of data. Geotechnical engineers commonly use a cumulative distribution plot to illustrate grain size distribution. The cumulative distribution plot is constructed by sorting values in the dataset from smallest to largest and numbering each from i = 1 to n, where n is equal to the number of cases in the dataset. A cumulative probability value (CP_i) for each value is calculated as

$$CP_i = \frac{i}{n+1} \tag{6.4}$$

The plot illustrates the relationship between a value and reliability. For example, assume that a value of 0.8 corresponds to a cumulative probability of 40 percent. This means 40 percent of the time the value is 0.8 or less.

6.3 DRIVEN CAPACITY VERSUS EN, GATES, AND WEAP

Estimates for pile capacity based on the static method used in DRIVEN are compared with estimates based on the behavior of the pile during driving. The three methods used to estimate capacity based on pile driving resistance are the EN formula, the FHWA-modified Gates formula, and WEAP.

The computer program, DRIVEN was used for estimating the pile capacity with a static method. Driven has several options for implementing the static method, and methods consistent with those used by Wisconsin DOT were selected. The options selected Tomlinson (1971) relationships for determining unit side resistance in fine-grained soils, and the Nordlund (1963, 1979) and Thurman (1964) for determining the unit side resistance and unit end bearing resistance. Friction values in coarse grained soils were determined from standard penetration test values corrected for overburden. Soils at some sites exhibited high penetration test values that resulted in estimates for friction angle greater than 36 degrees. In these cases, values higher than 36 degrees were used.

Pile capacities were also estimated using dynamic formulae. Estimates using the FHWA-modified Gates method are compared with estimates from DRIVEN in Fig. 6.1. The agreement is poor. Estimates using the Gates method are greater than estimates from DRIVEN up to about 600 kips, and then the Gates method predicts less capacity than DRIVEN. A wider range of capacities is estimated with DRIVEN. Capacities estimated with DRIVEN range from 40 to 1500 kips, while the estimates with Gates range from about 300 to 900 kips. The overall mean is for the ratio of Gates/DRIVEN is 1.45 and the coefficient of variation is 0.98 (Table 6.1). The cov is high and indicative of poor agreement. For comparison with previous studies (Long et al, 2009) as discussed in Chapter 3, the cov for static methods compared with static load tests results ranged from 0.50 to 0.66 and the cov for FHWA-modified Gates to static load test results was 0.42. Combining both these cov results into one estimate for cov for Gates/DRIVEN results in a cov between 0.65 and 0.78.

Agreement between the EN formula and DRIVEN (Fig. 6.2), and agreement between WEAP and DRIVEN (Fig. 6.3) are similar to those found for the agreement between Gates and DRIVEN. Specifically, it appears the Gates, EN, and WEAP estimate capacities greater than DRIVEN for lower capacity piles, and estimate capacities less than DRIVEN for higher capacity piles. The cov associated with EN, and WEAP are also very high (Table 6.1) and indicate significant scatter.

Previous studies have shown that the Gates method is more precise (lower cov) than DRIVEN when comparing predicted capacity and measured capacity. Therefore, adjustments to improve the agreement are applied to the static method for determining capacity rather than modifying the dynamic formula. Accordingly, it is more appropriate to consider the FHWA-modified Gates estimate as the independent variable, and the estimate of capacity using DRIVEN as the dependent variable. This means the axes are switched and redrawn with Gates on the x-axis (Fig. 6.4). The trend of the data in Fig. 6.4 provides some indication as to what modification may be necessary to improve the agreement between DRIVEN and FHWA-modified Gates. DRIVEN is shown to significantly under-predict capacity at low capacities estimated with Gates and slightly over-predict capacities for higher capacities estimated with Gates.

6.4 AGREEMENT BETWEEN DYNAMIC METHODS

The agreement of estimates for pile capacity based on measurements made during pile driving exhibit good agreement. For example, the ratio of capacity estimated with the EN formula compare to the FHWA-modified Gates estimate exhibited a mean of 0.43 and a cov of 0.19. The mean value (0.43) is small because the EN formula provides a safe bearing load whereas the Gates method estimates ultimate pile capacity. However, the cov value of 0.19 indicates a small degree of scatter.

The agreement between estimates of capacity made with WEAP and estimates made with Gates also indicates good agreement (Fig. 6.5). The agreement has a mean of 0.68 and a cov of 0.13. The mean value of 0.68 is primarily because the Gates formula is empirical and accounts for pile setup in an approximate way, whereas the estimates made with WEAP did not assume any setup. Accordingly, the Gates method estimates higher capacity than WEAP. The cov of 0.13 is indicative of a small degree of scatter.

6.5 AGREEMENT BETWEEN ESTIMATED PILE LENGTHS

Another way to investigate agreement between methods is to compare the length of pile penetration necessary to attain the desired pile capacity. The target pile capacity for DRIVEN was based on the FHWA-modified Gates capacity as determined from the observed pile penetration resistance at the end of driving.

Estimates for pile penetration were determined by finding the depth required for DRIVEN capacity to equal the FHWA-modified Gates capacity. A comparison of the estimated pile length versus field penetration is shown in Fig. 6.6. The statistics for penetration estimates (Table 6.1) result in a mean value of 1.18 and cov of 0.40. Therefore, DRIVEN has exhibits a mild tendency to overestimate the length of pile penetration needed to reach capacity. The tendency to overestimate length is most significant for the shorter pile. DRIVEN tends to underestimate pile penetration requirements for the longer piles.

Table 6.1 – Statistics for estimates of capacity using different methods with no limit on friction angle used in static analysis.

Case*	Mean (μ)	Standard Dev (σ)	Coefficient of Variation (cov)	Number (n)
GTS/DVN	1.448	1.415	0.977	173
EN/DVN	0.570	0.464	0.814	173
WEP/DVN	1.034	1.155	1.117	173
DRV/GTS	1.350	1.319	0.977	173
EN/GTS	0.432	0.083	0.193	182
WEP/GTS	0.675	0.088	0.130	182
LDRVN/LFLD	1.182	0.472	0.399	178

*Note: abbreviations are defined below
DVN = Results from computer program, DRIVEN
EN = Engineering New Formula historically used by WisDOT
GTS = FHWA-modified Gates
WEP = GRLWEAP
LFLD = length of pile driven in the field
LDVN = length of pile necessary to achieve Gates capacity predicted using the computer program DRIVEN

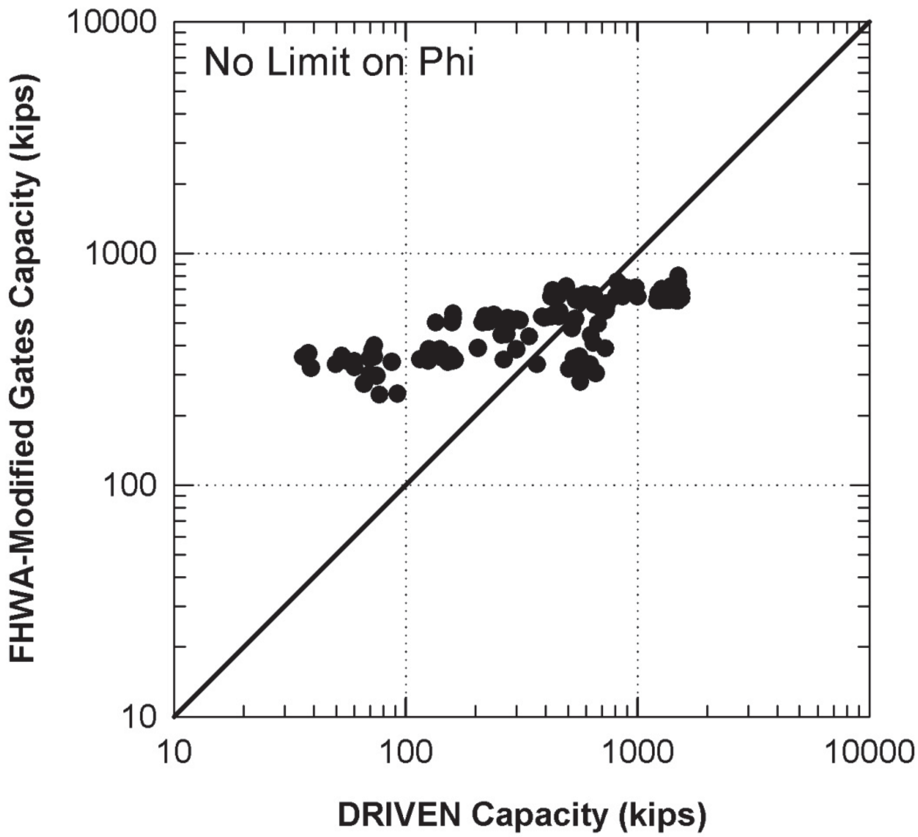

Figure 6.1 Estimated capacity using FHWA-modified Gates versus capacity estimated with DRIVEN.

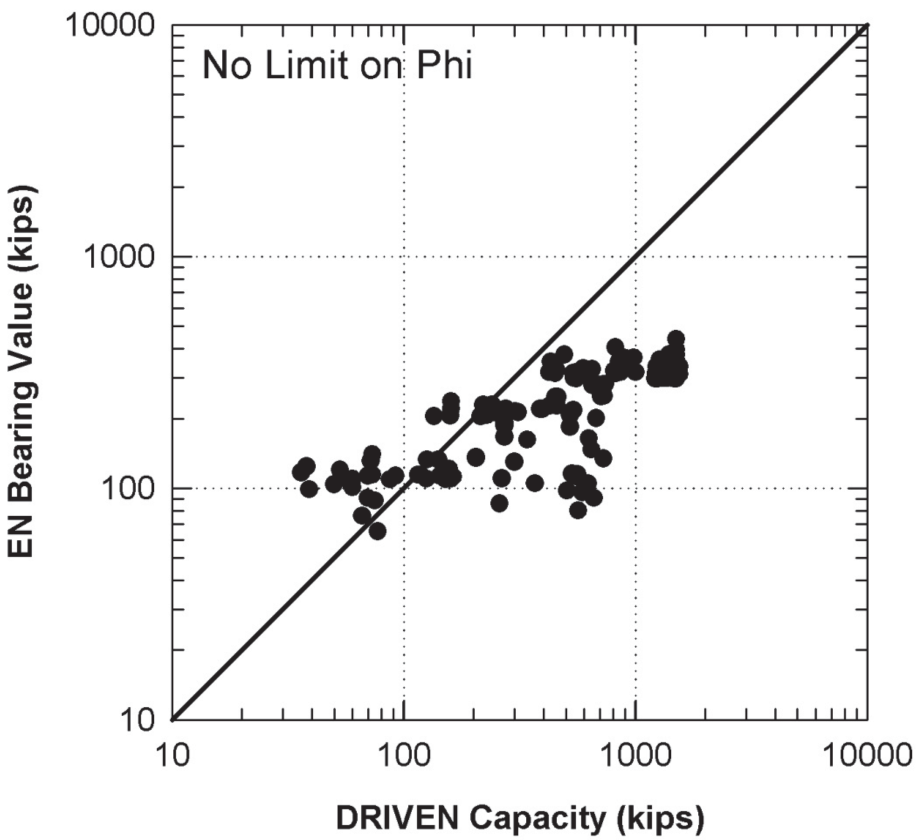

Figure 6.2 Estimated capacity using the EN formula versus capacity estimated with DRIVEN.

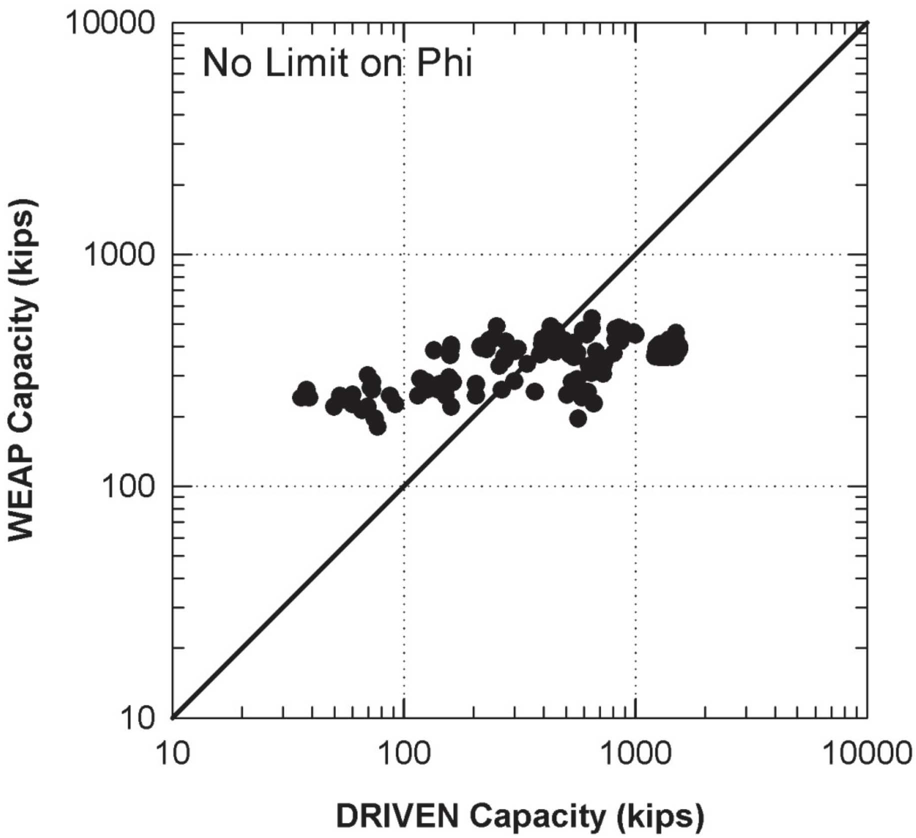

Figure 6.3 Estimated capacity using WEAP versus capacity estimated with DRIVEN.

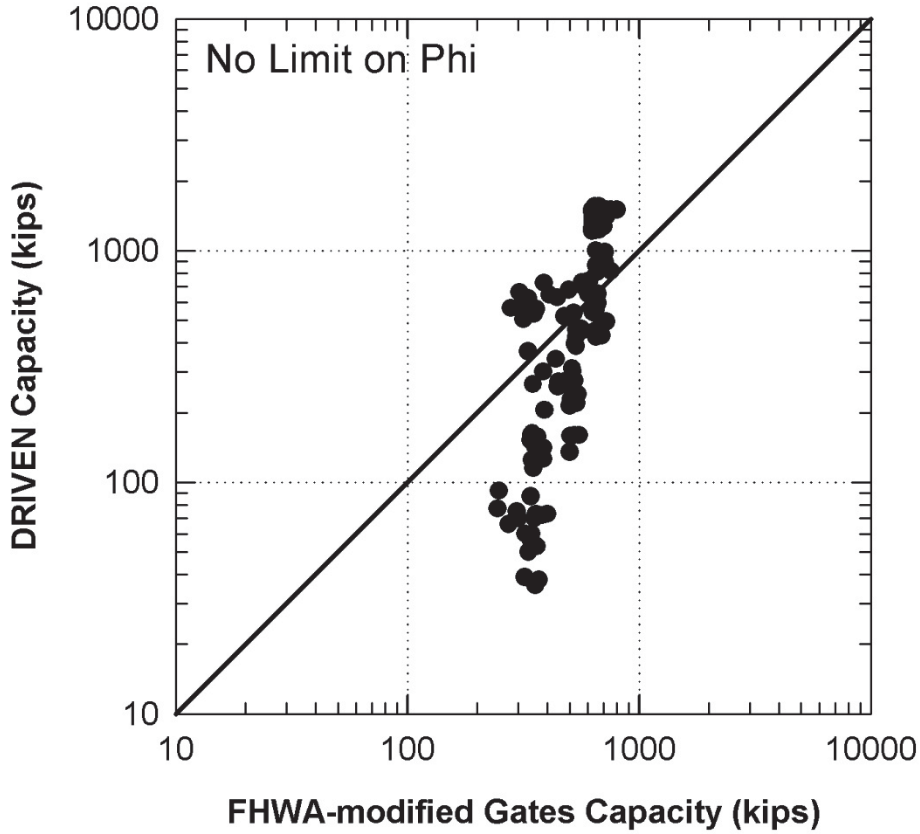

Figure 6.4 Estimated capacity using DRIVEN versus FHWA-modified Gates.

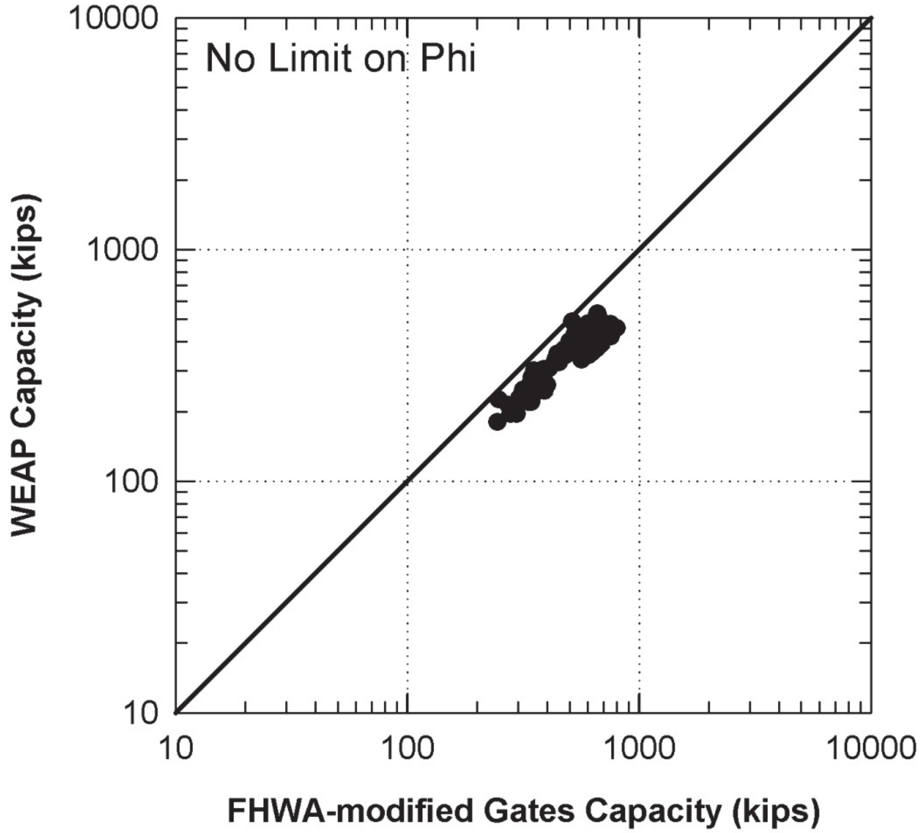

Figure 6.5 Estimated capacity using WEAP versus capacity estimated with FHWA-modified Gates.

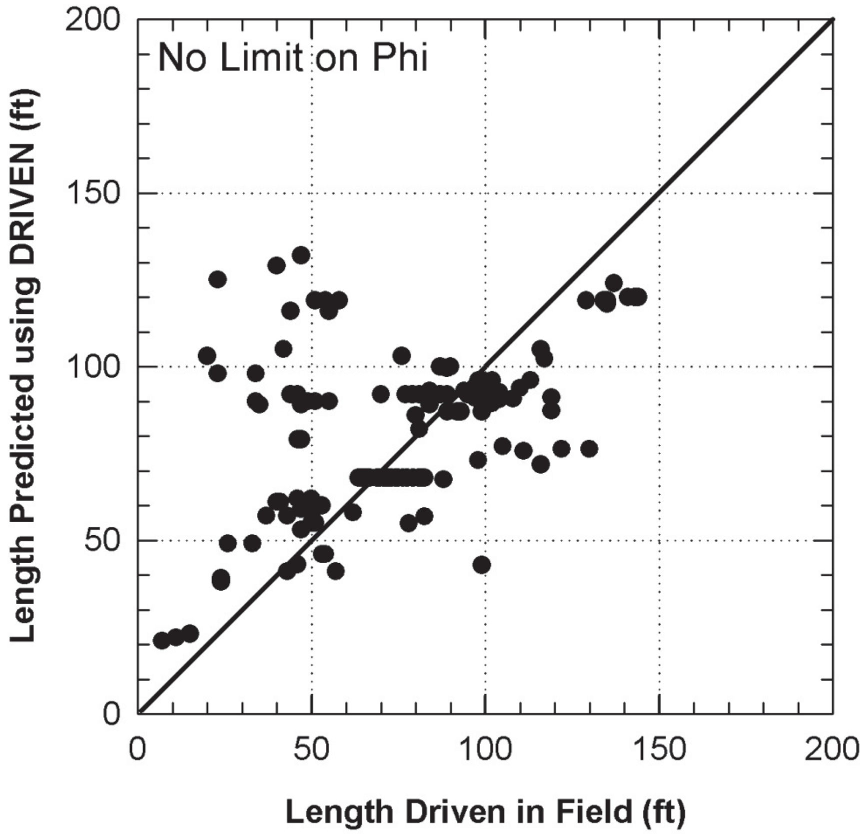

Figure 6.6 A comparison of estimated length of pile based on DRIVEN with actual length of pile driven in the field.

7.0 IMPROVEMENT OF AGREEMENT BETWEEN FHWA-MODIFIED GATES AND DRIVEN

7.1 INTRODUCTION

Modifications were made to the static method (DRIVEN) to improve the agreement between estimates of capacity made with the FHWA-modified Gates formula and estimates of pile capacity made with DRIVEN. Two factors that appear to significantly affect DRIVEN estimates of capacity were 1) the limiting value of friction angle used to represent granular soil strength, and 2) the depth of the driven pile. Improvements due to limiting the friction angle are presented first, followed by improvements achieved by including effect of pile depth.

7.2 LIMITING FRICITON ANGLE TO 36 DEGREES

The user's manual for DRIVEN states that the friction angle specified for a granular soil should not exceed 36 degrees. The reason stated in the user's manual is that the capacity equations become unrealistically high for friction angles greater than 36 degrees. The recommendation to limit the soil friction angle to 36 degrees was implemented for the 182 cases and results are discussed below.

7.2.1 Effect on agreement between methods

Estimates for pile capacity based on the static method used in DRIVEN are compared with estimates based on the behavior of the pile during driving. The three methods used to estimate capacity based on pile driving resistance are the EN formula, the FHWA-modified Gates formula, and WEAP. The statistics in Table 7.1 reflect mean and cov values for agreement between methods with DRIVEN restricted to using a limiting friction angle of 36 degrees. The results in Table 7.1 can be compared with the statistics reported in Table 6.1, which is the same table, but for the condition where DRIVEN was used without restricting the friction angle. In all cases, the comparisons of capacities between DRIVEN and dynamic methods show less scatter (smaller cov) when the friction angle was restricted to be no greater than 36 degrees. For example, the cov for the agreement between DRIVEN and Gates improved from 0.98 to 0.73 by implementing the limiting friction angle of 36 degrees Therefore, the effect of limiting the friction angle to 36 degrees or less results in better agreement between methods (but 0.73 is still a high value for cov).

The agreement between DRIVEN and FHWA-modified Gates is shown in Fig. 7.1. The trend is for DRIVEN to estimate capacities significantly less than FHWA-modified Gates for low pile capacities, and slightly overestimate capacity for high pile capacities. The trend is similar to the trend shown in the previous chapter (Fig. 6.4). The other relationships between DRIVEN and EN and DRIVEN and WEAP, and WEAP and Gates show trends similar to those seen in Chapter 6.

7.2.2 Agreement Of Estimated Pile Lengths

Estimates for pile penetration were determined by finding the depth required for DRIVEN capacity to equal the FHWA-modified Gates capacity. This is similar to what was done in Chapter 6, but the limiting value of friction angle was applied to DRIVEN. A comparison of the estimated pile length versus field penetration is shown in Fig. 7.2. The statistics for penetration estimates (Table 7.1) result in a mean value of 1.3 and cov of 0.45. The mean value of 1.3 means lengths are overestimated using DRIVEN.

7.3 EFFECT OF PILE DEPTH AND IMPROVEMENT FOR DRIVEN

The effect of depth on unit side resistance and unit end bearing was discussed in Chapter 2. Vesic (1967) and Coyle and Castello (1981) discussed and presented results of both model pile tests and full scale piles that illustrated that the unit side resistance and unit end bearing can be affected greatly by depth and the trend is non-linear. Equations used in DRIVEN determine the unit side resistance and end bearing as a linear function of effective vertical stress, up to a limiting stress. Thus the trend is a resistance that is linear increasing, and then constant for greater depths (or stresses). This bilinear simplification can result in what is termed herein as a depth effect. As discussed in Chapter 2, Dennis (1982) found depth affects for methods that used the bilinear approach for determining unit side and end bearing resistance. Accordingly, the effect of depth was investigated for DRIVEN.

The ratio of estimated capacity using DRIVEN/estimated capacity using the FHWA-modified Gates method was used as a value to compare agreement. DRIVEN capacities were determined using the limit of 36 degrees for friction angle. The relationship of the ratio of DRIVEN/Gates capacity is shown in Fig. 7.3. Ideally, the data would plot along a horizontal line with a ratio of 1.0, which would mean the agreement between the two estimates would be perfect for all depths. However, the data show a strong trend for the capacity ratio to increase from small values at shallow depth to larger values for greater depths. The trend means that DRIVEN under-predicts capacity (with respect to FHWA-modified Gates) for shallow depths, and over-predicts capacity for depths greater than about 80 ft. This trend is consistent with the findings of Dennis (1982) and Coyle and Castello (1981).

7.3.1 Effect of Effective Stress

Depth is not a fundamental parameter that affects soil behavior, however, as depth increases, so does effective stress. Since effective stress is a fundamental parameter that governs soil behavior, the capacity ratio (DRIVEN/Gates) was plotted versus the effective stress at the tip of the pile (Fig. 7.4). The result is the trend is shown to be stronger with less scatter than when depth was used as the horizontal axis. Accordingly, effective stress at the tip of the pile is taken to be an important parameter for improving estimates made with DRIVEN.

7.3.2 Effect of Soil Type

Other parameters, such as soil type and soil strength can also play an important role. Each case was filtered to identify what soils contributed to capacity. Piles that developed more than 67 percent capacity in clay soils are identified as piles in clay. Piles that developed more than 67 percent of their capacity in granular soils were identified as piles in sand. Piles that fit in neither category were identified as piles in mixed soil. The capacity ratio versus effective stress at the tip of the pile was plotted for all soil types and is shown in Fig. 7.5. There is no clear trend to distinguish a different behavior for each soil type. Therefore, the effect of soil type is taken to have little effect on the overall trend of capacity ratio versus effective stress.

7.3.3 Effect of Soil Strength

Effect of soil strength was investigated by separating the cases according to friction angle. The average friction angle was determined for cases in which piles developed more than 67 percent of their capacity from granular soil. All other cases were identified as mixed. Soils with friction angles from 30, 31-32, 33-34, and 35-36 degrees were identified separately on a plot of capacity ratio versus effective stress (Fig. 7.6). There were no strong trends observed to further refine the relationship of capacity ratio versus effective stress.

7.3.4 Effect of Side Resistance and End Bearing and Correction Factor

The effect of distribution of pile resistance was investigated by determining the portion of total load carried in side resistance and end bearing. Piles were identified as primarily side resistance if the side resistance was determined to be greater than 67 percent of the total capacity. Piles were identified as primarily end bearing is greater than 67 percent of total capacity was developed in end bearing. The rest of the piles were identified as mixed. Results were plotted as capacity ratio versus effective stress and there appears to be a different trend for friction piles and end bearing piles (Fig. 7.7). Thus, two relationships were developed to represent the trend for side resistance and end bearing.

The correction factor for side resistance (CF_{side}) versus effective stress is shown in Fig. 7.7 and can be represented with the following equation:

$$CF_{side} = 0.2 \leq -0.4615 + 1.4615 \cdot \sigma'_{v\,tip}/4750 \leq 1.2 \qquad (7.1)$$

where, $\sigma'_{v\ tip}$ is the vertical effective stress (psf) at the tip of the pile. The correction factor for end bearing is also shown in Fig. 7.7 and is represented with the following equation:

$$CF_{end\ bearing} = 0.2 \leq -0.185 + 1.185 \cdot \sigma'_{v\ tip}/4750 \leq 1.2 \qquad (7.2)$$

The correction is applied to determine the overall capacity as follows:

$$Corr\ Side\ Capacity = DRIVEN\ Side\ Capacity/CF_{side} \qquad (7.3)$$

$$Corr\ EB\ Capacity = DRIVEN\ EB\ Capacity/CF_{end\ bearing} \qquad (7.4)$$

7.4 APPLICATION OF CORRECTION FACTOR

Correction factors for side and end bearing were applied to each of the 182 cases and results were reviewed. Of the 182 cases 19 cases predicted pile lengths significantly greater than observed in the field. These cases had soil profiles with very dense granular soil layers at depths that corresponded to the depth of pile termination, but DRIVEN failed to predict the depth because the limiting friction angle of 36 degrees. These cases were re-evaluated and allowed to have friction angles up to 40 degrees, if standard penetration values exceeded 80 bpf.

Application of the correction factors for side and end bearing as a function of stress resulted in a significant improvement for the agreement between DRIVEN and the FHWA-modified Gates method (Fig. 7.8). The mean value of the ratio of DRIVEN/Gates capacity is 1.06 with a cov of 0.28 (Table 7.2). Values of mean and cov also show improvement with DRIVEN and the other dynamic methods. Interestingly, the statistical parameters do not indicate an improvement in the ability to predict pile lengths driven in the field. The corrected DRIVEN method resulted in a mean of 1.83 and a cov of 0.49. Pile lengths predicted with the corrected DRIVEN compared to lengths driven in the field are shown in Fig. 7.9. Most of the cases show improvement in agreement between predicted length and length driven in the field. However, there are several cases in which the piles drove to between 20 and 50 ft in the field, but DRIVEN predicts the length of piling to be much greater. The tendency to over predict pile length is made worse by the correction factor applied for vertical effective stress. As the piles get longer, and the vertical effective stress gets greater, the correction factor reduces side and end bearing by up to 20 percent. A review of these cases showed soil profiles that were mostly loose sands with no indication of layers that could support the pile at shallow depths.

A cumulative distribution plot is provided (Fig. 7.10) for the ratio of the length estimated using DRIVEN/length driven in the field. Three versions of the DRIVEN length are determined:1)Original DRIVEN in which are values of length are determined using DRIVEN with no restriction for friction angles, 2) DRIVEN where friction angles are limited to be no greater than 36 degrees, and 3) DRIVEN with correction factors for overburden, and a limit for maximum friction angle equal to 36 degrees. However, values up to 40 degrees can be used when N_{spt} values exceed 80.

Interpreting a cumulative distribution plot is similar to interpreting a grain size curve. A flat curve represents a wide range of values, whereas a steep curve represents values that are very similar. Therefore a flat curve would represent a distribution of length predictions that vary widely – from severely under-predicting length to greatly over-predicting length. A steep curve would represent predictions that are consistently close to measured lengths. The three curves in Fig. 7.10 form a general S-shape. The distribution for DRIVEN with no limit on friction angle is shown as hollow circles. The distribution for DRIVEN with a limit of friction angle equal to 36 degrees is shown as a small solid circle. The effect of applying the limiting friction angle to predictions for length show that there is a smaller tendency for DRIVEN to predict lengths shorter than driven in the field, but the method predicts more frequently a pile length that is greater than driven in the field. The DRIVEN method, with correction for overburden stress, and a conditional correction for soil friction angle is illustrated with small crosses in Fig. 7.10. There is a slightly greater tendency for the corrected method to predict lengths greater than the original method; however, there is significantly less tendency to over-predict length. However, there are about 20 cases where there is significant over-prediction for all three cases. All these cases were reviewed, but there was nothing in the soil exploration, soil profile, or driving records that could be found to explain the reason for DRIVEN predicting greater lengths than observed.

Table 7.1 Statistics for estimates of capacity using different methods with a limiting friction angle of 36 degrees used in static analysis.

Case*	**Mean (μ)**	**Standard Dev (σ)**	**Coefficient of Variation (cov)**	**Number (n)**
GTS/DVN	1.724	1.264	0.733	175
EN/DVN	0.699	0.438	0.626	175
WEP/DVN	1.206	1.006	0.834	175
DRV/GTS	0.892	0.654	0.733	175
EN/GTS	0.432	0.083	0.193	182
WEP/GTS	0.675	0.087	0.130	182
LDRVN/LFLD	1.297	0.579	0.446	161

*Note: abbreviations are defined below

DVN = Results from computer program, DRIVEN

EN = Engineering New Formula historically used by WisDOT

GTS = FHWA-modified Gates

WEP = GRLWEAP

LFLD = length of pile driven in the field

LDVN = length of pile necessary to achieve Gates capacity predicted using the computer program DRIVEN

Table 7.2 Statistics for estimates of capacity using different methods with a correction for vertical stress and a conditional limiting friction angle of 36 degrees used in static analysis.

Case*	**Mean (μ)**	**Standard Dev (σ)**	**Coefficient of Variation (cov)**	**Number (n)**
GTS/DVN	1.020	0.285	0.279	182
EN/DVN	0.445	0.166	0.373	182
WEP/DVN	0.684	0.197	0.288	182
DRV/GTS	1.057	0.295	0.279	182
LDRVN/LFLD	1.183	0.577	0.488	166

*Note: abbreviations are defined below
DVN = Results from computer program, DRIVEN
EN = Engineering New Formula historically used by WisDOT
GTS = FHWA-modified Gates
WEP = GRLWEAP
LFLD = length of pile driven in the field
LDVN = length of pile necessary to achieve Gates capacity predicted using the computer program DRIVEN with correction factor applied

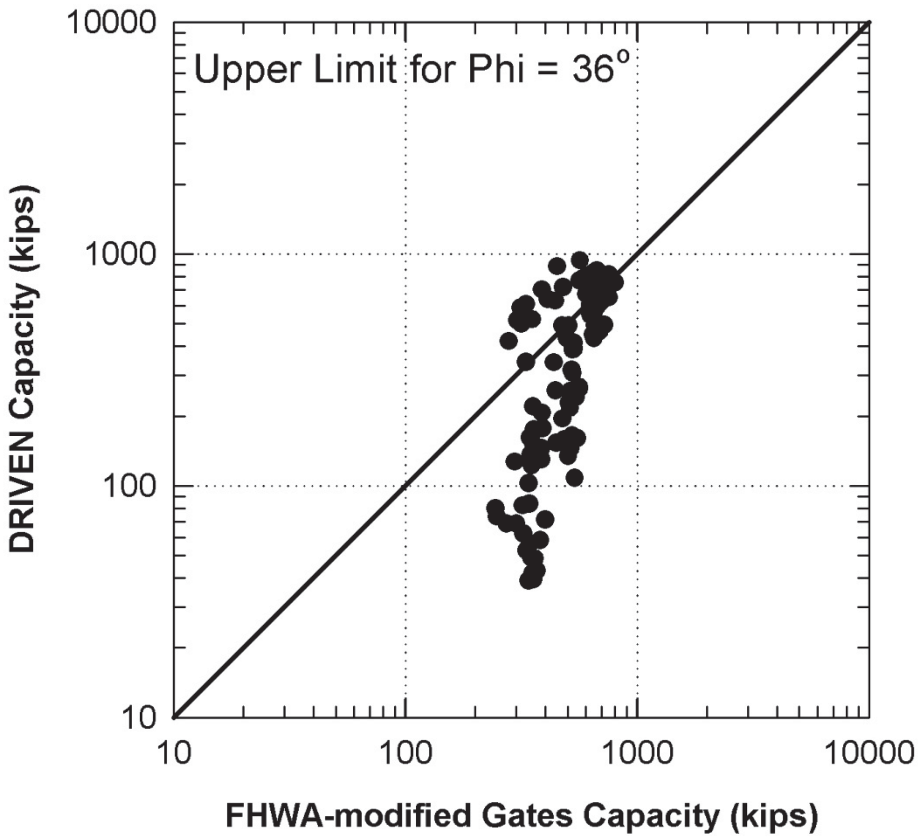

Figure 7.1 Estimated capacity using DRIVEN and limiting the friction angle to be no greater than 36 degrees, and the FHWA-modified Gates.

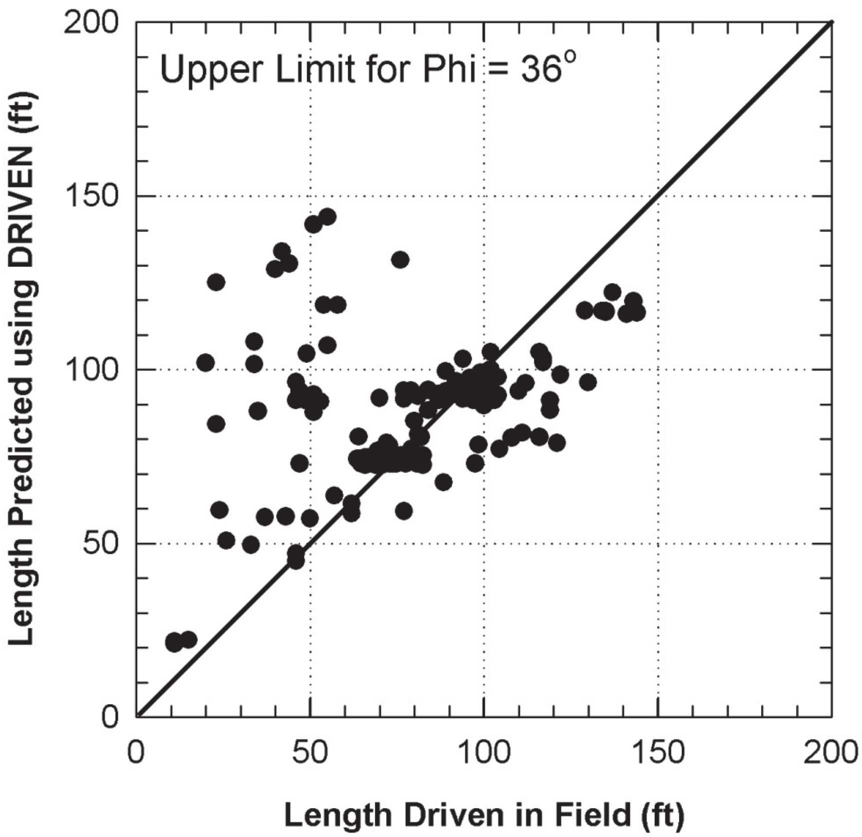

Figure 7.2 A comparison of estimated length of pile based on DRIVEN with restriction of friction angle to 36 degrees and actual length of pile driven in the field.

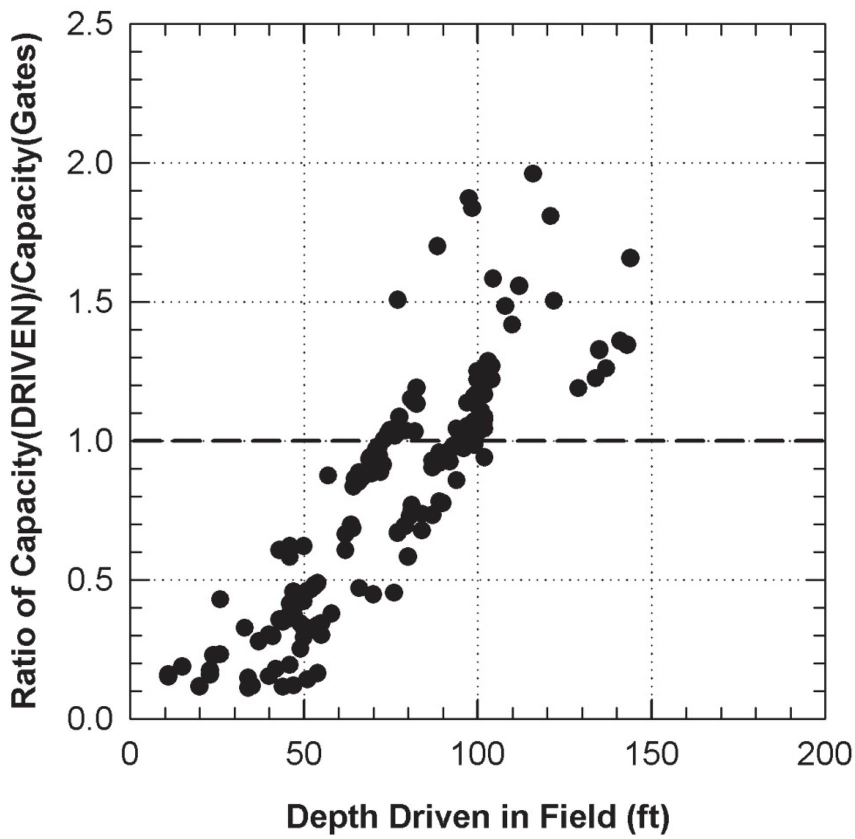

Figure 7.3 Ratio of estimated pile capacity using DRIVEN (with 36 degree limit) to the capacity using FHWA-modified Gates versus depth driven in the field.

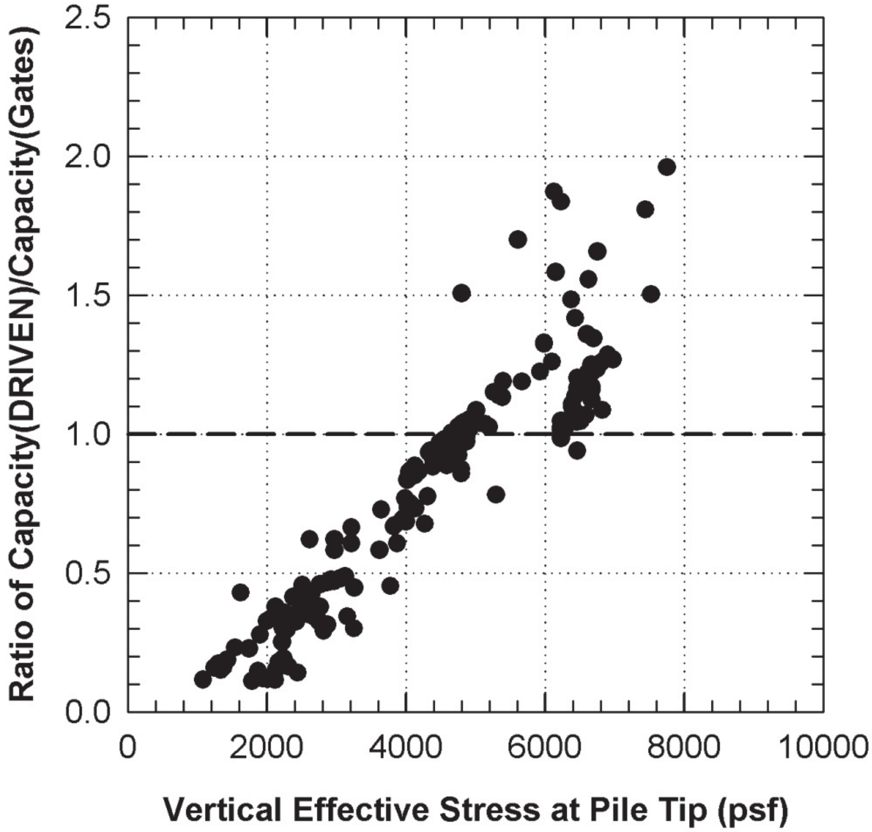

Figure 7.4 Ratio of estimated pile capacity using DRIVEN (with 36 degree limit) to the capacity using FHWA-modified Gates versus effective stress at tip of pile.

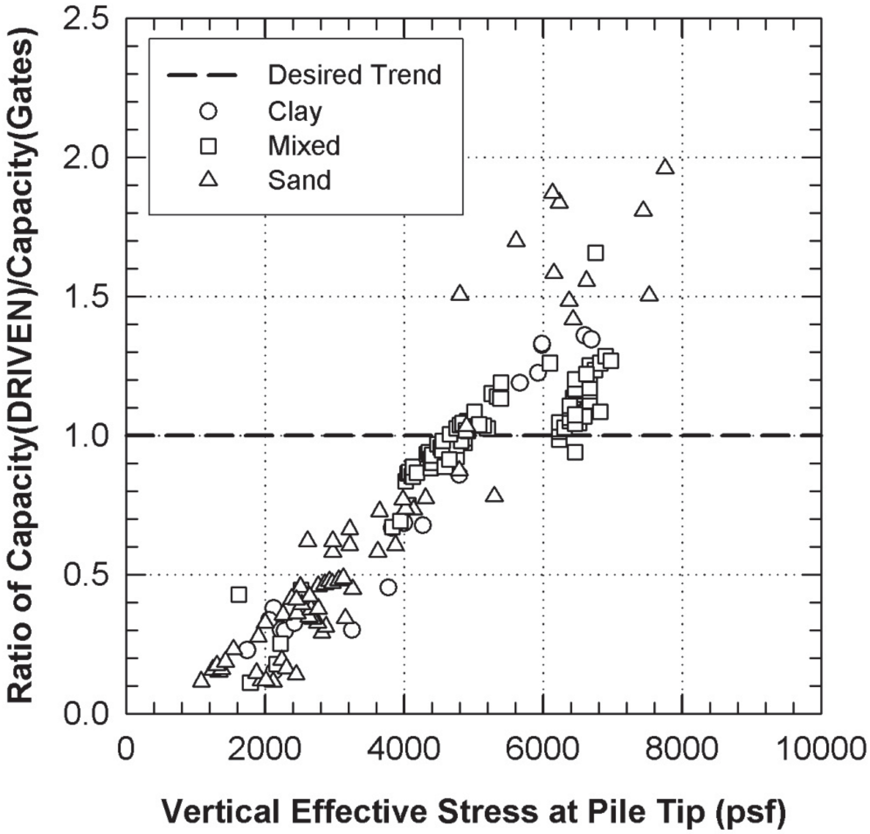

Figure 7.5 Effect of soil type on ratio of estimated pile capacity using DRIVEN (with 36 degree limit) to the capacity using FHWA-modified Gates versus effective vertical stress.

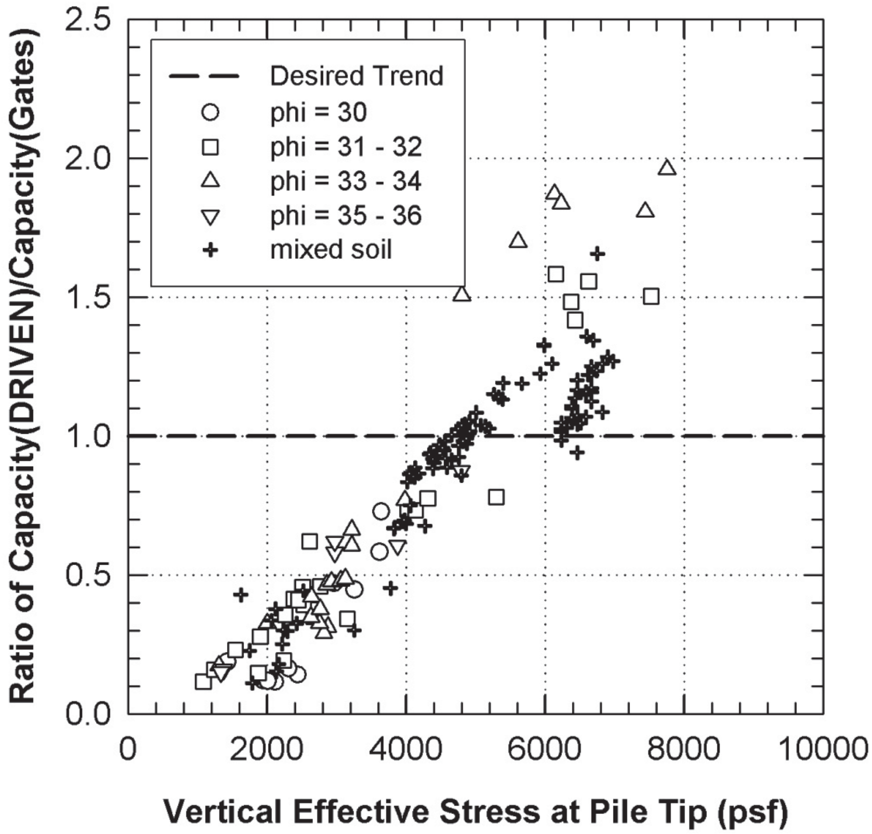

Note: + represents cases in which less than 60 percent of total capacity is developed in sand.

Figure 7.6 Effect of soil strength on ratio of estimated pile capacity using DRIVEN (with 36 degree limit) to the capacity using FHWA-modified Gates versus effective vertical stress.

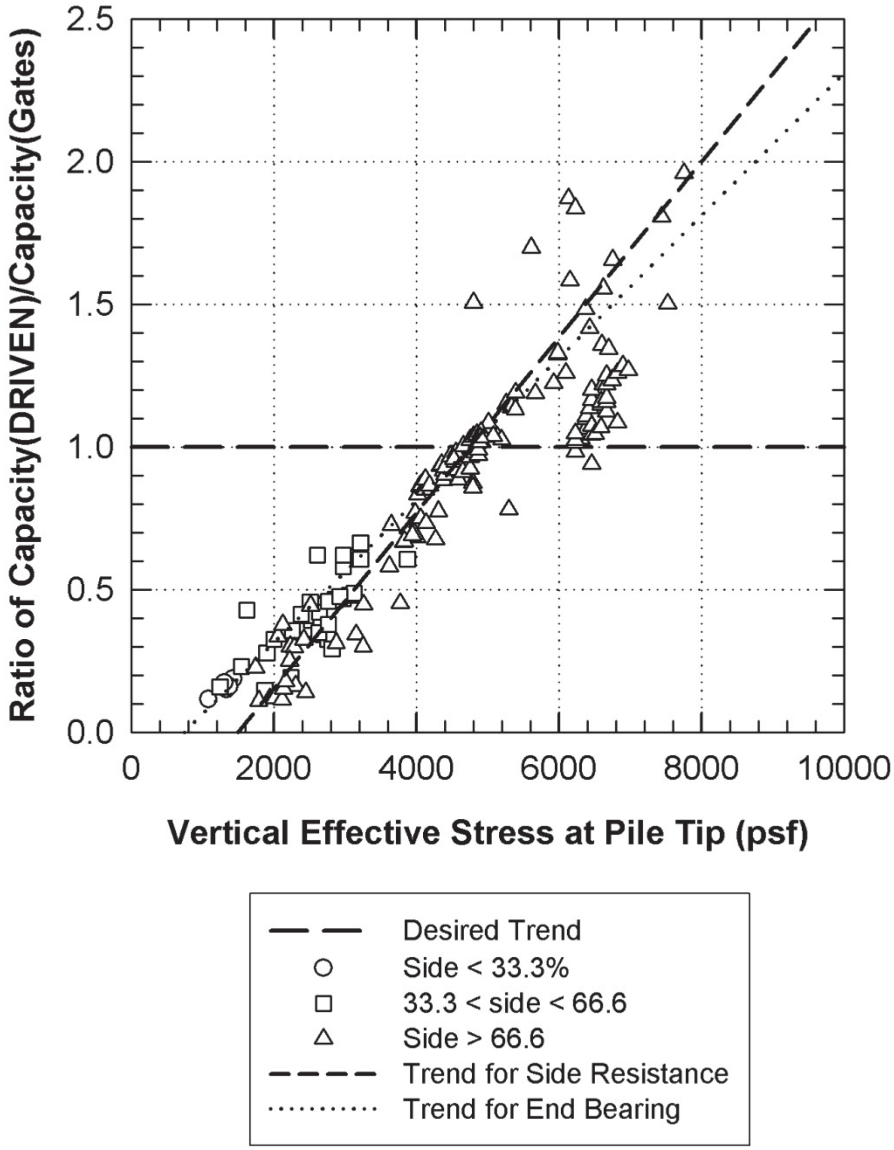

Figure 7.7 Effect of distribution of end bearing and side resistance on ratio of estimated pile capacity using DRIVEN (with 36 degree limit) to the capacity using FHWA-modified Gates versus effective vertical stress.

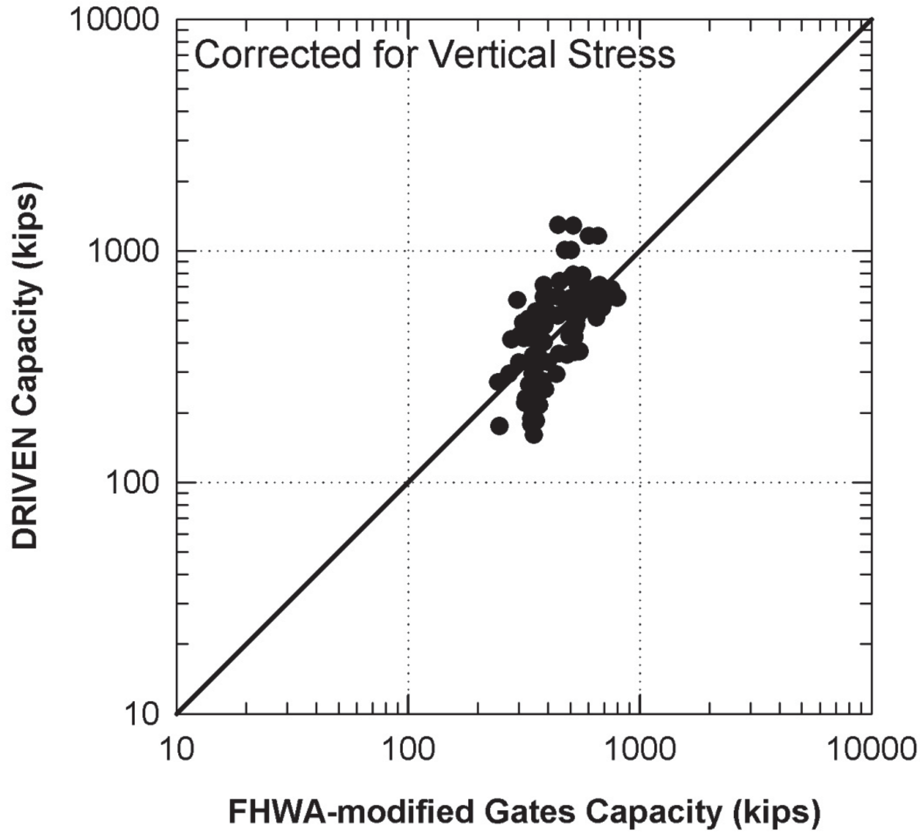

Figure 7.8 Estimated capacity using DRIVEN with correction factor for vertical effective stress and a conditional limit on friction angle versus the FHWA-modified Gates.

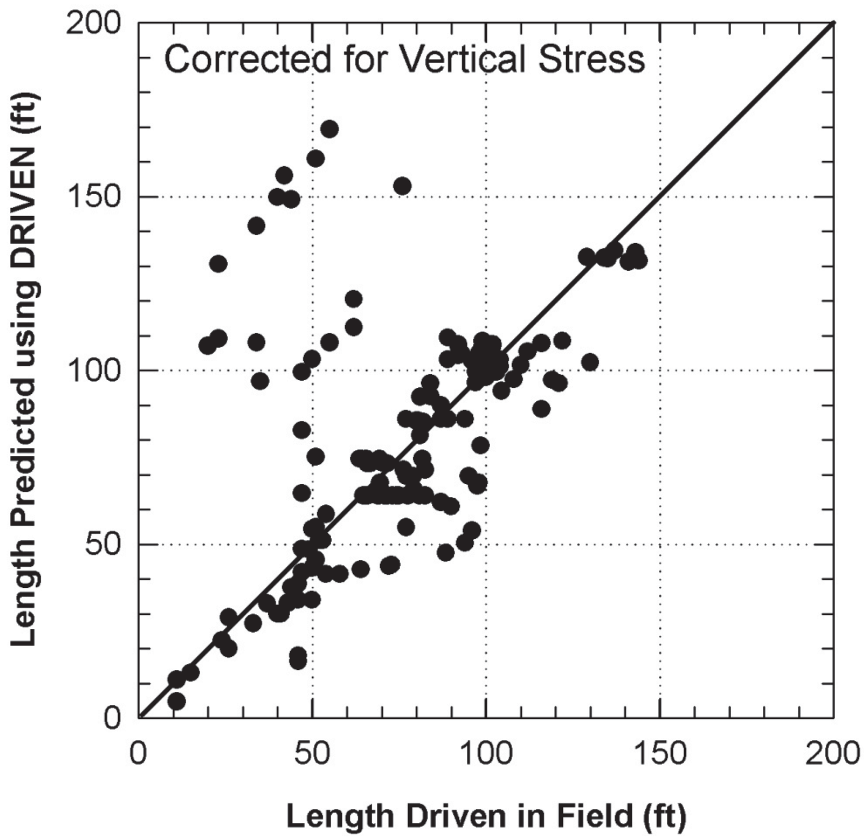

Figure 7.9 A comparison of estimated length of pile based on DRIVEN with correction factor for vertical stress and conditional limit for friction angle to 36 degrees versus actual length of pile driven in the field.

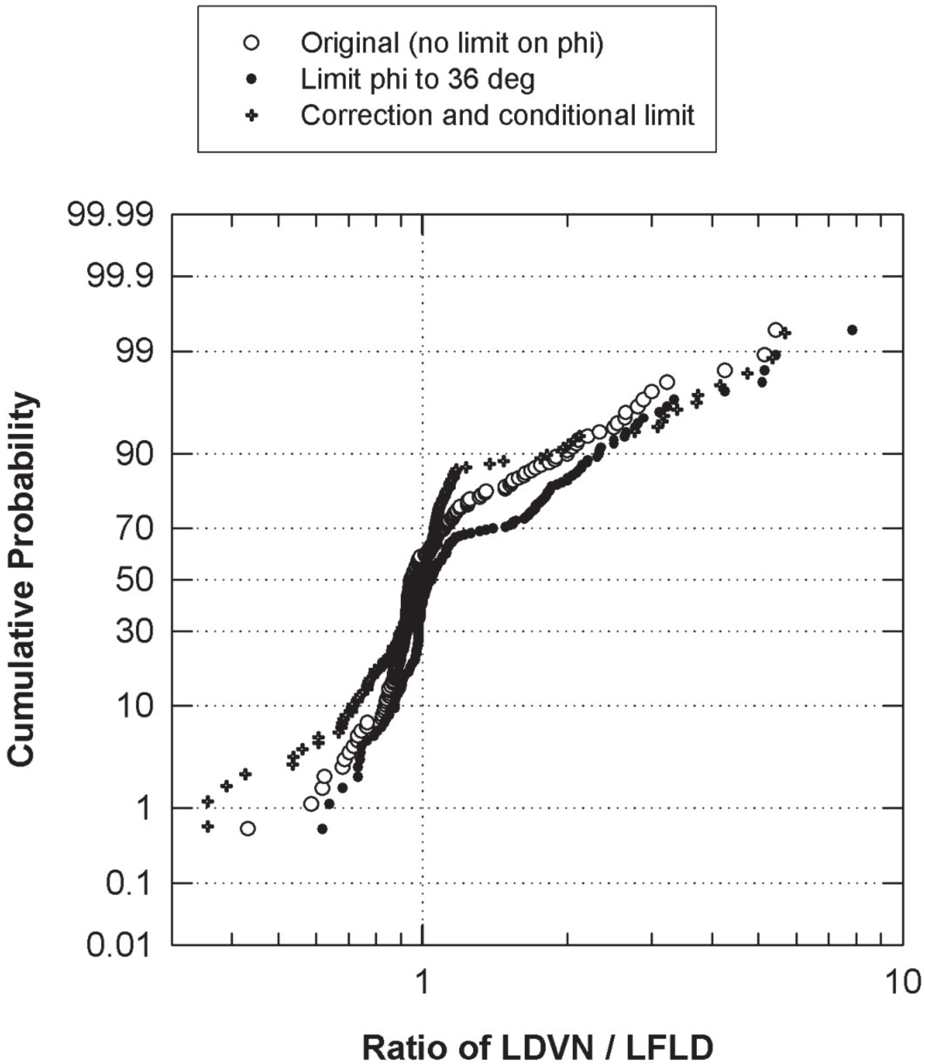

Figure 7.10 Cumulative distribution for the ratio of length predicted by DRIVEN/length driven in field for two conditions, no limit of Phi with DRIVEN, and DRIVEN with stress correction factor and conditional limit on friction angle..

8.0 SUMMARY AND CONCLUSIONS

The agreement between estimates of capacity using static methods and dynamic formula requires knowledge of how well the static method can predict capacity, and how well the dynamic formula can predict capacity. The static method developed within the computer program DRIVEN was used herein as the static method for determining pile capacity. Options selected from DRIVEN include using the Tomlinson (1971) relationships for determining pile capacity in fine-grained soil, and Nordlund (1963)/Thurman (1964) relationships for determining pile capacities in coarse-grained soils.

The relationships and options selected within DRIVEN for determining pile capacity in sand use a unit side resistance proportional to effective stress until a limiting value of side resistance is reached. The unit end bearing also is proportional to effective stress until a limiting value is reached. This approach for determining capacity is common for static methods, however, the approximation results in a method that tends to under-predict pile capacity for short piles, and over-predict capacity for long piles as discussed in Chapter 2. These trends were observed by Coyle and Castello (1981) and Dennis (1982) and supported by data provided by Vesic (1967). Dennis developed a length correction factor with values similar to those found in this study.

All predictive methods are subject to uncertainties. Predicted capacities for the static method, DRIVEN, were compared with predicted capacities based on the resistance of the pile during pile driving using dynamic formulae. Comparisons between predictions of pile capacity using DRIVEN and FHWA-modified Gates method and were found to exhibit quite a bit of scatter. The coefficient of variation (cov) was high (greater than 0.9), indicating poor agreement between the two methods. High cov values were anticipated. Chapter 3 presents results by Long, et al, (2009) in which cov values were found to be range from 0.3 to 0.7 with an average of 0.6.

Cases were collected in which 182 CIP piles were driven for bridges in Wisconsin (Chapter 5). A soil profile was identified for each of these cases, and detail of the pile driving behavior was recorded. Information sufficient to predict capacity with static methods, with dynamic formula, and with WEAP was collected for each case. The predominant pile type was a 14-inch diameter pile. All piles were driven with single open-ended diesel hammer, and the most commonly used hammer was a Delmag D30-32. Eighty percent of the piling drove to depths between 45 and 100 ft, with a maximum pile penetration slightly less than 150 feet. Piles were typically driven to capacities between 240 and 800 kips. Most of the piles were friction piles. Seventy-five percent of the piles developed less than 30 percent of their total capacity from end bearing. Sixty percent of the piles developed more than half their capacity from granular soils. About 25 percent of the piles developed all capacity from granular soil.

Chapter 6 presents the results of comparisons between capacities predicted using DRIVEN with no restriction on soil friction angle with the EN formula, the FHWA-modified Gates formula, and WEAP. Efforts are focused mostly on the agreement between DRIVEN and Gates because these are the two methods currently used by Wisconsin DOT. The agreement between DRIVEN and Gates is poor. Comparisons between DRIVEN and EN, and DRIVEN and WEAP exhibited the same trend as DRIVEN vs. Gates and were also poor.

Modifications were made to the static method (DRIVEN) in an attempt to improve the agreement between estimates of capacity made with the FHWA-modified Gates formula and estimates of pile capacity made with DRIVEN (Chapter 7). The first modification was to limit the soil friction angle to be no greater than 36 degrees. This is a recommendation in the DRIVEN user's manual. This modification slightly improved the agreement between DRIVEN and Gates. The effect of applying a limiting friction angle resulted in slight improvement. The mean value changed from 1.4 to 0.9, and the cov decreased from 0.98 to 0.73.

Two additional factors that appear to affect DRIVEN estimates of capacity were 1) the depth of the driven pile, and 2) whether the resistance was in side or end bearing. Both of these factors were accounted for by developing a correction factor that adjusts the DRIVEN capacity based on effective stress at the tip of the pile and whether the resistance is side resistance or end bearing. The resulting formula is as follows:

$$Corr\ Side\ Capacity = DRIVEN\ Side\ Capacity/CF_{side} \tag{8.1}$$

and

$$Corr\ EB\ Capacity = DRIVEN\ EB\ Capacity/CF_{end\ bearing} \tag{8.2}$$

Where CF_{side} and $CF_{end\ bearing}$ are determined using the equations below:

$$CF_{side} = 0.2 \leq -0.4615 + 1.4615 \cdot \sigma'_{v\ tip}/4750 \leq 1.2 \tag{8.3}$$

where, $\sigma'_{v\ tip}$ is the vertical effective stress (psf) at the tip of the pile. The correction factor for end bearing is also shown below and is represented with the following equation:

$$CF_{end\ bearing} = 0.2 \le -0.185 + 1.185 \cdot \sigma'_{v\ tip}/4750 \le 1.2 \qquad (8.4)$$

Application of these correction factors significantly improves the agreement between DRIVEN and FHWA-modified Gates. A review of all the cases with the corrected DRIVEN indicated that soil profiles with Standard Penetration Test values greater than 80 would be better represented in DRIVEN by allowing friction angles to be as high as 40 degrees.

With the above modifications, significant improvement was observed in the agreement between estimates of capacity using DRIVEN and FHWA-Gates. The mean value changed from 1.36 to 1.06 and the cov decreased substantially from 0.97 to 0.28. Thus, the applied correction factors are very successful in improving the agreement between capacities estimated by DRIVEN and FHWA-modified Gates.

Estimates for pile length were also compared. The length of pile necessary to develop capacity was estimated using DRIVEN with correction factors applied. There were several sites with significant difference between predicted and measured length of piling. These sites were reviewed carefully, and there were no obvious reasons to explain the difference. However, the predictions for length show an overall improvement, but the improvement is less significant than observed for capacity comparison. Estimates for length are less sensitive than estimates for capacity.

9.0 REFERENCES

American Petroleum Institute, "Recommended Practice for Planning, Designing and Constructing Fixed Offshore Platforms, Section 1.6, Foundation Design," Sixteenth Edition, April 1, 1986.

American Society for Testing Materials, "Practice for Preparing Precision Statements for Test Methods for Construction Materials, C670-90a, Annual ASTM Book of Standards, Vol. 04.08, 1990.

Briaud, J-L., and L.M. Tucker, "Measured and Predicted Axial Response of 98 Piles," Journal of Geotechnical Engineering, ASCE, Vol. 114, No. 9, September, 1988, paper no. 22725, pp. 984-1028.

Cornell, C. A., "A Probability Based Structural Code," J. American Concrete Institute, Vol. 66, No.4, December, 1969, pp. 974-985.

Coyle, H.M. and R. R. Castello, "New Design Correlations for Piles in Sand," Journal of the Geotechnical Engineering Division, ASCE, Vol. 107, No. GT7, 1981, pp. 965-986.

Dennis, N. D. and R. E. Olson, "Axial Capacity of Steel Pipe Piles in Clay." Proceedings, ASCE Specialty Conference on Geotechnical Practice in Offshore Engineering, S. G. Wright, ed., April 27-29, 1983, Austin, Texas, 370-388.

Flaate, K., "An Investigation of the Validity of Three Pile-Driving Formulae in Cohesionless Material," Publication No.56, Norwegian Geotechnical Inst., Oslo, Norway: 11-22, 1964.

Fragaszy, R. J., D. Argo, and J. D. Higgins, "Comparison of Formula Predictions with Pile Load Test," Transportation Research Board, 22-26 January, 1989.

Fragaszy, R. J., J. D. Higgins, and D. E. Argo, "Comparison of Methods for Estimating Pile Capacity," Washington State Department of Transportation and in cooperation with U.S. Department of Transportation FHWA, August, 1988.

Gates, M., "Empirical Formula For Predicting Pile Bearing Capacity," Civil Engineering, Vol 27, No.3, March, 1957, pp 65-66.

Long, J., and M. Maniaci, Friction Bearing Design of Steel H-piles. IDOT ITRC 1-5-38911. Edwardsville: Illinois Transportation Research Center, Dec, 2000.

Long, J., J. Hendrix, and A. Baratta, Evaluation/Modification of IDOT Foundation Piling Design and Construction Policy. Report No. ICT-09-03. Findings of ICT-R27-24. Rantoul: Illinois Center for Transportation, Mar, 2009.

Long, J., J. Hendrix, and D. Jaromin, Comparison of Five Different Methods for Determining Pile Bearing Capacities, SPR# 0092-07-04, Wisconsin Highway Research Program, March, 2009.

Long, J. and A. Anderson, Improved Design for Driven Piles on a Pile Load Test Program in Illinois, Report No. ICT-R27-69, Rantoul: Illinois Center for Transportation, July, 2012.

Nordlund, R.L., "Bearing Capacity of Piles in Cohesionless Soils," ASCE, Journal of the Soil Mechanics and Foundations Division, No. SM-3, 1963.

Nordlund, R.L., "Point Bearing and Shaft Friction of Piles in Sand." Presented at the 5th Annual Short Course on Fundamentals of Deep Foundations Design, University of Missouri-Rolla. 1979.

Olson, R. E. and Dennis, N. D., "Reliability of Pile Foundations," Proc. ASCE Specialty Conference, Structures Congress, Houston, Texas, 1983.

Olson, R. E. and K. S. Flaate, "Pile-Driving Formulas for Friction Piles in Sand," Journal of the Soil Mechanics and Foundations Division, ASCE, Vol.93, No.SM6, November, 1967, pp 279-296.

Paikowsky, S. G., J. E. Regan, and J. J. McDonnell, "A Simplified Field Method For Capacity Evaluation Of Driven Piles," Publication No. FHWA-RD-94-042, U.S. Department of Transportation, Federal Highway Administration, McLean, Virginia, September 1994.

Paikowsky, S. G., Kuo, C., Baecher, G., Ayyub, B., Stenersen, K, O'Malley, K., Chernauskas, L., and O'Neill, M., Load and Resistance Factor Design (LRFD) for Deep Foundations, NCHRP Report 507, Transportation Research Board, Washington, DC, 2004.

Thurman, A. G., "Computed Load Capacity and Movement of Friction and End-Bearing Piles Embedded in Uniform and Stratified Soil," Phd. D. Thesis, Carnegie Institute of Technology, 1964.

Tomlinson, M. J., "The Adhesion of Piles Driven in Clay Soils." Proc. 4th Int. Conf. S.M. & F.E. vol. 2, 1957, pp. 66-71.

Tomlinson, M. J., Foundation Design and Construction. London: Pitman, 1985.

Tomlinson, M. J., "Some Effects of Pile Driving on Skin Friction," Proceedings of the Conference on "Behavior of Piles," ICE, London, 1971, Paper 9, pp. 107-114, 149-150.

U.S. Department of Transportation, FHWA (Federal Highway Administration), Research and Procurement, Design and Construction of Driven Pile Foundations. (Washington, D.C. :FHWA Contract No. DTFH61-93-C-00115, September 1995) I, II.

Vesic, A. B., "Bearing Capacity of Deep Foundations in Sand," National Research Council, Highway Research Record, Vol. 39, 1963, pp. 112-153.

Vesic, A. S., "A Study of Bearing Capacity of Deep Foundations." Final Rep., Proj. B-189, School of Civil Eng., Georgia Inst. Tech., Atlanta, Ga., 1967.

Wellington, A. M. (1892) discussion of "The Iron Wharf at Fort Monroe, Va.," by J. B. Duncklee, Transactions, ASCE, Vol. 27, Paper No. 543, Aug., 1892, pp. 129-137.

APPENDIX A CALCULATION OF MODIFIED PILE CAPACITY

A.1 INTRODUCTION

The report identifies formulae to modify the side resistance and end bearing capacity for a driven pile. Estimates of the original capacity versus depth are made with the computer program DRIVEN. Then the estimates of capacity from driven are modified to account for the effect of vertical effective stress.

A.2 ESTIMATING CAPACITY WITH DRIVEN

An example case is presented herein. A CIP pile, 10.75 inches in diameter, is driven into a mixed soil profile. The soil profile consists of 8.0 ft thick layer of loose granular soil with a friction angle of 28 degrees and a total unit weight of 80pcf. The granular soil below is 33.0 ft thick with a friction angle of 32 degrees and a unit weight of 115 pcf. The third layer is a clay layer 50 ft thick with a unit weight of 105 pcf and a shear strength of 1700 psf. Below this layer is a cohesionless soil, 10.5 ft thick with a unit weight of 129 pcf and a friction angle of 35 degrees. The groundwater table is located at a depth of 8 ft.

Output from DRIVEN is given in Figs. A.1 – A.3. Input information such as the diameter of the pile, the location of the groundwater table, and details of the soil profile are shown in Fig. A.1. The variation with depth of ultimate skin friction and ultimate end bearing as determined by DRIVEN are shown in Fig. 2. Summary values of capacity in side resistance, end bearing, and total resistance are given in Fig. 3. These values represent the unmodified values of ultimate capacity as determined by DRIVEN.

A.3 EFFECT OF PILE DEPTH ON ULTIMATE CAPACITY

The effect of depth on unit side resistance and unit end bearing was discussed in Chapter 7. It was shown in Chapter 7 that there was a strong relationship between the effective vertical stress at the tip of the pile and the ratio of predicted capacity (using DRIVEN)/predicted capacity (from FHWA-modified Gates). Accordingly, correction factors were developed to account for the effective stress. Chapter 7 provides the equations (Eqns. 7.1 – 7.4) to modify the side and end bearing values to improve agreement between capacities predicted by DRIVEN and FHWA-modified Gates. These equations are repeated below for convenience:

The equation for correcting DRIVEN side resistance to better agree with FHWA-modified Gates is as follows:

$$Corr\ Side\ Capacity = DRIVEN\ Side\ Capacity / CF_{side} \quad \text{(A.1)}$$

where CF_{side} is determined as follows:

$$CF_{side} = 0.2 \leq -0.4615 + 1.4615 \cdot \sigma'_{v\ tip}/4750 \leq 1.2 \quad \text{(A.2)}$$

Where σ'_v is the vertical effective stress at the tip of the pile.

The equation for correcting the end bearing capacity estimated with DRIVEN to better agree with FHWA-modified Gates is as follows:

$$Corr\ EB\ Capacity = DRIVEN\ EB\ Capacity / CF_{end\ bearing} \quad \text{(A.3)}$$

where CF_{end} is determined as follows:

$$CF_{end\ bearing} = 0.2 \leq -0.185 + 1.185 \cdot \sigma'_{v\ tip}/4750 \leq 1.2 \quad \text{(A.4)}$$

For example, for a pile penetration of 35 ft, DRIVEN determines the following
Depth = 100 ft
Skin Friction = 283 kips
End Bearing = 68 kips
Total Capacity = 351 kips

The effective stress determined by DRIVEN for a depth of 100 ft is 5106 psf. The value of effective stress at the tip of the pile is shown in the end bearing section in Fig. A.2. DRIVEN only reports the effective stress at the tip for cohesionless soil, therefore, effective stress must be determined by hand calculations if the soil is reported as cohesive.

Based on the values reported above, the modified skin resistance can be determined as follows:

CF_{side} = -0.4615 +1.4615*σ'_v/4750
= -0.4615 + 1.4615*5106/4750 = <u>1.109</u>
(which is between the limits 0.2 and 1.2)

Therefore the Modified skin resistance is

Modified Skin Resistance= 283 kips/1.109 = 256 kips

Based on the values reported above, the modified end bearing resistance can be determined as follows:

$CF_{end\ bearing} = -0.185 + 1.185*\sigma'_v/4750$
$= -0.185 + 1.185*5106/4750 = 1.089$
(which is between the limits 0.2 and 1.2)

Therefore the Modified end bearing capacity is

End Bearing Capacity = 67.8 kips/1.109 = 62.3 kips

The total modified pile capacity is the sum of the modified skin resistance and modified end bearing which is 256 + 62.3 = 318 kips.

Calculations for each depth identified by DRIVEN are provided in Fig. A.4.

DRIVEN 1.2

GENERAL PROJECT INFORMATION

Filename:
Project Name: Project Name   Project Date: 06/18/2013
Project Client: Client
Computed By: Initials
Project Manager: Project Manager

PILE INFORMATION

Pile Type: Pipe Pile - Closed End
Top of Pile: 0.00 ft
Diameter of Pile: 10.75 in

ULTIMATE CONSIDERATIONS

Water Table Depth At Time Of:	- Drilling:	8.00 ft
	- Driving/Restrike	8.00 ft
	- Ultimate:	8.00 ft
Ultimate Considerations:	- Local Scour:	0.00 ft
	- Long Term Scour:	0.00 ft
	- Soft Soil:	0.00 ft

ULTIMATE PROFILE

Layer	Type	Thickness	Driving Loss	Unit Weight	Strength	Ultimate Curve
1	Cohesionless	1.50 ft	0.00%	80.00 pcf	28.0/28.0	Nordlund
2	Cohesionless	6.50 ft	0.00%	80.00 pcf	28.0/28.0	Nordlund
3	Cohesionless	33.00 ft	0.00%	115.00 pcf	32.0/32.0	Nordlund
4	Cohesive	50.00 ft	0.00%	105.00 pcf	1700.00 psf	T-79 Steel
5	Cohesionless	10.50 ft	0.00%	129.00 pcf	35.0/35.0	Nordlund

Figure A.1 Output from DRIVEN providing information on general project information, pile properties, groundwater conditions, and soil profile.

ULTIMATE - SKIN FRICTION

Depth	Soil Type	Effective Stress At Midpoint	Sliding Friction Angle	Adhesion	Skin Friction
0.01 ft	Cohesionless	0.40 psf	14.81	N/A	0.00 Kips
1.49 ft	Cohesionless	59.60 psf	14.81	N/A	0.05 Kips
1.51 ft	Cohesionless	120.40 psf	14.81	N/A	0.05 Kips
7.99 ft	Cohesionless	379.60 psf	14.81	N/A	1.43 Kips
8.01 ft	Cohesionless	640.26 psf	16.93	N/A	1.44 Kips
17.01 ft	Cohesionless	876.96 psf	16.93	N/A	7.75 Kips
26.01 ft	Cohesionless	1113.66 psf	16.93	N/A	17.47 Kips
35.01 ft	Cohesionless	1350.36 psf	16.93	N/A	30.59 Kips
40.99 ft	Cohesionless	1507.64 psf	16.93	N/A	41.20 Kips
41.01 ft	Cohesive	N/A	N/A	1405.00 psf	41.25 Kips
50.01 ft	Cohesive	N/A	N/A	1405.00 psf	76.84 Kips
59.01 ft	Cohesive	N/A	N/A	1405.00 psf	112.43 Kips
68.01 ft	Cohesive	N/A	N/A	1405.00 psf	148.02 Kips
77.01 ft	Cohesive	N/A	N/A	1405.00 psf	183.60 Kips
86.01 ft	Cohesive	N/A	N/A	1405.00 psf	219.19 Kips
90.99 ft	Cohesive	N/A	N/A	1405.00 psf	238.88 Kips
91.01 ft	Cohesionless	4506.13 psf	18.52	N/A	238.97 Kips
100.01 ft	Cohesionless	4805.83 psf	18.52	N/A	283.45 Kips
101.49 ft	Cohesionless	4855.12 psf	18.52	N/A	291.30 Kips

ULTIMATE - END BEARING

Depth	Soil Type	Effective Stress At Tip	Bearing Cap. Factor	Limiting End Bearing	End Bearing
0.01 ft	Cohesionless	0.80 psf	22.80	8.40 Kips	0.01 Kips
1.49 ft	Cohesionless	119.20 psf	22.80	8.40 Kips	0.92 Kips
1.51 ft	Cohesionless	120.80 psf	22.80	8.40 Kips	0.93 Kips
7.99 ft	Cohesionless	639.20 psf	22.80	8.40 Kips	4.92 Kips
8.01 ft	Cohesionless	640.53 psf	40.40	20.80 Kips	10.20 Kips
17.01 ft	Cohesionless	1113.93 psf	40.40	20.80 Kips	17.75 Kips
26.01 ft	Cohesionless	1587.33 psf	40.40	20.80 Kips	20.80 Kips
35.01 ft	Cohesionless	2060.73 psf	40.40	20.80 Kips	20.80 Kips
40.99 ft	Cohesionless	2375.27 psf	40.40	20.80 Kips	20.80 Kips
41.01 ft	Cohesive	N/A	N/A	N/A	9.64 Kips
50.01 ft	Cohesive	N/A	N/A	N/A	9.64 Kips
59.01 ft	Cohesive	N/A	N/A	N/A	9.64 Kips
68.01 ft	Cohesive	N/A	N/A	N/A	9.64 Kips
77.01 ft	Cohesive	N/A	N/A	N/A	9.64 Kips
86.01 ft	Cohesive	N/A	N/A	N/A	9.64 Kips
90.99 ft	Cohesive	N/A	N/A	N/A	9.64 Kips
91.01 ft	Cohesionless	4506.47 psf	64.00	67.82 Kips	67.82 Kips
100.01 ft	Cohesionless	5105.87 psf	64.00	67.82 Kips	67.82 Kips
101.49 ft	Cohesionless	5204.43 psf	64.00	67.82 Kips	67.82 Kips

Figure A.2 Variation with depth of skin friction and end bearing as determined by DRIVEN.

ULTIMATE - SUMMARY OF CAPACITIES

Depth	Skin Friction	End Bearing	Total Capacity
0.01 ft	0.00 Kips	0.01 Kips	0.01 Kips
1.49 ft	0.05 Kips	0.92 Kips	0.97 Kips
1.51 ft	0.05 Kips	0.93 Kips	0.98 Kips
7.99 ft	1.43 Kips	4.92 Kips	6.35 Kips
8.01 ft	1.44 Kips	10.20 Kips	11.64 Kips
17.01 ft	7.75 Kips	17.75 Kips	25.50 Kips
26.01 ft	17.47 Kips	20.80 Kips	38.27 Kips
35.01 ft	30.59 Kips	20.80 Kips	51.39 Kips
40.99 ft	41.20 Kips	20.80 Kips	62.00 Kips
41.01 ft	41.25 Kips	9.64 Kips	50.90 Kips
50.01 ft	76.84 Kips	9.64 Kips	86.49 Kips
59.01 ft	112.43 Kips	9.64 Kips	122.07 Kips
68.01 ft	148.02 Kips	9.64 Kips	157.66 Kips
77.01 ft	183.60 Kips	9.64 Kips	193.25 Kips
86.01 ft	219.19 Kips	9.64 Kips	228.83 Kips
90.99 ft	238.88 Kips	9.64 Kips	248.53 Kips
91.01 ft	238.97 Kips	67.82 Kips	306.79 Kips
100.01 ft	283.45 Kips	67.82 Kips	351.27 Kips
101.49 ft	291.30 Kips	67.82 Kips	359.12 Kips

Figure A.3 Variation with depth of skin friction, end bearing, and total capacity as determined by DRIVEN.

	Original DRIVEN Capacities					Modified Capacities			
Pile Depth (ft)	Skin Friction (kips)	End Bearing (kips)	Total Capacity (kips)	Effective Stress at Depth (psf)	Cfside	Modified Skin Friction (kips)	Cfend	Modified End Bearing (kips)	Modified Total Capacity (kips)
0.01	0	0.01	0	1	0.200	0.0	0.200	0.1	0
1.49	0.05	0.92	1	119	0.200	0.3	0.200	4.6	5
1.51	0.05	0.93	1	121	0.200	0.3	0.200	4.7	5
7.99	1.43	4.92	6	639	0.200	7.2	0.200	24.6	32
8.01	1.44	10.2	12	641	0.200	7.2	0.200	51.0	58
17.01	7.75	17.75	26	1114	0.200	38.8	0.200	88.8	128
26.01	17.47	20.8	38	1587	0.200	87.4	0.211	98.6	186
35.01	30.59	20.8	51	2061	0.200	153.0	0.329	63.2	216
40.99	41.2	20.8	62	2375	0.269	153.0	0.408	51.0	204
41.01	41.25	9.64	51	2376	0.270	153.0	0.408	23.6	177
50.01	76.84	9.64	86	2760	0.388	198.3	0.503	19.1	217
59.01	112.43	9.64	122	3143	0.506	222.4	0.599	16.1	238
68.01	148.02	9.64	158	3527	0.624	237.4	0.695	13.9	251
77.01	183.6	9.64	193	3910	0.742	247.6	0.790	12.2	260
86.01	219.19	9.64	229	4293	0.860	255.0	0.886	10.9	266
90.99	238.88	9.64	249	4506	0.925	258.3	0.939	10.3	269
91.01	238.97	67.82	307	4506	0.925	258.3	0.939	72.2	331
100.01	283.45	67.82	351	5106	1.109	255.5	1.089	62.3	318
101.49	291.3	67.82	359	5204	1.140	255.6	1.113	60.9	316

Figure A.4 Calculation Table for determining modified skin friction, modified end bearing, and modified total capacity.

Wisconsin Highway Research Program
University of Wisconsin-Madison
1415 Engineering Drive
2204 Engineering Hall
Madison, WI 53706
608.890.4966
http://wisdotresearch.wi.gov/whrp